UNIVERSITY OF OTTAWA
Department of Chemical and Biological Engineering

Performance Improvement of Latex-Based PSAs using Polymer Microstructure Control

by
Lili Qie

A thesis submitted to the Faculty of Graduate and Postdoctoral Studies
in partial fulfillment of the requirements for the degree of

Doctor of Philosophy in
Chemical Engineering

© Lili Qie, Ottawa, Canada, 2011

STATEMENT OF CONTRIBUTIONS OF COLLABORATORS

I hereby declare that I am the sole author of this thesis. I performed all the polymerization experiments, polymer characterization and pressure-sensitive adhesive (PSA) performance testing as well as the associated data analysis. The PSA's surface images were characterized by Dr. Gabriela Fonseca with Atomic Force Microscopy (AFM) at the University of Ottawa. PSA film surface tension measurements and latex particle size analysis were carried out by me in the Department of Chemical and Biological Engineering at the University of Ottawa.

The scientific guidance throughout the project and editorial comments of the written work were provided by my thesis supervisor Dr. Marc A. Dubé of the Department of Chemical and Biological Engineering at the University of Ottawa.

Name: Lili Qie

Date: January/2011

ABSTRACT

This thesis aims to improve the performance of latex-based pressure-sensitive adhesives (PSAs). PSA performance is usually evaluated by tack, peel strength and shear strength. Tack and peel strength characterize a PSA's bonding strength to a substrate while shear strength reflects a PSA's capability to resist shear deformation. In general, increasing shear strength leads to a decrease in tack and peel strength. While there are several commercial PSA synthesis methods, the two most important methods consist of either solvent-based or latex-based techniques. While latex-based PSAs are more environmentally compliant than solvent-based PSAs, they tend to have much lower shear strength, at similar tack and peel strength levels. Therefore, the goal in this thesis was to greatly improve the shear strength of latex-based PSAs at little to no sacrifice to tack and peel strength.

In this study, controlling the polymer microstructure of latexes or their corresponding PSA films was used as the main method for improving the PSA performance. The research was sub-divided into four parts. First, the influence of chain transfer agent (CTA) and cross-linker on latex polymer microstructure was studied via seeded semi-batch emulsion polymerization of butyl acrylate (BA) and methyl methacrylate (MMA). Three techniques were used to produce the latexes: (1) adding CTA only, (2) adding cross-linker only, and (3) adding both CTA and cross-linker. It was found that using CTA and cross-linker simultaneously allows one to expand the range of latex microstructural possibilities. For example, latexes with similar gel contents but

different M_c (molecular weight between cross-links) and M_w (molecular weight of sol polymers) could be produced if CTA and cross-linker concentration are both increased. However, for the corresponding PSAs with similar gel contents, the relationship between their polymer microstructure and performance was difficult to establish as almost all of the medium and high gel content PSAs showed very low tack and peel strength as well as extremely large shear strength readings.

In the second part of this thesis, in order to improve the tack and peel strength of medium and high gel content PSAs, the monomer composition and emulsifier concentration were varied. It was found that changing the monomer mixture from BA/MMA to BA/acrylic acid (AA)/2-hydroxyethyl methacrylate (HEMA) while simultaneously decreasing emulsifier concentration dramatically improved the corresponding PSAs' shear strength as well as tack and peel strength. The addition of polar groups to the PSA increased its cohesive strength due to the presence of strong hydrogen bonding; meanwhile, PSA films' surface tension increased.

In the third part, two series of BA/AA/HEMA latexes were generated by varying the amounts of CTA either in the absence or presence of cross-linker. The latexes produced in the absence of cross-linker exhibited significantly larger M_c and M_w compared to their counterparts with similar gel contents prepared with cross-linker. The PSAs with the larger M_c and M_w showed much larger shear strengths due to improved entanglements between the polymer chains.

In the final part of the thesis, the performance of the BA/AA/HEMA PSAs was further improved by post-heating. Compared with original latex-based PSAs with similar gel contents, heat-treated PSAs showed not only significantly improved shear strengths,

but also much larger tack and peel strengths. The different shear strengths were related to the PSAs' gel structures, which were discrete in the original PSAs but continuous in the heat-treated PSAs. The improved tack and peel strengths were related to the PSA films' surface smoothness. During the post-heating process, the PSA polymer flowed, resulting in much smoother surfaces than the original PSA films. In addition, the effect of post-heating was related to the polymer microstructure of the untreated PSAs. Decreasing the amount of very small or very big polymers or simultaneously increasing M_c and M_w could lead to post-treated PSAs with significantly better performance. Moreover, it was found that by optimizing the polymer microstructure of the original latex-based PSAs, it was possible to obtain a treated PSA with similar or even better performance than a solvent-based PSA with similar polymer microstructure.

Our original objective was surpassed: in two cases, not only was shear strength greatly improved, but so were tack and peel strength due to the simultaneous modification of PSA bulk and surface properties.

RÉSUMÉ

Cette thèse vise à améliorer la performance des adhésifs sensibles à la pression (ASP) à base de latex. La performance des ASPs est généralement évaluée par leur habileté à adhérer à une surface. L'adhérance à coller et la résistance au décollement caractérisent une force de liaison d'ASP à un substrat tandis que la résistance au cisaillement reflète la capacité d'un ASP à résister à la déformation de coupe. En général, ce qui augmente la résistance au cisaillement conduit à une diminution de l'adhérance à coller et la résistance au décollement. Bien qu'il existe plusieurs méthodes de synthèse commerciale d'ASP, les deux méthodes les plus importantes diffèrent par milieu de fabrication: à base de solvant ou à base de latex. Alors que les ASP à base de latex sont plus conformes aux normes environnementales que les ASP à base de solvant, ils ont tendance à avoir une résistance au cisaillement beaucoup plus faible. Par conséquent, l'objectif de cette thèse était d'améliorer considérablement la résistance au cisaillement des ASPs à base de latex sans sacrifier leur adhérance et leur résistance au décollement.

Dans cette étude, le contrôle de la microstructure des polymères de latex ou des films de l'ASP a été utilisé comme la méthode principale pour améliorer la performance de l'ASP. La recherche a été sous-divisée en quatre parties. Premièrement, l'influence de l'agent de transfert de chaîne (ATC) et de réticulation sur la microstructure du polymère de latex a été étudiée par polymérisation d'acrylate de butyle (AB) et de méthacrylate de méthyle (MAM) en émulsion ensemencée semi-continu. Trois techniques ont été utilisées pour produire le latex: (1) en ajoutant que de l'ATC, (2) en ajoutant seulement l'agent de

réticulation, et (3) en ajoutant les deux. Il a été constaté que l'utilisation simultanée d'ATC et d'agent de réticulation permet d'élargir l'éventail des possibilités de la microstructure du latex. Par exemple, les latex avec des contenus de gel similaires, mais avec des différentes valeurs de M_c (poids moléculaire entre réticulations) et de M_w (poids moléculaire de polymères sol) peuvent êtres produits si les concentrations de l'ATC et de l'agent de réticulation sont augmentées. Toutefois, pour les ASPs correspondant à une teneur en gel similaire, il a été difficile d'établir la relation entre leur microstructure du polymère et de la performance parce que presque la totalité des ASPs à moyen et à haut contenu en gel a montré une très faible habileté à coller et de résister au décollement, ainsi que des mesures très grandes de résistance au cisaillement.

Dans la deuxième partie de cette thèse, afin d'améliorer l'habileté à coller et la résistance au décollement des ASPs avec des moyens et hauts contenus en gel, la composition de monomères et la concentration d'émulsifiant ont été variées. Il a été constaté que la modification du mélange de monomères de AB/MAM à AB/acide acrylique (AA)/2-hydroxyéthyl méthacrylate (HEMA) simultanément avec la diminution de la concentration d'émulsifiant, ont considérablement amélioré la résistance au cisaillement des ASPs ainsi que leur habileté à coller et de résister au décollement. L'ajout de groupes polaires sur l'ASP a accru sa force de cohésion en raison de la présence d'une liaison d'hydrogène forte, et en même temps, la tension de surface des films ASP a augmenté.

Dans la troisième partie, deux séries de latex avec AB/AA/HEMA ont été générées en variant les quantités d'ATC, soit en l'absence ou la présence d'agent de réticulation. Le latex produit en absence d'agent de réticulation a montré un niveau plus

large du M_c et M_w, comparativement à leurs homologues ayant les mêmes teneurs en gel préparé avec agent de réticulation. Les ASPs avec les plus grands M_c et M_w ont montré une résistance supérieure au cisellement la plus grande en raison de l'augmentation de l'enchevêtrement entre les chaînes de polymères.

Dans la dernière partie de la thèse, la performance des ASPs du AB/AA/HEMA a été encore améliorée par post-chauffage. Par comparaison avec les ASPs d'origine à base de latex avec des teneurs similaires de gel, les ASPs traités avec la chaleur ont montré non seulement une considérable amélioration à la résistance au cisaillement, mais aussi une plus grande habileté à coller et à résister au décollement. Les différentes résistances au cisaillement ont été liées aux structures de gel, qui ont été discrets dans les ASP originaux, mais continues dans les ASPs avec traitement thermique. L'augmentation de l'habileté à coller et la résistance au décollement a été liée à la rugosité de surface des films d'ASPs. Au cours du processus de post-chauffage, le polymère ASP a coulé, entraînant des surfaces beaucoup plus lisses que les films d'ASP originaux. En plus, l'effet de post-chauffage est lié à la microstructure du polymère des ASP non-traitées. La diminution de la quantité des polymères très petits ou très grands ou en augmentant simultanément le M_c et le M_w pourrait conduire aux ASPs post-traitées avec de biens meilleures performances. D'ailleurs, il a été constaté que par l'optimisation de la microstructure du polymère des ASPs à base de latex originaux, il a été possible d'obtenir un ASP avec des performances similaires ou encore mieux que l'ASP à base de solvant avec une microstructure similaire.

Notre objectif initial a été surpassé: dans deux cas, non seulement la résistance au cisaillement a été améliorée grandement, mais aussi l'habilité à coller et la résistance au

décollement en raison à la modification simultanée des propriétés en vrac et des surfaces des ASPs.

TABLE OF CONTENTS

LIST OF FIGURES

Chapter 6

Chapter 7

Appendix

LIST OF TABLES

Appendix

NOMENCLATURE

CMC = Critical micelle nucleation

G' = Storage modulus (Pa)

G'' = Loss modulus (Pa)

G* = Composite modulus (Pa)

[I] = Initiator concentration

J = Creep compliance (Pa^{-1})

k_P = Propagation rate coefficient

[M] = Monomer concentration

M_c = Molecular weight between crosslink points (g mol^{-1})

M_e = Molecular weight between entanglements (g mol^{-1})

M_w = Weight-average molecular weight of sol polymers (g mol^{-1})

M_n = Number-average molecular weight of sol polymers (g mol^{-1})

$\bar{n}$ = average number of radicals per particle

N_A = Avogadro's number (mol^{-1})

R = Universal ideal gas constant, [cm^3 bar mol^{-1} K^{-1}]

R_I = Rate of radical generation (or initiation)

R_P = Rate of polymerization

T = temperature (K)

T_g = Glass transition temperature (°C)

x_n = number-average degree of polymerization

Greek symbols

τ = Relaxation time

ω_1 = Debonding frequency of peel strength testing (Hz)

ω_2 = Bonding frequency of peel strength testing (Hz)

χ = Polymer and solvent interaction parameter ((cal cm^{-3})$^{1/2}$)

ρ = Density (g cm^{-3})

δ = Polymer's solubility parameter ((cal cm^{-3})$^{1/2}$)

θ = Contact angle (^{o})

γ = Surface tension (N m^{-1})

LIST OF ABBREVIATIONS

AA = Acrylic acid

AFM = Atomic force microscopy

AMA = Allyl methacrylate

BA = Butyl acrylate

CTA = Chain transfer agent

DLS = Dynamic light scattering

DMA = Dynamic mechanical analysis

DSC = Differential scanning calorimetry

EHA = 2-Ethyl hexyl acrylate

GPC = Gel permeation chromatography

HEMA = 2-Hydroxy ethyl methacrylate

HQ = Hydroquinone

KPS = Potassium persulfate

MAA = Methacrylic acid

MMA = Methyl methacrylate

MWD = Molecular weight distribution

NDM = n-Dodecyl mercaptan

PDI = Polydispersity index

phm = parts per hundred parts of monomer

PSA = Pressure sensitive adhesive

PSD = Particle size distribution

PTFE = Polytetrafluoroethylene

SDS = Sodium dodecyl sulphate

THF = Tetrahydrofuran

LIST OF MOLECULAR FORMULAE

Acrylic acid: $CH_2=CHCOOH$

Allyl methacrylate: $CH_2=C(CH_3)-COO-CH_2-CH=CH_2$

Butyl acrylate: $CH_2=CH-COO-(CH_2)_3-CH_3$

n-Dodecyl mercaptan: $CH_3-(CH_2)_{11}-SH$

2-Hydroxy ethyl methacrylate: $CH_2=C(CH_3)-COO-(CH_2)_2-OH$

Hydroquinone: $HO-(C_6H_4)-OH$

Methyl methacrylate: $CH_2=C(CH_3)-COO-CH_3$

Potassium persulfate: $K_2(SO_4)_2$

Sodium bicarbonate: $NaHCO_3$

Sodium dodecyl sulfate: $CH_3-(CH_2)_{11}-(SO_4)-Na$

ACKNOWLEDGMENTS

I would like very much to thank all the people that have helped, supported and inspired me during my doctoral studies.

First, I want to express my sincere gratitude to my supervisor, Dr. Marc A. Dubé, for accepting me in his research group and also for his continuous encouragement, patience and guidance over the years. He has taught me a lot about how to do research and write research papers. In addition, Dr. Dubé has been very supportive. I had a baby during my PhD study, and for about two years I was in Ottawa alone with my daughter. When she was sick, I could not make it to school. Dr. Dubé was very understanding and supportive regarding this. I have to say that without Dr. Dubé, I would not have been able to finish my studies.

Secondly, I want to thank my committee members, Dr. Arturo Macchi, Dr. Jules Thibault, and Dr. Christopher Lan for their constructive feedback. I am also grateful to other professors, as well as the office and technical staff of the Department of Chemical and Biological Engineering at the University of Ottawa. In particular, I thank Louis Tremblay, Franco Ziroldo and Gérard Nina for their technical help.

Third, I thank the National Science and Engineering Research Council of Canada and Omnova Solutions Inc for their financial support.

Fourth, I thank my colleagues for their kind help. Especially, I would like to express my appreciation to Dr. Gabriela Fonseca for her sincere help with experiments, valuable research discussions, as well as her genuine, moral support. Whenever my experiments were running late, she would give me a hand and babysit my daughter.

Lastly, I want to thank my husband Jinsheng Zhou for his encouragement and support.

CHAPTER 1

INTRODUCTION

A pressure sensitive adhesive (PSA) can adhere immediately to a substrate upon application of light pressure.[1] PSAs are viscoelastic, usually polymeric, materials, and their performance is mainly evaluated by three properties: tack, peel strength and shear strength. Tack reflects a PSA's capability to deform and adhere quickly. Peel strength shows its ability to resist removal by peeling. Shear strength measures its ability to resist flow under shear forces and is mostly related to the cohesive strength of the PSA. In general, it is not possible to increase shear strength simultaneously with tack and peel strength. The reason is that in order to increase shear strength, the cohesive strength of the PSAs must be enhanced; however, this will lower the PSA's capability to deform and flow, and accordingly its capability to wet the substrate.

PSAs are used widely in many commonplace articles such as tapes, labels and shoes to high technology products such as electronic parts and controlled drug delivery systems. PSAs can be classified into four categories based on their mode of production: latex-based, solvent-based, hot melt and radiation cured PSAs.[2] Among these PSAs, latex-based and solvent-based PSAs are more widely used. Moreover, lately latex-based PSAs have become dominant in the PSA market due to their environmental compliance and lower production cost. However, in some applications where very large shear strength is needed, latex-based PSAs still cannot compete with solvent-based PSAs. The reason is that in general, latex-based PSAs have much lower cohesive strength and consequently much smaller shear strength, compared with solvent-based PSAs.

It is known that PSA performance is strongly related to its bulk properties (or viscoelastic properties) as well as surface properties such as surface tension and surface smoothness.[3-7] PSA viscoelastic properties can be measured via dynamic mechanical

analysis (DMA) and these properties are controlled by the PSA's polymer properties; for example, the PSA's copolymer composition, glass transition temperature (T_g) as well as its polymer microstructure (i.e., gel content, molecular weight of sol polymers (M_w), molecular weight between cross-linking points (M_c) and molecular weight between entanglement points (M_e)).[8-11] For PSAs with similar bulk properties, increasing their surface tension and smoothness will lead to higher tack and peel strength.[12] In addition, for PSAs with similar surface properties and composition, increasing their gel content will result in larger shear strength but smaller tack and peel strength. Moreover, for similar gel content PSAs with the same composition, the one having a continuous gel network will have a larger cohesive strength and consequently, larger shear strength compared to the one with the discontinuous network.[9-10] Although much research has been done in the past to study the influence of PSAs' polymer microstructure on their performance, most of the work has focused on either latex-based or solvent-based PSAs. To our knowledge, only Tobing et al.[8,9] have systematically studied the polymer microstructure difference between these two kinds of PSAs. They pointed out that the gel network is discrete in latex-based PSAs, but continuous in solvent-based PSAs (see image "a" and "b" of Figure 1.1). The discontinuous gel network endows latex-based PSAs with a lower cohesive strength and accordingly, a lower shear strength.

The polymer microstructure of latex-based PSA films is related to the process for forming these films. Images "b" and "c" of Figure 1.1 provide a good illustration of this process. First, latexes are cast on a backing film (see image b for an example of latex's polymer microstructure). Then, the water in the latexes evaporates and at the same time, some sol polymers of one latex particle will diffuse across the particle boundary. If the

latex polymer microstructure is appropriate (i.e., $M_w > 2M_e$ and $M_c >= M_e$), the diffused sol polymers will entangle with the sol polymer or gel polymers from another particle.[9,10] Meanwhile, the latex particles will deform and the particle boundary will disappear gradually, and finally latex-based PSA films will form (see image c). From image "c" of Figure 1.1, one can see that in latex-based PSA films, the gel is discrete, and the small microgel polymers are connected by the sol polymer chains via entanglement. Actually, this is the best scenario, and in some cases, the microgels cannot entangle. By analysis of the film formation process, one can envisage that the polymer microstructure of latex-based PSA films is directly related to that of their corresponding latexes.

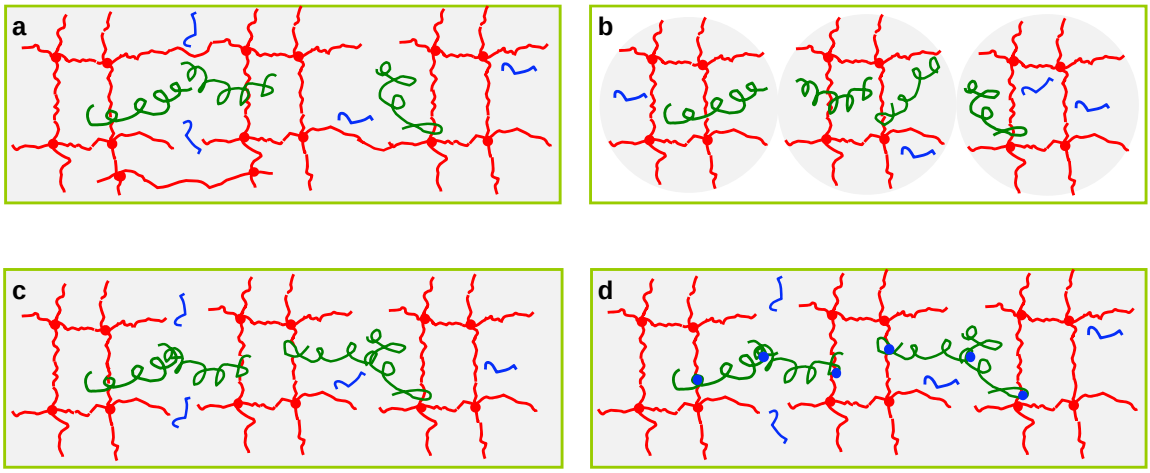

Figure 1.1: Polymer microstructures of PSA films and latex-based PSA film formation process. (a: solvent-based PSA film, b: latex particles, c: latex-based PSA film, d: Post-treated latex-based PSA film.)

(Note: In images a through d, the grids and associated solid dots represent the gel polymers and their cross-link points, respectively; the long curled lines represent sol polymers with size larger than $2M_e$; and the short lines refer to the small sol polymers incapable of entanglement with other sol polymers or gel polymers. The solid dots in image d linking the grids and sol polymers represent newly formed cross-linking points during the post-treatment process for the latex-based PSA films.)

By comparing the polymer microstructures of latex-based and solvent-based PSAs, one can see that in order to improve the performance of latex-based PSAs to the same level as that of solvent-based PSAs, their discrete microgel structure must be changed into a continuous gel network. One possible way to achieve this is to produce latex-based PSA films with functional groups and then post-treat these films. Tobing et al.[9] reported that for gel free latex-based PSAs, if the M_w was larger than $2M_e$, then the sol polymers could entangle with each other; for gel-containing PSAs, if M_c was larger than M_e and M_w was larger than $2M_e$ but smaller than $20M_e$, then the sol polymers could entangle with the microgels. After post-treating these two types of latex-based PSAs under suitable conditions, some of the entanglement points could become cross-linking points if there were functional groups in their vicinity able to react during the post-treatment process. As a result, a continuous gel network could form in the post-treated latex-based PSA films (see image d of Fig. 1), and consequently the shear strength could be greatly increased. The post-treatment method was also used in other studies, but these studies focused on optimizing the functional groups.[13-17] Up to now, even post-treated latex-based PSAs still have a much lower shear strength compared to solvent-based PSAs with similar properties such as gel content, M_c and M_w. Hence, more research is still needed in order to improve the performance of latex-based PSA films.

The present study aimed to improve the performance of latex-based PSA films by controlling their polymer microstructure. By verifying the microstructure of post-treated latex-based PSAs, it was found that although their gel network is continuous, it is not uniform. Weak points often exist around the edges of the original microgels in the treated PSAs if the microgels are not connected by a sufficient number of cross-linking points.

The presence of these weak points can lead to lower cohesive strength of the treated PSA films and accordingly, lower shear strengths for these PSAs. The elimination of these weak points could be accomplished in two steps: (1) Optimize the latex polymer microstructure, so that a sufficient number of sol polymers entangle the microgels in the latex-based PSA films; (2) post-treat the latex-based PSA films with good polymer entanglements under appropriate conditions to ensure that a sufficient number of entanglement points become cross-linking points in the gel network of the treated PSAs.

1.1 Objectives of the Research

The principal objective of this research was to improve the performance of latex-based PSA films. In particular, we sought to improve shear strength at little or no sacrifice to tack and peel strength. To achieve this, the following tasks were established:

(1) Study the influence of chain transfer agent and cross-linker concentration on the polymer microstructure of latexes produced via a seeded semi-batch emulsion polymerization approach.
(2) Study the influence of the polymer microstructure and surface properties of latex-based PSAs on their performance.
(3) Study the influence of polymer microstructure of latex-based PSAs on their viscoelastic properties.
(4) Study the influence of polymer microstructure of latex-based PSAs on the performance of their corresponding post-treated PSAs.

1.2 Structure of the Thesis

The research was accomplished following a systematic plan that contemplated the requirements needed to achieve the main goal of improving the performance of latex-based PSAs by controlling their polymer microstructure. The research was divided into several sections, with each section designed to fulfill one of the tasks outlined above. A schematic diagram of the research methodology is shown in Figure 1.2.

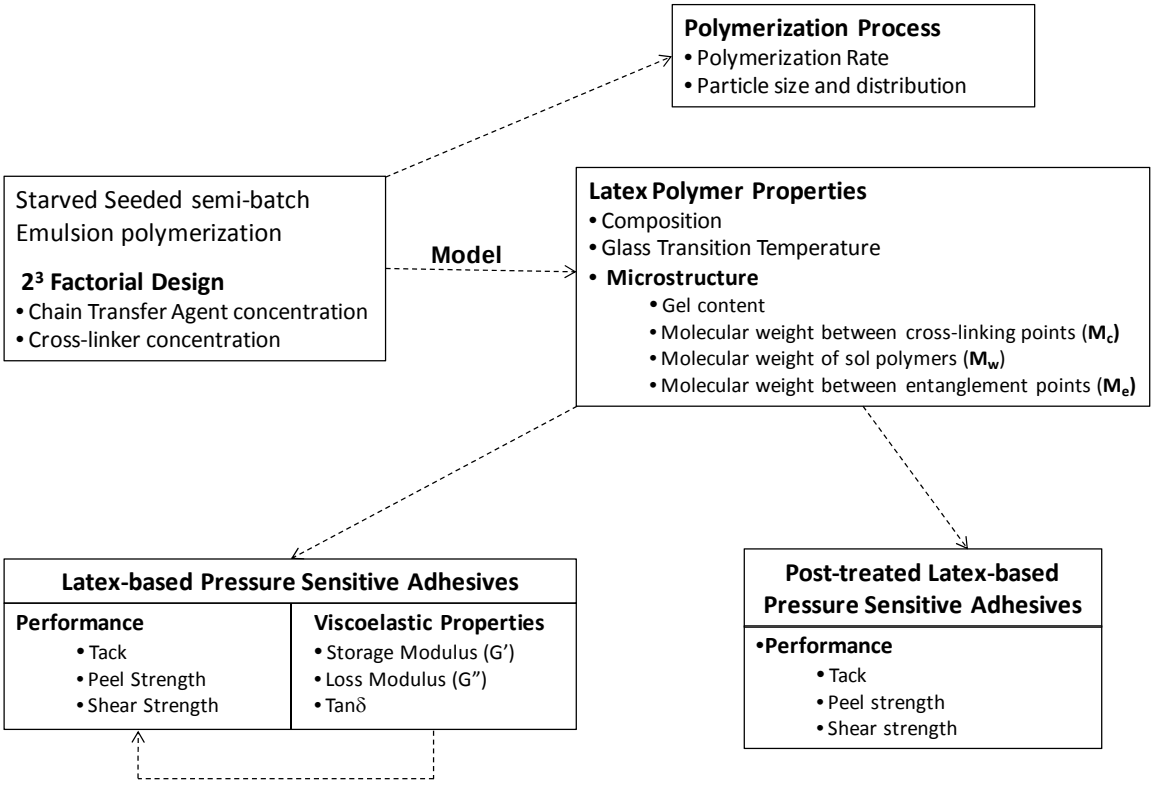

Figure 1.2 Schematic overview of research methodology

The thesis is prepared in a journal article format and includes seven chapters. With the exception of this introductory chapter, the theoretical background chapter (Chapter 2) and the general discussion and conclusion chapter (Chapter 7), each chapter

is associated with a section in the research plan shown in the scheme. In addition, each chapter corresponds to an independent publication that has been or will be submitted to a scientific journal. The details of each chapter are provided below.

Chapter 2: Theoretical Background and Research Methodology

This chapter provides the reader with concise background and fundamental information necessary for understanding the subsequent chapters. It covers the principles of emulsion polymerization as well as information related to PSA performance. This chapter also includes a research methodology section. The section contains detailed information on polymerization and characterization methods, which may not be provided in the following chapters due to the concise nature of journal publications. Citations to thorough reviews are also given for those readers who wish to expand their knowledge on emulsion polymerization and latex-based PSAs.

Chapter 3: Manipulation of Chain Transfer Agent and Cross-linker Concentration to Modify Latex Polymer Microstructure for Pressure Sensitive Adhesives. Qie L., Dubé M. A., European Polymer Journal 2010, 46(6): 1225-1236.

In this chapter are presented the results regarding the influence of CTA and cross-linker concentration on the latexes' polymer microstructure as well as the influence of the latexes' polymer microstructure on the corresponding PSAs' performance. A starved seeded semi-batch emulsion polymerization approach was used to produce butyl acrylate (BA)/methyl methacrylate (MMA) latexes. During the polymerization process, the CTA and cross-linker were added in three ways: (1) only CTA, (2) only cross-linker, (3) both

CTA and cross-linker. The focus was on using both CTA and cross-linker to adjust latex polymer microstructure. A range of BA/MMA latexes with differing polymer microstructures was produced. However, the relationship between polymer microstructure and PSA performance was difficult to establish for PSAs with similar gel content, because almost all of medium and high gel content PSAs showed very low tack and peel strength as well as extremely large shear strength readings.

Chapter 4: The Influence of Butyl Acrylate/Methyl Methacrylate/2-Hydroxy Ethyl Methacrylate/Acrylic Acid Latex Properties on Pressure Sensitive Adhesive Performance, Qie L., Dubé M. A., International Journal of Adhesion and Adhesives 2010, 30(7): 654-664.

This chapter describes our aims to resolve the poor PSA performance of the latexes described in Chapter 3. More specifically, improving the tack and peel strength at no or small sacrifice of the shear strength for medium and high gel content PSAs. For this purpose, the CTA, cross-linker and emulsifier concentrations as well as the monomer mixture composition were manipulated to produce latexes with versatile polymer microstructures and compositions. The influence of the latexes' polymer microstructure and composition on the corresponding PSAs' performance and viscoelasticity were reported.

Chapter 5: Manipulating Latex Polymer Microstructure using Chain Transfer Agent and Cross-linker to Modify PSA Performance and Viscoelasticity. Qie L., Dubé M. A., accepted by Macromolecular Reaction Engineering, in 2010.

The similar gel content BA/AA (acrylic acid)/HEMA (2-hydroxy ethyl methacrylate) latexes were produced via two different techniques and the results of this effort are presented in Chapter 5. One technique was to vary the amount of CTA in the absence of cross-linker, and the other was to use both CTA and cross-linker during a starved, seeded, semi-batch emulsion polymerization process. The polymer microstructures of these latexes were compared. In addition, the influence of the latexes' polymer microstructure on the corresponding PSAs' viscoelastic properties and performance was studied.

Chapter 6: Influence of the Polymer Microstructures of Latex-based Pressure Sensitive Adhesives on the Performance of their Post-treated PSAs. Qie L., Dubé M. A. This chapter will be submitted to the Journal of Applied Polymer Science.

This chapter reports on a study of the influence of the polymer microstructures of BA/AA/HEMA latexes (or their corresponding latex-based PSAs) on the performance of the corresponding post-treated PSAs. More specifically, gel-free or very low gel content latexes were used to study the influence of the amount of very small sol polymers (i.e., size < $2M_e$) in the original PSAs on the performance of the treated PSAs, under the condition that the original PSAs had M_w larger than $2M_e$. For gel-containing latex-based PSAs, the influence of the amount of either very small or very large sol polymers (i.e., size < $2M_e$ or size > $20M_e$) in the original PSAs on the performance of post-treated PSAs was studied under the condition that original PSAs had M_c larger than M_e and also M_w larger than $2M_e$ but smaller than or close to $20M_e$. The possibility of simultaneously increasing the M_c and M_w of the original latex-based PSAs on improving the performance of their corresponding post-treated PSAs was also explored under the condition that the

original PSAs had M_c larger or close to M_e and also M_w larger than $2M_e$ but smaller than $20M_e$ In addition, the treated latex-based PSAs were compared with original latex-based PSAs and solvent-based PSAs, under the condition of similar polymer properties (e.g., gel content, M_w and M_c) with respect to their gel network and PSA performance.

Chapter 7: General Discussion and Conclusions

This final chapter presents a general discussion relating all aspects of the thesis. A summary of several possible ways for achieving this objective is provided.

1.3 References

1. Benedek I., Pressure-sensitive Adhesives and Applications 2004, 2nd Edition, Marcel Dekker Inc., New York.
2. Jovanovic R., Dubé M. A., Journal of Macromolecular Science. Polymer Reviews 2004, C44: 1-51.
3. Deplace F., Carelli C., Mariot S., Journal of Adhesion 2009, 85: 18-54.
4. Lakrout H., Sergot P., Creton C., Journal of Adhesion 1999, 69: 307-359.
5. Qie L., Dubé M. A., International Journal of Adhesion and Adhesives 2010, 30(7): 654-664.
6. Zosel A., Journal of Adhesion 1994, 44: 1-16.
7. Li L., Tirrell M., Korba G. A., Journal of Adhesion 2001, 76: 307-334.
8. Tobing S. D., Klein A., Journal of Applied Polymer Science 2001, 79: 2230-2244.
9. S. D. Tobing, A. Klein, Journal of Applied Polymer Science 2001, 79: 2558-2564.
10. S. D. Tobing, A. Klein, Journal of Applied Polymer Science 2001, 81: 2109-2117.

11. Zosel A., International Journal of Adhesion and Adhesives 1998, 18: 265-271.

12. Yang H. W. H., Journal of Applied Polymer Science 1995, 55: 645-652.

13. Papsin J., George A., Patent No.: US 6281298B1.

14. Kavanagh M. A., Anderson K.S., Erdogan B., Patent No.: US 7652103B2.

15. Krepski L.R., Filiatrault T. D., Mccracken S. D., Patent No.: US 7714076.

16. Filiatrault T. D., Kavanagh M. A., Anderson K. S., Patent No.: US 7652095.

17. Farwaha R., Boutillier D. N., Phan L., Patent No.: US 6541566.

CHAPTER 2

THEORETICAL BACKGROUND

AND RESEARCH METHODOLOGY

This chapter includes two sections. The first section covers the principles of emulsion polymerization as well as the basic knowledge needed to understand PSA performance. The second part provides detailed information about the research methodology employed in this study.

2.1 Theoretical Background

2.1.1 Emulsion polymerization

Emulsion polymerization is a widely used process for producing synthetic latexes. It is a chain growth reaction initiated by free radicals. It has an important feature of heterogeneity: multiple phases (e.g., organic and inorganic phases) exist during the whole polymerization process.[1]

The main ingredients for conducting emulsion polymerization include monomers, water, emulsifier, and water-soluble initiator. In addition, chain transfer agent (CTA) and cross-linker are often used in order to modify the latexes' polymer properties.[1]

Emulsion polymerizations can be carried out in several ways; e.g., via a batch process or a seeded semi-batch process. A schematic diagram of a batch process is shown in Figure 2.1. In the batch process, usually water and emulsifier are first added to the reactor and mixed. The amount of emulsifier equivalent to the critical micelle concentration (CMC) will dissolve in the water, but any amounts beyond the CMC will aggregate and form micelles. Next, monomer (or a monomer mixture) is added. Most of the monomer will form large droplets (e.g., micrometer size) with emulsifier on their

surface to stabilize them. The monomer will partition between the water phase, the monomer droplets and the micelles (e.g., nanometer size) (see image 2-1A). The reactants are heated to the desired temperature and, at that point, water-soluble initiator is added to the reactor. The initiator dissociates in the aqueous phase and forms highly reactive free radicals, which will polymerize the monomer dissolved in water, and thereafter become primary radicals (see image 2-1B). Once these primary radicals reach a size where they become hydrophobic, they will begin to migrate into the monomer-swollen micelles and initiate the polymerization therein. At this point, the "nucleated micelle" is referred to as a growing latex particle containing both monomer and polymer. As the polymerization proceeds, the number of micelles decreases and the number of growing latex particles increases until micelles are no longer present in the reaction mixture. After that, the number of growing latex particles is constant. Under these conditions, the main locus of polymerization is inside the growing latex particles. The monomer from the droplets diffuses into the growing latex particles until the droplets disappear. After that point, the number of latex particles remains constant, but the monomer concentration in the latex particles gradually decreases with time. At the end of the polymerization, essentially all of the monomer inside the latex particles is polymerized (although under a variety of instances, residual monomer may be present). Hence, the final product, latex, consists of polymer particles stabilized with emulsifiers and suspended in water (see image 2-1C).

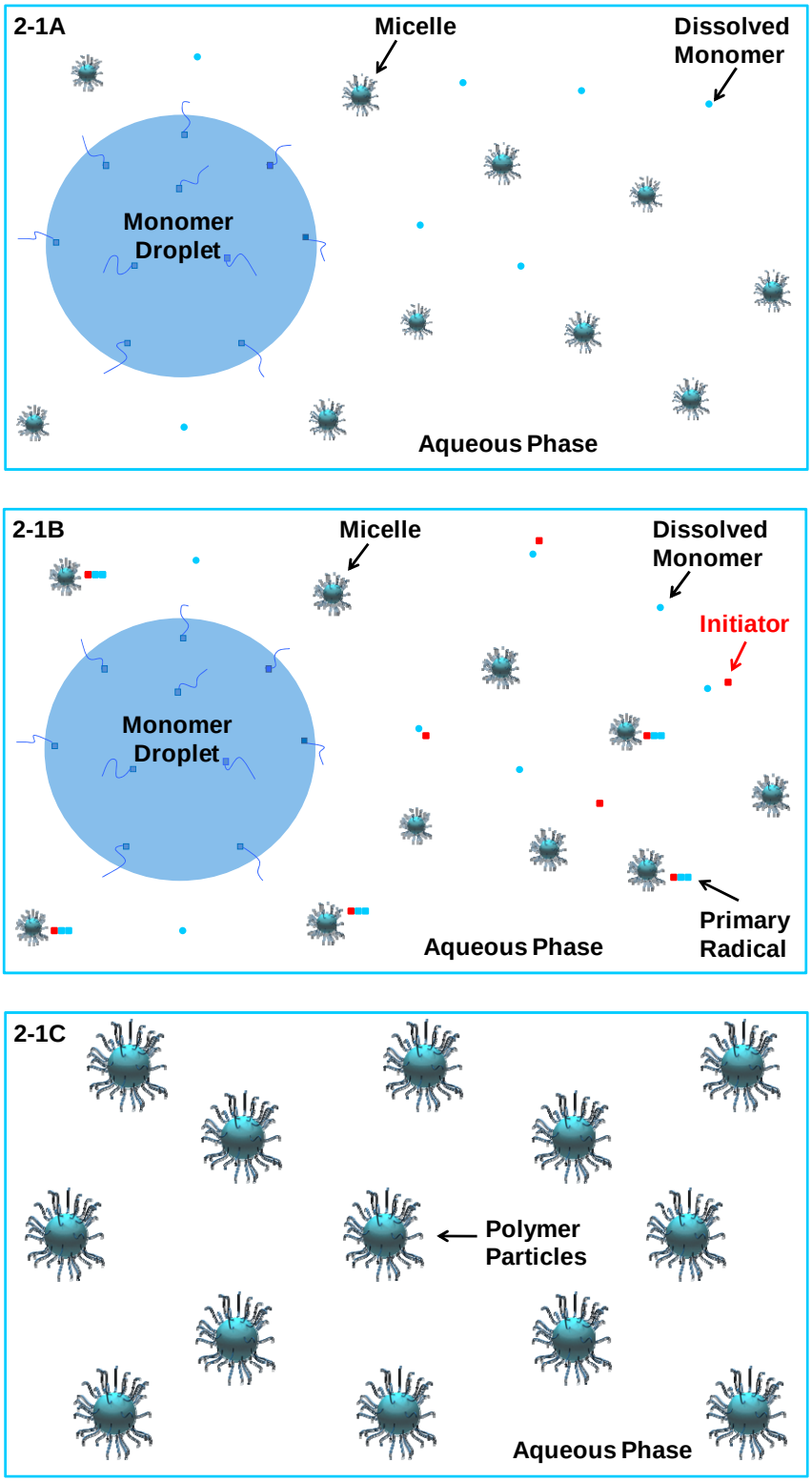

Figure 2.1: Scheme of batch emulsion polymerization process.

It is known that the polymerization rate is associated with the number of latex particles (N), the monomer concentration in the growing particle ([M]) as well as the rate coefficient for propagation (k_P), which depends on both the monomer composition and polymerization temperature (see Equation 2-1[1]).

$$R_P = \frac{k_P[M]\bar{n}N}{N_A} \qquad (2-1)$$

In Equation 2-1, $\bar{n}$ is the average number of radicals per particle, and N_A is Avogadro's number.

The molecular weight of the latex polymer is related to the number of latex particles (N), the rate coefficient for propagation (k_P), and the initiator and monomer concentrations (see Equation 2-2[1]).

$$x_n = \frac{k_P[M]\bar{n}N}{R_I} \qquad (2-2)$$

In Equation 2-2, x_n is the number-average degree of polymerization, which is associated with the size of the latex polymer chains; and R_I is the rate of radical generation, which is related to the initiator concentration as well as the polymerization temperature. (Note: The effect of CTA and cross-linker concentration on the size of the latex polymer chains is not considered in Equation 2-2.)

As mentioned earlier, during batch emulsion polymerization, the monomer concentration in the growing latex particles [M] is not constant for the whole process.

Hence, according to Equations 2-1 and 2-2, one can see that the polymerization rate and the size of the latex polymer chains will drift during the polymerization process. In addition, Equations 2-1 and 2-2 are for batch homo-polymerization. When two monomers are copolymerized, the polymerization rate and number-average degree of polymerization can be described with Equations 2-3 and 2-4.

$$R_P = \frac{(k_{P11}[M_1] + k_{P12}[M_2] + k_{P21}[M_1] + k_{P22}[M_2])\bar{n}N}{N_A} \qquad (2-3)$$

$$x_n = \frac{(k_{P11}[M_1] + k_{P12}[M_2] + k_{P21}[M_1] + k_{P22}[M_2])\bar{n}N}{R_I} \qquad (2-4)$$

where k_{pij} is the propagation rate coefficient for the addition of monomer j to a polymer radical ending in monomer i. $[M_1]$ and $[M_2]$ are the concentrations of monomers 1 and 2, respectively.

With Equation 2-3, one can see that when two monomers with very different polymerization coefficients (k_P) are copolymerized in a batch process, then one monomer will react much faster than the other. As a result, the monomer composition will change during the polymerization process and the latex copolymer will have a heterogeneous composition.

The seeded, semi-batch process was developed to avoid the drift in latex properties as well as in polymerization rate associated with the batch process.[1] In general, a seeded semi-batch process includes three stages: (1) A short batch stage where a small amount of monomer or monomer mixture (i.e., ~5 wt% of the total monomers) are polymerized batch-wise to produce a seed latex with a narrow particle size

distribution; (2) A substantially longer feeding stage during which a monomer emulsion and aqueous initiator solution are often added very slowly to grow the seed latex without generating new particles (Note: Monomer emulsion generally includes monomers, water, emulsifiers, and in some cases CTA and/or cross-linker); (3) A short cook stage to fully react the remaining monomer in the latex particles. From the above description, one can see that almost all of the latex polymers are produced in the feeding stage during a seeded semi-batch emulsion polymerization process. In addition, compared with the batch process, the seeded semi-batch process offers improved latex polymer property control. For example, if a proper polymerization formulation and feeding rates are adopted, then no coagulation between latex particles or formation of secondary latex particles will occur. Hence the number of latex particles (N) will be constant. Meanwhile, if the feeding rates of the monomer emulsion and initiator solution are constant, then the monomer and initiator concentrations in the growing latex particles will be constant during the whole feeding stage. Under this condition (i.e., constant number of latex particles as well as constant monomer and initiator concentrations), the latex polymers produced during the feeding stage will have consistent polymer properties (see Equation 2-4). Moreover, compared with the batch process, seeded semi-batch processes can also offer better control of the latex copolymer composition. For example, if the monomer emulsion and initiator solution are fed slowly enough (i.e., a monomer-starved feed condition), then the fed monomers will be able to react more or less instantaneously. Hence, under this condition, even though monomers with different reactivity are present, the resulting latex copolymer will have a homogeneous composition equal to the composition of the monomer mixture in the monomer emulsion feed. One should keep in

mind that the starved-feed condition results in high polymer concentrations throughout the polymerization and a higher propensity for branching and cross-linking reactions may exist. This is sometimes a desirable property but may also be deleterious to the eventual polymer properties.

Since the seeded semi-batch emulsion polymerization process has so many advantages over the batch process, it is more widely used in industry. In addition, it is also used in this study to produce latexes for making latex-based PSA films.

2.1.2 Control of latexes' polymer microstructure

In a polymer material, the size of polymer chains varies a lot (e.g., from small movable and dissolvable sol polymers to very larger polymer network (or gel polymer)). Polymer microstructure is often used to describe the size and packing of the polymer chains in a polymer material. It covers molecular weight of sol polymers (M_w), gel content and structure, molecular weight between cross-linking points (M_c) and molecular weight between entanglement points (M_e). Polymer microstructure greatly affects the polymer material's bulk properties (or viscoelastic properties) as well as the performance of the final products (e.g., PSAs).[2-16] Hence, in the past, much research has been done on manipulating the latexes' polymer microstructures. The method used including varying initiator, CTA and cross-linker concentrations, initiator and monomer feed rates, monomer composition, and seed properties, during a seeded semi-batch emulsion polymerization process.[17-24]

Among the above mentioned polymerization conditions, CTA and cross-linker concentrations are the two most effective and commonly used factors for tailoring

emulsion polymer microstructural properties. It is well known that adding CTA can decrease M_w in the case of gel-free latex, or in the case of gel-containing latex, decrease gel content.[18,21,25-26] Adding cross-linker can increase gel content, but decrease M_c and M_w.[19] In any of these two cases, it is not possible to manipulate the gel content independently of the M_w. In contrast, the effect of combining CTA and cross-linker is not well studied. Chauvet et al.[22] reported some unique phenomena caused by combining CTA and cross-linker in a seeded semi-batch emulsion polymerization of butyl acrylate (BA) and acrylic acid (AA). They showed how gel content and M_w could be increased simultaneously at the same cross-linker concentration by decreasing the concentration of CTA. However, the latexes produced with both CTA and cross-linker covered a narrow gel content range from 71 to 88%. Kajtna et al.[27] also studied the effect of combining CTA and cross-linker but in a batch suspension polymerization of ethyl-hexyl acrylate and ethyl acrylate. They reported that at the same cross-linker concentration, the addition of CTA could lead to a lower gel content and higher M_w. The trend in M_w is contradictory to what was reported by Chauvet et al. In addition, they found the polymer molecular weight distribution (MWD) of the sol polymer was very broad when CTA and cross-linker were combined; i.e., the polydispersity ranged from 21 to 27. The molecular weight between cross-linking points (M_c), which has a crucial influence on the properties of high gel content polymer, was not reported in either of the above two studies.

Based on the above information regarding manipulating latexes' polymer microstructure, it was decided to use three techniques in this study to produce latexes with versatile polymer microstructure via a seeded semi-batch emulsion polymerization approach. The three techniques were using CTA only, using cross-linker only, as well as

using both CTA and cross-linker. My research focused on studying the polymer microstructures of the latexes produced with the third technique. More specifically, our goal was to study the M_c and M_w change over a broad gel content range for latexes produced by simultaneously using CTA and cross-linker. In addition, the latexes produced with the three different techniques were compared with respect to their polymer microstructures, their corresponding polymer materials' bulk properties (or viscoelastic properties) as well as their corresponding final products' (i.e., PSAs') performance. This way, the better polymer microstructures of latexes for improving the performance of latex-based PSAs could be identified.

2.1.3 Control of the polymer microstructure of latex-based PSAs

Besides controlling the latexes' polymer microstructure, post-treating a latex-based PSA is another effective way to manipulate a PSA's polymer microstructure.[12,13] For example, it is well known that if post-treating gel-containing latex-based PSAs with proper polymer microstructure, their discrete microgel structure can be transformed into a continuous gel network, which can lead to great improvement in the PSA's performance.[12,13] In this study, post-treating latex-based PSAs was also used to modify their polymer microstructure. In addition, the influence of the original PSAs' polymer microstructures on the treated PSAs' polymer microstructures and performance was also studied. Information on how to optimize the polymer microstructures of latex-based PSAs in order to get treated PSAs with better performance is provided.

2.1.4 Pressure sensitive adhesives

Pressure sensitive adhesives (PSAs) are viscoelastic materials. They are permanently tacky and can stick to a substrate even under light, finger pressure. The performance of PSAs is typically evaluated by tack, peel strength and shear strength. Tack reflects the adhesive's capability to deform and adhere quickly. Peel strength refers to its ability to resist removal by peeling. Shear strength is a measure of its ability to resist flow under shear forces.[28]

To achieve desirable performance, commercial PSAs are commonly produced using at least two monomers.[28] One monomer, such as butyl acrylate (BA) and 2-ethyl hexyl acrylate (EHA), will yield a polymer with a low glass transition temperature (T_g) (e.g., <-40°C), and therefore impart good deformability and flow ability to the PSA. In contrast, the other monomer, such as methyl methacrylate (MMA), methacrylic acid (MAA), and acrylic acid (AA), will lead to a polymer with a high T_g (e.g., >100°C), and accordingly endow the PSA with sufficient cohesive strength. In this study, BA/MMA, BA/MMA/HEMA (2-hydroxy ethyl methacrylate), and BA/AA/HEMA were chosen as the monomer systems.

Commercial PSAs are often produced via three techniques: hot-melt techniques, solution polymerization and emulsion polymerization.[29] The first method uses melt copolymer to make PSA films, the second uses polymer organic solutions, and the third one uses latex, which is polymer particles stabilized by emulsifiers and suspended in water. Among these three methods, the emulsion polymerization technique is considered more environmental friendly, since the production and application of latex and latex-based PSA involve water instead of organic solvents. Latex-based PSAs have become

dominant in the PSA market due to their environmental compliance and lower production costs. However, they still cannot replace solvent-based PSAs in some applications where very large shear strength is required, since at similar tack and peel strength, solvent-based PSAs usually have much larger shear strength, compared with latex-based PSAs.[12-13] The better performance of solvent-based PSAs is due to their continuous gel network; in latex-based PSAs, the gel is present as discrete microgels.[12-13] Thus, the performance of latex-based PSAs must be improved in order to expand their range of applications, and the effective way to achieve this is to optimize their polymer microstructure.

It is well known that the PSA performance is related to surface properties as well as bulk properties (or viscoelastic and/or rheological properties).[30-33] For example, increasing a PSA's surface tension and smoothness as well as decreasing the amount of impurity (e.g., emulsifier) on a PSA's surface could lead to higher tack and peel strength. In addition, a PSA's rheological properties in the small strain regime have been characterized with dynamic mechanical analysis (DMA) at small strain (e.g., ~1%). It was found that the larger the storage modulus (G'), the larger the PSA's capability to resist deformation and consequently the larger its shear strength.[34] The peel strength was proportional to the ratio of the loss modulus at the debonding test frequency to the storage modulus at the bonding test frequency (i.e., G"(ω_1)/G'(ω_2)) as shown in Equation 2-5.[35]

$$Peel\ strength \propto \frac{G''(\omega_1)}{G'(\omega_2)} \qquad (2-5)$$

Equation 2-5 was established according to the peel strength test procedure, which involves both a bonding and debonding process. If a PSA's storage modulus at the bonding frequency is smaller, then the PSA can deform and flow more easily, leading to better wetting of the PSA on a substrate during the bonding process and consequently, larger peel strength. If a PSA's loss modulus at the debonding frequency is larger, then the PSA can dissipate more energy during the debonding process. In order to peel such a PSA off the substrate, a larger force will be needed, and therefore the PSA shows larger peel strength.

A PSA's elastic properties have been characterized with a tensile test, which involves a much larger strain scale than for the DMA test and is related to the PSA's peel strength.[35-36] If a PSA experiences a larger strain during the tensile test, then it is very possible that it would form longer fibrils during the debonding processing of a tack and peel strength test. Consequently, it would experience larger strain during the debonding process, dissipate more energy, and therefore exhibit larger tack and peel strength.

A PSA's bulk properties depend on their composition, T_g and polymer microstructure. At similar T_g and polymer microstructure, compared with a PSA with a non-polar group, a PSA with polar groups tends to have larger cohesive strength, due to the larger interaction force between the polymer chains. Consequently, it will exhibit larger shear strength.[28] At similar polymer microstructure, increasing the T_g of a PSA will lead to larger cohesive strength and consequently larger shear strength. The influence of polymer microstructure on a PSA's bulk properties and consequently, its performance, has attracted much more research interest, compared with that of composition and T_g. The reason is that the polymer microstructure is very versatile, and therefore

manipulating a PSA's microstructure is a very effective way to modify its bulk properties and performance.

Hereafter, the effect of polymer microstructure is summarized for PSAs made with polymer generated using traditional methods (i.e., using only CTA, only cross-linker or neither). For gel free or low gel content PSAs, with increasing molecular weight, their cohesive strength will increase while deformability and flow ability will decrease. As a result, their shear strength increases, but tack and peel strength will exhibit a maximum point then decrease (see Figure 2.2). Gel content is usually the dominant factor among all the polymer microstructure properties (e.g., gel content, M_c, M_w and M_e) with respect to their influence on a PSA's bulk properties and performance. In general, increasing gel content tends to increase a PSA's cohesive strength while decreasing their deformability. Consequently, with the increase in gel content, shear strength increases, while tack and peel strength decrease. Prior to our research, latex polymers with similar composition and gel contents, which were generated using traditional methods, were never compared for microstructural properties to those generated with the simultaneous use of CTA and cross-linker. Moreover, the influence of their polymer microstructure on their PSAs' viscoelastic properties and performance have never been studied either.

A PSA's gel structure plays an important role on bulk properties and performance. For example, at similar gel contents, a continuous gel structure will endow a PSA with significantly larger shear strength compared with discrete one possessing a microgel structure.[12-13] In latex-based PSAs, the gel is present as a discrete microgel. Thus, in order to improve their performance, the microgel structure should be transformed into a continuous gel network by post-treating the PSAs. Tobing et al.

showed that the gel structure of treated PSAs depend on the polymer microstructure of the original latex-based PSAs. If a PSA has $M_c \geq M_e$ as well as $2M_e \leq M_w \leq 20M_e$, then its microgels could be converted into a continuous gel network.[12-13] In this study, the influence of polymer molecular weight distribution on the performance of post-treated latex-based PSAs was studied. More specifically, the influence of the presence of a significant amount of very small sol polymers (i.e., $< 2M_e$) or very larger sol polymers (i.e., $> 20M_e$) in the original latex-based PSAs with $M_c \geq M_e$ as well as $2M_e \leq M_w \leq 20M_e$ was investigated.

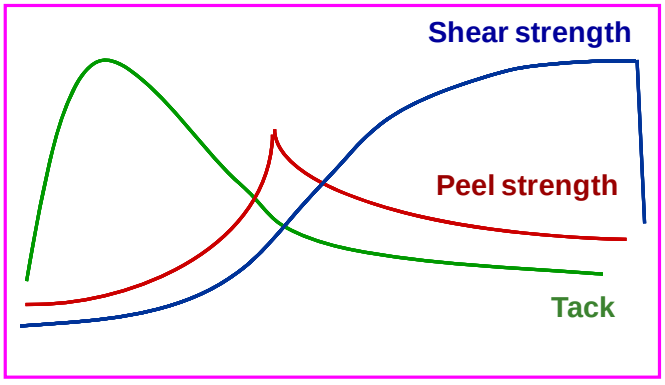

Figure 2.2: Influence of molecular weight on a PSA's performance (ref. 37)

2.2 Research Methodology

2.2.1 Materials

Butyl acrylate (BA), methyl methacrylate (MMA), acrylic acid (AA), 2-hydroxyl methacrylate (HEMA) monomers, allyl methacrylate (AMA) cross-linker, 1-dodecanethiol (NDM) chain transfer agent (CTA), sodium dodecyl sulphate (SDS)

surfactant, sodium bicarbonate ($NaHCO_3$) buffer, potassium persulfate (KPS) initiator and hydroquinone (HQ) inhibitor were all obtained from Sigma Aldrich and were used as supplied. All the above materials were reagent grade except HEMA, which had a purity of 97 wt%. Distilled deionized water (DI-H_2O) was used throughout the study. Ammonia (30 wt% in H_2O for pH control) was obtained from British Drug House. All solvents used in the polymer characterization such as tetrahydrofuran (THF, HPLC grade, EMD Chemicals), toluene (99.8%, Fisher Scientific) and di-iodomethane (99%, Sigma-Aldrich) were also used as supplied by the manufacturer. Nitrogen gas (Linde Canada) was used to purge the reactor. PTFE porous membranes with pore size of 0.2 μm, for use in gel content measurements, were purchased from Cole-Parmer Canada.

2.2.2 Polymer latex preparation

All latexes were produced via a starved seeded semi-batch emulsion polymerization approach. The polymerization process includes three stages. The first stage was a batch seed production step, the second was a continuous stage involving feeding a monomer mixture and initiator stock solution, and the third stage was a batch finishing stage to increase the monomer conversion to completion.

For the initiator stock solution, 0.8996 g KPS was dissolved into 90 g DI-H_2O. The amount of KPS fed to the reaction was 0.26 parts per hundreds parts monomer (phm) for all runs. The monomer emulsion stock solution consisted of 6.7 g SDS dissolved into 89 g DI-H_2O, along with 338.4 g monomer mixture. The composition of the monomer mixture was not the same for all runs. Varying amounts of the chain transfer agent,

NDM, and cross-linker, AMA, were added to the monomer emulsion stock solution prior to the reaction.

A homogeneous aqueous solution containing 202 g DI-H_2O, 0.048 g $NaHCO_3$, and 0.45 g SDS was charged into a one-litre Mettler-Toledo LabMax™ reactor. The stainless steel reaction vessel was equipped with an anchor stirring blade and various feed and sampling ports. The stirring speed was maintained at 250 rpm throughout the runs. The reactor was purged with N_2 and the reactor temperature was increased to 70˚C within 30 min. An initiator solution containing 0.45 g KPS and 15 g DI-H_2O and a monomer mixture containing 12 g monomer mixture were charged to the reactor to form the seed latex. The composition of the monomer mixture was not the same for all runs. The temperature was then raised to 75˚C within 5 min and the seed polymerization was continued for an additional 10 min. At that point, the initiator and monomer emulsion stock solutions were added slowly to the reactor using two separate metering pumps (Model: Prominent gamma G/4b; Prominent Fluid Controls Inc.). The feeding times for the initiator and the monomer emulsion stock solutions were 3.5 and 3.0 h, respectively, for some experiments, or 3 and 2.5 h, respectively, for the others. After the feed was completed, the reaction was allowed to proceed for an additional 50 min to increase monomer conversion. The latex was then cooled to below 30°C, and NH_4OH (30 wt.%) was added to increase the pH to about 3.5 or 5.5 in order to enhance the shelf stability of the latex.

2.2.3 Latex particles characterization

The latexes' particle size and size distribution were measured using a Dynamic Light Scattering (DLS) instrument (Malvern NanoS Zetasizer) with an angle of 176°. One drop of the latex was diluted with 2 mL DI-H_2O in a 4 mL polystyrene cuvette. The reported diameter is an intensity-weighted average particle size. The polydispersity index values (PDI) given by the instrument reflect a narrower distribution with PDI values closer to 0.01. Latexes having a PDI smaller than 0.4 were considered to have a narrow particle size distribution. The detection range of the instrument was 0.6 nm to 6 μm.

2.2.4 Latex solid content

A gravimetric method was used to calculate latex solid content. About 1 g latex was weighed and put in an aluminum dish, then the dish was dried in a fume hood at room temperature for a week and then in an vacuum oven at 30℃ for 2 days to get dry polymers. The solid content (*S*) was calculated with the following equation.

$$S = \frac{W_{DLS}}{W_{LS}} \qquad (2-6)$$

In the above equation, W_{DLS} is the weight of the dry latex sample; W_{LS} is the weight of the latex sample.

2.2.5 Monomer Conversion Characterization

Instantaneous monomer conversion was calculated based on the total amount of monomer added to the reactor up to the sampling time; while overall monomer

conversion was calculated based on the total amount of monomer in the polymerization recipe. The calculation was complicated, and used the information about both the polymerization (i.e., formulation and feeding rate) and latex (i.e., solid content). In the Appendix, the detailed calculation procedure for Run 1 from Chapter 3 is provided. In this chapter, only two basic equations are provided for calculating the monomer conversions as follows:

$$x_{I,t} = \frac{W_{P,t}}{W_{TM,t}} \qquad (2-7)$$

$$x_{O,t} = \frac{W_{P,t}}{W_{TM}} \qquad (2-8)$$

In the above two equations, $x_{I,t}$ and $x_{O,t}$ are the instantaneous and overall monomer conversion at feeding time t, respectively; $W_{P,t}$ is the amount of polymer produced in the reactor up to feeding time t; $W_{TM,\,t}$ is the total amount of monomer added to the reactor up to the sampling time; and W_{TM} is the total amount of monomer in the formulation, which is the same as the total amount of monomer added to the reactor up to the end of polymerization.

2.2.6 Latex polymer characterization

Gel content

For gel content measurement, a modification of the method by Tobing and Klein[14] was used. Around 0.03 g dry polymer was weighed and sealed in a PTFE coated membrane pouch. Then the membrane pouch was immersed into 25 mL THF in a 100 mL glass

bottle. The bottle was then tightly capped and put on a shaker for 24 h. The membrane pouch was then removed and dried in a fume hood until it reached a constant weight. The weight of the remaining dry gel was measured and the gel content was calculated using:

$$gel\ content = \frac{W_{DG}}{W_{DP}} \qquad (2-9)$$

In the above equation, W_{DG} and W_{DP} are the weight of the dry gel and dry polymer, respectively.

Weight- and number-average molecular weight of the sol polymers (M_w and M_n)

The THF solution remaining from the gel content test was concentrated, if necessary, and analyzed for sol polymer molecular weight (i.e., M_w and M_n). The solution was filtered using a 0.45 μm syringe PTFE filter (Pall Corporation) and then analyzed with a Waters Gel Permeation Chromatography (GPC) instrument equipped with a Differential Refractive Index detector, a manual injector and three Waters Styragel columns (HR6, HR4 and HR3) in series. THF was used as the eluent and the flow rate was set at 0.3 mL/min. The internal temperature was set at 37°C. The data were analyzed using Empower 2 software from Waters. The calibration curve included a set of 12 polystyrene standards (EasiCal from Polymer Laboratories) with a range of 162 to 6,035,000 g/mol. In the Mark-Houwink equation ($[\eta] = kM^{\alpha}$), the k and α parameters of the latex copolymers were calculated according to their composition. For example, the Mark-Houwink parameters, K and α, for BA and MMA are 1.1 x 10^{-4} dL/g and 0.708, and 1.28 x 10^{-4} dL/g and 0.690, respectively.[41] If the copolymer composition was BA/MMA

(weight ratio: 90/10), then the K and α would be 1.12 x 10^{-4} dL/g and 0.706. For the copolymer having a very large amount of BA and a small and negligible amount of HEMA and/or AA, the K and α of the copolymer were taken as that of the polyBA.

Measurement of the molecular weight between cross-linking points (M_c)

To measure M_c, a new method was established. About 0.03 g of dry gel polymer was weighed and put in a 15 mL glass vial with a diameter of ~10 mm, and then 10 mL toluene was added. The bottle was then tightly sealed with a plastic cap and put on a shaker for a range of times (0.5, 1, 5 and 20 h). Next, the toluene was removed using a glass pipette, and the solvent-swelled gel was weighed. It was found that the amount of toluene absorbed by the dry gel did not change significantly with swelling time. Thus, the shortest swelling time, 0.5 h, was chosen for future M_c tests. To calculate M_c, the following Equation was used:[14]

$$M_c = \frac{\left\{V_1 \rho_P \left[\phi^{1/2} - \frac{\phi}{2}\right]\right\}}{\{-[ln(1-\phi) + \emptyset + \chi\phi^2]\}} \qquad (2-10)$$

In the above equation, V_1 is the molar volume of toluene, 106.3 cm^3/mol;[14] and ρ_P is the density of copolymer. The density was calculated according to the copolymer composition. For example, given that the density of PBA and PMMA are 1.06 g/cm^3 and 1.19 g/cm^3, respectively,[1] the density of BA/MMA (weight ratio: 90/10) copolymer is 1.073g/cm^3. ϕ is the volume fraction of gel polymer in the swollen gel and can be calculated as:[14]

$$\phi = \frac{W_P \rho_S}{W_P \rho_S + W_S \rho_P} \qquad (2-11)$$

In the above equation, W_P and W_S are the weight fractions of the gel polymer and solvent (toluene) in the swollen gel, respectively. ρ_S and ρ_P are the densities of solvent (0.8669 g/cm^3) and copolymer (1.073 g/cm^3), respectively.[14]

In Equation 2-10, χ is the copolymer and solvent interaction parameter calculated as:[14]

$$\chi = 0.34 + \frac{V_1(\delta_1 - \delta_2)}{RT} \qquad (2-12)$$

δ_1 is the solubility parameter of the copolymer. It was calculated accordingly to the composition of the copolymer. For example, given that the solubility parameters for polyBA and polyMMA are 8.9 and 9.2 (cal/cm^3)$^{1/2}$, respectively, the solubility parameter of BA/MMA (weight ratio: 90/10) copolymer is calculated as 8.93 (cal/cm^3)$^{1/2}$. δ_2 is the solubility parameter for toluene, 8.9 (cal/cm^3)$^{1/2}$.[1,14]

Molecular weight between entanglement points (M_e)

All of the latex copolymer produced in this study had a polydisperse molecular weight distribution. Their molecular weight between entanglement points (M_e or $M_{e,\ polydisperse}$) was calculated with the plasticizer model:[38]

$$M_{e,polydisperse} = \frac{M_{e,monodisperse}}{\phi^{2.3}} \qquad (2-13)$$

$M_{e,monodisperse}$ is the entanglement molecular weight for copolymers with narrow molecular weight distribution, and it can be obtained with the copolymer composition. For example, given that the $M_{e,monodisperse}$ for polyBA and polyMMA are 20773 and 10013 g/mol, respectively,[14,39] the $M_{e,monodisperse}$ for BA/MMA (weight ratio: 90/10) copolymer is calculated as 19697 g/mol. For gel free copolymers, ϕ is the weight percentage of the sol polymers having size larger than $M_{e,monodisperse}$, and this value can be obtained with the molecular weight distribution curve from GPC measurement. For gel containing copolymers, ϕ is the total weight percentage of the sol polymers having size larger than $M_{e,monodisperse}$ and the gel polymers having M_c larger than $M_{e,mondisperse}$.

Glass transition temperature (T_g)

Two methods were used to measure T_g: Differential Scanning Calorimetry (DSC) and dynamic mechanical analysis (DMA), the latter to be described in the DMA test section below. A DSC Model Q1000 from TA Instruments was used. It was equipped with an auto sampler, a refrigerated cooling system and nitrogen as the purge gas. For the measurement, ~0.04 g of dry polymer was weighed into standard DSC hermetic aluminum sample pans. The analysis was performed using a modulated DSC method with modulation amplitude of ±1°C every 60 s. The sample was cooled to -80°C and followed by a heating ramp of 3°C/min until the sample reached 150°C for BA/MMA and BA/MMA/HEMA copolymers or 80°C for BA/AA/HEMA copolymers. The lower

temperature of 80°C was adopted for BA/AA/HEMA copolymers in order to avoid possible reaction between AA and HEMA at high temperature (e.g., >100°C). The T_g was calculated from the inflection point in the Reversed Heat Flow curve using the software provided.

2.2.7 Latex-based PSAs

PSA films preparation

In this study, there were two kinds of latex-based PSA films: the original ones and their post-treated counterparts. To prepare the original PSA films, two steps were taken. First, latexes were coated on a 50 μm thick Mylar sheet with either a 30# or 60# Meyer rod to make PSA films with thicknesses of either ~33 μm or 60 μm. Then, the films were dried and conditioned for 24 h at 23°C and relative humidity of 50% before being tested. To prepare the post-treated PSA films, the conditioned films with thickness of ~33 μm were heated via two steps: (1) heating at 90°C for 10 min in order to remove the remaining water in the PSAs; (2) heating at a higher temperature (e.g., 120 or 126°C) in order to react the carboxyl and hydroxyl groups from AA and HEMA units. The post-treated PSA films were also conditioned for 24 h at 23°C and relative humidity of 50% prior to testing.

Testing the performance of latex-based PSA films

Tack, peel strength and shear strength were measured at 23°C and relative humidity of 50% according to the Pressure Sensitive Tape Council standards PSTC-6, PSTC-1 and PSTC-7, respectively.[40] A Universal Instron tester was used to evaluate loop tack and

peel strength. For tack, a strip of 25.4 mm x 177.8 mm was cut from the film and was formed into a loop with the adhesive side facing outward. Approximately 25.4 mm at both ends of the strip was masked with tape and inserted into the upper grip. The instrument moved the upper grip downward at a speed of 300 m/min until an area of 25.4 mm x 25.4 mm came into contact with the stainless steel substrate mounted into the lower grip. Next, the tester moved the upper grip upwards at the same speed while recording the force needed to de-bond the loop from the substrate. The maximum force per unit length of the contact area necessary to remove the adhesive was reported as loop tack. PSTC-1 Test Method A evaluates peel strength at a peel angle of 180°. A PSA film specimen of 25.4 mm x 304.8 mm was cut. The strip was laminated onto a stainless steel substrate with the help of a 2040 g roll coater. The roll coater was passed through the film front to back twice (i.e., along the length of the film). The dwell time did not exceed one minute. The substrate and the strip were inserted into the grips and the upper grip was set to move upward at a speed of 300 mm/min. The average force per unit length of the contact area required to peel the strip from the substrate was recorded and reported as peel strength. Lastly, PSTC-7 measures shear strength. A specimen of 25.4 mm x 152.4 mm of the film was cut. The strip was laminated onto a stainless steel substrate with a contact area of 25.4 mm x 25.4 mm and then placed in the home-built shear tester using a C-clamp. A 500 g weight was suspended at the end of the strip. The time needed for the PSA films to fall off the testing panel was recorded automatically using Labview™ software as the shear strength. In addition, some PSA films had shear strengths too large to be measured within a practical time period with a contact area of 25.4 mm x 25.4 mm. Hence a

modified method based on PSTC-7 was used to measure the shear strength. In this case, the contact area of the PSA film on the testing panel was 12.7 mm x 12.7 mm.

Measurement of surface tension of PSA films as well as calculation of the chemical interaction energy between the surfaces of PSA films and stainless steel testing panels.

A contact angle method was used to measure the surface tension of the PSA films with VCA Optima contact angle equipment from AST Products Inc. DI water and di-iodomethane were used as the testing liquids with known surface tensions. The surface tension of the PSA film (γ_P) and the chemical interaction energy between the surfaces of the PSA film and stainless steel testing panel (I) were calculated with Equations 2-16 through 2-17:[32]

$$(1 + cos\theta_1)\gamma_1 = 4\left(\frac{\gamma_1^d\gamma_P^d}{\gamma_1^d + \gamma_P^d} + \frac{\gamma_1^p\gamma_P^p}{\gamma_1^P + \gamma_P^p}\right) \qquad (2-14)$$

$$(1 + cos\theta_2)\gamma_2 = 4\left(\frac{\gamma_2^d\gamma_P^d}{\gamma_2^d + \gamma_P^d} + \frac{\gamma_2^p\gamma_P^p}{\gamma_2^P + \gamma_P^p}\right) \qquad (2-15)$$

$$\gamma_P = \gamma_P^d + \gamma_P^p \qquad (2-16)$$

$$I = 2\left(\gamma_P^d\gamma_S^d\right)^{1/2} + 2\left(\gamma_P^p\gamma_S^p\right)^{1/2} \qquad (2-17)$$

In the above Equations, θ_1 and θ_2 were the contact angles measured with water and di-iodomethane (CH_2I_2), respectively; γ_P, γ_P^d and γ_P^p were the PSA film's surface tension,

its dispersion and polar components; γ_1 (72.8 dyne/cm), γ_1^d (22.1 dyne/cm) and γ_1^p (50.7 dyne/cm) are the surface tension of water, its dispersion and polar components, respectively; γ_2 (50.8 dyne/cm), γ_2^d (44.1 dyne/cm) and γ_2^p (6.7 dyne/cm) are surface tension of di-iodomethane, its dispersion and polar components, respectively; γ_S^d (29 dyne/cm) and γ_S^p (15 dyne/cm) are the dispersion and polar component of the surface tension of the stainless steel testing panel.[32] (Note: 1 dyne/cm = 10^{-3} N/m)

Characterization of the surface of PSA films with Atomic Force Microscopy (AFM)

The PSA film surfaces were imaged by AFM in tapping mode using a Multimode Scanning Probe Microscope (Veeco Instruments) and silicon cantilevers (Vistaprobes from NanoScience Instruments). The tip of the cantilever had a pyramidal geometry and the tip radius was 10 nm. The cantilevers had a resonant frequency of 300 kHz with a spring constant of 40 N/m. Height and phase images were taken in air at ambient temperature. The scan speed was 0.9 Hz and the scanned area was about 5 μm x 5 μm.

Measurement of the viscoelastic properties of PSA films

The viscoelastic properties of PSA films were characterized using DMA with a RDA III rheometer (TA Instruments). The geometry used was a pair of parallel plates with diameter of 25 mm, and the PSA sample thickness was 1.8+/-0.2 mm. The PSA samples were prepared as follows: First, a certain amount of latexes were put in home-made silicon release paper dishes (3.5 cm x 3.5 cm). Then, the latexes were dried for 4 weeks to obtain PSA films with constant weight as well as a thickness of about 0.6 mm. Finally,

three of these films were pressed together with the DMA plates to form one PSA sample with a thickness of ~1.8 mm.

The DMA measurements were done in two ways to measure the PSA films' storage modulus (G') and loss modulus (G"): temperature sweep and frequency sweep. Both measurements were done under a compression mode and with a small and constant strain of 1%. The temperature sweep curves were measured by heating the PSA sample from -30 to 180°C (or 150^{o}C) at a rate of 3°C/min and under a shear frequency of 1.591 Hz. The PSA copolymers' T_g could also be obtained via temperature sweep. It is the temperature corresponding to the maximum point of the tanδ curve. The frequency sweep tests were performed in two ways: (1) In order to get a frequency master curve, frequency sweeps were carried out at different temperatures including -35, -23, 0, 23, 50 and 80°C; for each temperature, the frequency sweep data were obtained at 0.05, 0.1, 0.2, 0.5, 1, 2, 5, 10, 20 and 50 Hz. The frequency master curve was built with the 23^{o}C frequency sweep as reference. (2) The frequency sweep tests were performed at 23 and 83°C over a frequency range of about 80 to 0.02 Hz. A frequency master curve was built using the time-temperature superposition method and with the data at 23^{o}C as the reference. It was found that the frequency master curves generated for a PSA film via the above two methods were identical. In addition, compared with the former method, the latter method was easier.

2.3 References

1. Lovell P. A., El-Aasser M. S., Emulsion Polymerization and Emulsion Polymers 1997, John Wiley & Sons, New York.

2. Elizalde O., Vicente M., Leiza J. R., Polymer Reaction Engineering 2002, 10(4): 265-283.
3. Elizalde O., Vicente M., Plessis C., Journal of Coatings Technology and Research 2004, 1(1): 45-51.
4. Gower M. D., Shanks R. A., Macromolecular Chemistry and Physics 2004, 205(16): 2139-2150.
5. Gower M. D., Shanks R. A., Journal of Applied Polymer Science 2004, 93(6): 2909-2917.
6. Gower M. D., Shanks R. A., Macromolecular Chemistry and Physics 2005, 206(10): 1015-1027.
7. Gower M. D., Shanks R. A., Journal of Polymer Science Part B-Polymer Physics 2006, 44(8): 1237-1252.
8. Jovanovic R., McKenna T. F., Dubé M. A., Macromolecular Materials and Engineering 2004, 289(5): 467-474.
9. Jovanovic R., Ouzineb K., McKenna T. F., Dubé M. A., Macromolecular Symposium 2004, 206: 43-56.
10. Jovanovic R., Dubé M. A., Industrial and Engineering Chemistry Research 2005, 44(17): 6668-6675.
11. Jovanovic R., Dubé M. A., The Canadian Journal of Chemical Engineering 2007, 85(3): 341-349.
12. Tobing S. D., Klein A., Sperling L.H., Journal of Applied Polymer Science 2001, 81(9): 2109-2117.

13. Tobing S. D., Klein A., Journal of Applied Polymer Science 2001, 79(14): 2558-2564.
14. Tobing S. D., Klein A., Journal of Applied Polymer Science 2001, 79(12): 2230-2244.
15. Zosel A., Ley G., Macromolecules 1993, 26(9): 2222-2227.
16. Zosel A., International Journal of Adhesion and Adhesives 1998, 18(4): 265-271.
17. Plessis C., Arzamendi G., Leiza J. R., Macromolecules 2000, 33(14): 5041-5047.
18. Plessis C., Arzamendi G., Leiza J. R., Journal of Polymer Science Part A: Polymer Chemistry 2001, 39(7): 1106-1119.
19. Bouvier-Fontes L., Pirri R., Asua J. M., Journal of Polymer Science Part A: Polymer Chemistry 2005, 43(20): 4684-4694.
20. Bouvier-Fontes L., Pirri R., Magnet S, Asua J. M., Macromolecules 2005, 38(7): 2722-2728.
21. Shen H. Z., Zhang J. Y., Liu S. J., Journal of Applied Polymer Science 2008, 107(3): 1793-1802.
22. Chauvet J., Asua J. A., Leiza J. R., Polymer 2005, 46(23): 9555-9561.
23. Elizalde O., Arzamendi G., Leiza J. R., Industrial and Engineering Chemistry Research 2004, 43(23): 7401-7409.
24. Plessis C., Arzamendi G., Agnely M., Journal of Polymer Science Part A: Polymer Chemistry 2002, 40(16): 2878-2883.
25. Barudio I., Guillot J., Fevotte G., Journal of Polymer Science Part A: Polymer Chemistry 1998, 36(1): 157-168.

26. Former C., Castro J., Fellows C. M., Journal of Polymer Science Part A: Polymer Chemistry 2002, 39(20): 3335-3349.
27. Kajtna J., Golob J., Krajnc M., International Journal of Adhesion and Adhesives 2009, 29(2): 186-194.
28. István B., Pressure-Sensitive Adhesives and Applications 2004, Marcel Dekker Inc., New York.
29. Jovanovic R., Dubé M. A., Journal of Macromolecular Science. Polymer Reviews 2004, C44(1): 1-51.
30. Flanigan C. M., Crosby A. J., Shull K. R., Macromolecules 1999, 32(21): 7251-7262.
31. Li L. H., Tirrell M., Korba G. A., Journal of Adhesion 2001, 76(4): 307-334.
32. Yang H. W. H., Chang E. P., Trends in Polymer Science 1997, 5(11): 380-384.
33. Zosel A., Colloid and Polymer Science 1985, 263(7): 541-553.
34. Chang E. P., Journal of Adhesion 1991, 34, 189-200.
35. Deplace F., Carelli C., Mariot S., Journal of Adhesion 2009, 85, 18-54.
36. Lakrout H., Sergot P., Creton C., Journal of Adhesion1999, 69, 307-359.
37. Satas D., Handbook of Pressure Sensitive Adhesive Technology 1989, 2nd Edition, Van Nostrand Reinhold, New York.
38. Wool R. P., Polymer Interfaces, Structure, and Strength 1995, Hanser/Gardner Publications, Cincinnati.
39. Fetters L. J., Lohse D. J., Richter D., Macromolecules 1994, 27(17): 4639-4647.
40. Pressure Sensitive Tape Council, Test Methods for Pressure Sensitive Adhesive Tapes 2004, Northbrook, Illinois.

41. Brandrup J., Immergut E.H., Grulke E.A., Polymer Handbook 1999, 4th Edition, John Wiley & Sons.

CHAPTER 3

MANIPULATION OF CHAIN TRANSFER AGENT AND CROSS-LINKER CONCENTRATION TO MODIFY LATEX POLYMER MICROSTRUCTURE FOR PRESSURE SENSITIVE ADHESIVES

Manipulation of Chain Transfer Agent and Cross-linker Concentration to Modify Latex Polymer Microstructure for Pressure Sensitive Adhesives

Lili Qie and Marc A. Dubé
Department of Chemical and Biological Engineering,
University of Ottawa, 161 Louis Pasteur Pvt., Ottawa, Ontario, Canada K1N 6N5

Abstract

N-dodecyl mercaptan (NDM) chain transfer agent and allyl methacrylate (AMA) cross-linker were used to manipulate latex properties in a starved seeded semi-batch emulsion polymerization of butyl acrylate (BA) and methyl methacrylate (MMA) or with a third monomer, acrylic acid (AA). Latexes with higher gel content and lower sol polymer molecular weight (M_w) were produced by adding only AMA. On the other hand, latexes with lower gel content and M_w were produced by adding only NDM. In addition, at a constant AMA concentration (0.2 phm), the addition of NDM (0.2 phm) decreased gel content, increased molecular weight between cross-linking points (M_c), and decreased M_w. Adding more NDM (to a total of 0.4 phm) further decreased the gel content, while decreasing the tested M_c and increasing M_w. It was also found that using higher concentrations of both AMA and NDM could produce latex with similar gel content, but smaller M_c and M_w, compared to the latex produced at lower concentrations of both NDM and AMA. Regarding the influence of AA, gel content was increased and M_w was significantly decreased with an increase in AA concentration and a decrease in MMA

concentration. The performance of the latexes was evaluated for application as a pressure sensitive adhesive (PSA).

3.1 Introduction

Emulsion polymers are becoming increasingly important due to their environmental compliance.[1] They are widely used in many applications such as pressure sensitive adhesives (PSA),[2] coatings,[3,4] paints and binders. The performance of these products greatly depends on the latex polymer properties such as composition, glass transition temperature (T_g), gel content and structure, molecular weight between cross-linking points (M_c), molecular weight of sol polymers (M_w), and molecular weight between entanglement points (M_e).[5-9]

Acrylic monomers are extensively used to produce latex; usually two or more monomers are copolymerized via a seeded semi-batch approach to provide latexes with desirable properties. With this approach, much research has been performed on manipulating polymer properties by using different reaction conditions such as initiator, chain transfer agent (CTA) and cross-linker concentrations,[10-15] initiator and monomer feed rates,[10] monomer composition,[11,16] seed properties,[17] etc.

Among the above mentioned polymerization conditions, CTA and cross-linker concentrations are the two most effective and commonly used factors for tailoring emulsion polymer micro-structural properties. It is well known that adding CTA can decrease M_w in the case of gel-free latex, or in the case of gel-containing latex, decrease gel content.[11,14,18-19] Adding cross-linker can increase gel content, but decrease M_c and M_w.[12] In any event, it is not possible to manipulate the gel content independently of the

M_w. However, the effect of combining CTA and cross-linker is not well studied.[15,20] Chauvet et al. reported some unique phenomena caused by combining CTA and cross-linker in a seeded semi-batch emulsion polymerization of butyl acrylate (BA) and acrylic acid (AA).[15] They showed how gel content and M_w could be increased simultaneously at the same cross-linker concentration by decreasing the concentration of CTA. However, the latexes produced with both CTA and cross-linker covered a narrow gel content range from 71 to 88%. Kajtna et al. also studied the effect of combining CTA and cross-linker but in a batch suspension polymerization of ethyl-hexyl acrylate and ethyl acrylate.[20] They reported that at the same cross-linker concentration, the addition of CTA could lead to a lower gel content and higher M_w. The trend in M_w is contradictory to what was reported by Chauvet et al.[15] In addition, they found the polymer molecular weight distribution (MWD) of the sol polymer was very broad when CTA and cross-linker were combined; for example, the polydispersity ranged from 21 to 27. The molecular weight between cross-linking points (M_c), which has a crucial influence on the properties of high gel content polymer, was not reported in either study.

In the present study, the combined influence of CTA and cross-linker on various polymer micro-structural properties was studied via starved seeded semi-batch emulsion polymerizations of BA/methyl methacrylate (MMA) and BA/MMA/AA. Our goal was to explore a broad gel content range, measure the M_c, and test bulk polymer properties using dynamic mechanical analysis (DMA) in order to produce latexes with similar gel contents but differing M_c and M_w. The influence of AA on the polymer micro-structural properties was also studied.

The BA/MMA or BA/(MMA + AA) weight ratio was set at 90/10 in order to produce latexes for use as PSAs. PSAs are viscoelastic materials and can stick to a surface even under very light pressure. They are usually polymerized from two or more monomers, one with a low T_g (e.g., BA) to provide tackiness and the other with a high T_g (e.g., MMA and AA) to provide cohesive strength. The performance of PSAs is usually evaluated by tack, peel strength and shear strength. Tack measures how easily a PSA can stick to a substrate, peel strength tests how difficult a PSA can be removed from a substrate by peeling, and shear strength reflects the cohesive strength of the PSA and is defined as the time needed for a PSA to fall from a testing panel under a certain vertical shear force.

Up to now, many studies have been focused on studying the influence of polymer micro-structural properties on PSA performance.[5-9] Armed with a better understanding of the combined effects of CTA and cross-linker on polymer micro-structural properties, in this study, we attempted to relate the PSA performance to these properties.

3.2 Experimental Methods

3.2.1 Materials

The monomers including BA (reagent grade), MMA (reagent grade), AA (reagent grade), and allyl methacrylate (AMA, reagent grade), the chain transfer agent, 1-dodecanethiol (NDM, reagent grade), the surfactant, sodium dodecyl sulphate (SDS, GC grade), the buffer, sodium bicarbonate ($NaHCO_3$), the initiator, potassium persulfate ($K_2S_2O_8$) and the inhibitor hydroquinone (HQ) were obtained from Sigma Aldrich and were used as supplied. Distilled deionized water (DDI-H_2O) was used throughout the study. Ammonia

(30% by weight in H_2O) was obtained from British Drug House. All solvents used in the polymer characterization such as tetrahydrofuran (THF, HPLC grade, EMD Chemicals) and toluene (99.8%, Fisher Scientific), were also used as supplied by the manufacturer. Nitrogen gas (Linde Canada) was used to purge the reactor. PTFE porous membranes with pore size of 0.2 μm, for use in gel content measurements, were purchased from Cole-Parmer Canada.

3.2.2 Latex preparation

All runs were performed as seeded semi-batch emulsion polymerizations in three stages. The first stage was a batch seed production step, the second was a continuous stage involving feeding a monomer mixture and initiator stock solution, and the third stage was a batch finishing stage to increase the monomer conversion to completion.

For the initiator stock solution, 0.8996 g KPS was dissolved into 90 g DDI-H_2O. The amount of KPS fed to the reactor was 0.26 parts per hundreds parts monomer (phm) for all runs. The monomer emulsion stock solution consisted of 6.7 g SDS dissolved into 89 g DDI-H_2O, along with 304.6 g BA and 33.8 g MMA. Varying amounts of the chain transfer agent, NDM, and cross-linker, AMA, were added to the monomer emulsion stock solution prior to the reaction.

To start the polymerization, a homogeneous aqueous solution containing 202 g DDI-H_2O, 0.048 g $NaHCO_3$, and 0.45 g SDS was charged into a one-liter Mettler-Toledo LabMax™ reactor. The stainless steel reaction vessel was equipped with an anchor stirring blade and various feed and sampling ports. The stirring speed was maintained at 250 rpm throughout the runs. The reactor was purged with N_2 and the reactor temperature

was increased to 70 ^{o}C within 30 min. Then an initiator solution containing 0.45 g KPS and 15 g DDI-H_2O and a monomer mixture containing 10.8 g BA and 1.2 g MMA were charged to the reactor to form the seed latex. The temperature was then raised to 75 ^{o}C within 5 min and the seed polymerization was continued for an additional 10 min. At that point, the stock initiator solution and monomer emulsion were added slowly to the reactor using two separate metering pumps (Model: Prominent gamma G/4b; Prominent Fluid Controls Inc.). The feeding times for the initiator and the monomer emulsion stock solutions were 3.5 and 3.0 h, respectively. After the feed was completed, the reaction was allowed to proceed for an additional 50 min to increase monomer conversion. The latex was then cooled to below 30°C, and NH_4OH (30 wt%) was added to increase the pH to about ~3.5 in order to enhance the shelf stability of the latex.

3.2.3 Polymer latex characterization

Particle sizes were measured using a Dynamic Light Scattering (DLS) instrument (Malvern NanoS Zetasizer) with an angle of 176°. One drop of the latex was diluted with 2 mL DDI-H_2O in a 4 mL polystyrene cuvette. The reported diameter is an intensity-weighted average particle size. The polydispersity index values (PDI) given by the instrument reflect a narrower distribution with PDI values closer to 0.01. Latexes having a PDI smaller than 0.4 were considered to have a narrow particle size distribution. The detection range of the instrument was from 0.6 nm to 6 μm.

A standard gravimetric method was used to calculate the monomer conversion to polymer. The calculation was complicated, and used the information of both the polymerization (i.e., formulation and feeding rates) and the latex (i.e., solid content). The

detailed monomer conversion calculation procedure is provided in the Appendix of this thesis. To calculate latex solid content, around 1 g of latex sample was weighed and put in an aluminum dish, then the dish was dried in a fume hood at room temperature and then in an vacuum oven at 30°C for 2 days to remove the unreated monomer and water. The solid content was the weight ratio of the dry latex to wet latex.

For the measurement of gel content, a modification of the method by Tobing and Klein[6] was used. Around 0.03 g dry polymer was weighed and sealed in a PTFE coated membrane pouch. Then the membrane pouch was immersed into 25 mL THF in a 100 mL glass bottle. The bottle was then tightly capped and put on a shaker for 24 h. The membrane pouch was then removed and dried in a fume hood until it reached a constant weight. The weight of the remaining dry gel was taken and the gel content was calculated using:

$$gel\ content = \frac{W_{DG}}{W_{DP}} \qquad (3-1)$$

In the above equation, W_{DG} and W_{DP} are the weight of dry gel and dry polymer, respectively.

The THF solution remaining from the gel content test was concentrated, if necessary, and analyzed for sol polymer molecular weight. The solution was filtered using a 0.45 μm syringe PTFE filter (Pall Corporation) and then analyzed with a Waters Gel Permeation Chromatography (GPC) instrument equipped with a Differential Refractive Index detector, a manual injector and three Waters Styragel columns (HR6, HR4 and HR3) in series. THF was used as the eluent and the flow rate was set at 0.3

mL/min. The internal temperature was set at 37°C. The data were analyzed using Empower 2 software from Waters. The calibration curve included a set of 12 polystyrene standards (EasiCal from Polymer Laboratories) with a range of 162 to 6,035,000 g/mol. The Mark-Houwink parameters, K and α, for BA and MMA are 1.1 x 10^{-4} dL/g and 0.708, and 1.28 x 10^{-4} dL/g and 0.690, respectively.[44]

To measure M_c, a new method was established. About 0.03 g of dry gel polymer was weighed and put in a 15 mL glass vial with a diameter of ~10 mm, and then 10 mL toluene was added. The bottle was then tightly sealed with a plastic cap and put on a shaker for a range of times (0.5 h, 1 h, 5 h and 20 h). Next the toluene was removed using a glass pipette, and the solvent-swelled gel was weighed. It can be seen from Figure 3.1 that the amount of toluene absorbed by the dry gel did not change significantly with swelling time. Thus, the shortest swelling time, 0.5 h, was chosen for future M_c tests. To calculate M_c, the following Equation was used:

$$M_C = \frac{V_1 \rho_P \left[\phi^{1/2} - \frac{\phi}{2}\right]}{-[\ln(1-\phi) + \phi + \chi\phi^2]} \qquad (3-2)$$

where V_1 is the molar volume of toluene, 106.3 cm^3/mol;[6] and ρ_P is the density of polymer (1.06 g/cm^3 and 1.19 g/cm^3 for PBA and PMMA respectively,[1] 1.073g/cm^3 for the BA/MMA (90/10 by weight) copolymer). ϕ is the volume fraction of gel polymer in the swollen gel and can be calculated as follows:

$$\phi = \frac{W_P \rho_S}{W_P \rho_S + W_S \rho_P} \qquad (3-3)$$

where W_p and W_s are the weight fractions of the gel polymer and solvent (toluene) in the swollen gel, respectively. ρ_s and ρ_p are the densities of solvent (0.8669 g/cm^3) and polymer, respectively. In Equation 3-2, χ is the polymer and solvent interaction parameter, and can be calculated as:

$$\chi = 0.34 + \frac{V_1(\delta_1 - \delta_2)}{RT} \qquad (3-4)$$

δ_1 is the solubility parameter of the BA/MMA copolymer. As the solubility parameter value of poly(butyl acrylate (hereafter referred to as PBA) is 8.9 (cal/cm^3)$^{1/2}$,[6] that of poly(methyl methacrylate) (hereafter referred to as PMMA) is 9.2 (cal/cm^3)$^{1/2}$,[1] δ_1 should be 8.93 (cal/cm^3)$^{1/2}$ for the BA/MMA (90/10 by weight) copolymer; and δ_2 is the solubility parameter for toluene, 8.9 (cal/cm^3)$^{1/2}$.[6]

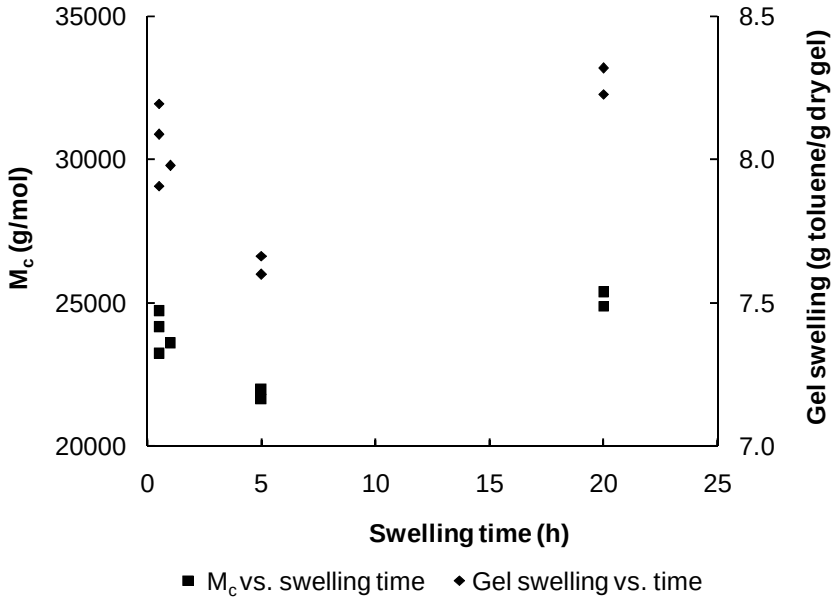

Figure 3.1: Gel swelling and M_c changes with swelling time
(gel samples from latex 8; see Table 3.1)

3.2.4 Glass transition temperature measurement

Two methods were used to test the polymers' glass transition temperatures (T_g): differential scanning calorimetry (DSC) and dynamic mechanical analysis (DMA), the latter to be described in the DMA test section below.

A differential scanning calorimeter (DSC) Model Q1000 from TA Instruments was used. It was equipped with an auto sampler, a refrigerated cooling system and nitrogen as the purge gas. To do the test, about 0.04 g of dry polymer was weighed into standard DSC hermetic aluminum sample pans. The analysis was performed using a modulated DSC method with modulation amplitude of ±1°C every 60 s. The sample was cooled to -80°C and followed by a heating ramp of 3°C/min until the sample reached 150°C. The T_g was calculated from the inflection point in the Reversed Heat Flow curve using the software provided.

3.2.5 PSA performance testing

Tack, peel strength and shear strength were measured according to the Pressure Sensitive Tape Council standards PSTC-6, PSTC-1 and PSTC-7, respectively.[21] The latex was filtered using glass wool and cast onto a 50 um Mylar® sheet with a 30# Meyer rod. The cast film was dried at room temperature and conditioned for 24 h at standard conditions of temperature and humidity (23 ±1°C and 50% ±5 Relative Humidity). A Universal Instron tester was used to evaluate loop tack and peel strength. For tack, a strip of 25.4 mm x 177.8 mm was cut from the film and was formed into a loop with the adhesive side facing outward. Approximately 25.4 mm at both ends of the strip was masked with tape

and inserted into the upper grip. The instrument moved the upper grip downward at a speed of 300 m/min until an area of 25.4 mm x 25.4 mm came into contact with the stainless steel substrate mounted into the lower grip. Next, the tester moved the upper grip upwards at the same speed while recording the force needed to de-bond the loop from the substrate. The maximum force per unit length of the contact area necessary to remove the adhesive was reported as loop tack. PSTC 1 Test Method A evaluates peel strength at a peel angle of 180°. A PSA film specimen of 25.4 mm x 304.8 mm was cut. The strip was laminated onto a stainless steel substrate with the help of a 2040 g roll coater. The roll coater was passed through the film front to back twice (i.e., along the length of the film). The dwell time did not exceed 1 minute. The substrate and the strip were inserted into the grips and the upper grip was set to move upward at a speed of 300 mm/min. The average force per unit length of the contact area required to peel the strip from the substrate was recorded and reported as peel strength. Lastly, PSTC 7 measures shear strength. A specimen of 25.4 mm x 152.4 mm of the film was cut. The strip was laminated onto a stainless steel testing panel with a contact area of 25.4 mm x 25.4 mm, and then placed in the home-built shear tester using a C-clamp. A 500 g weight was suspended at the end of the strip. The time needed for a PSA film to fall off the testing panel was recorded automatically using Labview™ software as its shear strength.

3.2.6 Testing PSAs' viscoelastic properties with dynamic mechanical analysis

The viscoelastic properties of the PSAs were characterized via a RDA III rheometer (TA Instruments) with 25 mm-diameter parallel plate geometry. The sample thickness was 1.7+/-0.2 mm. The DMA measurements were done by heating the sample from -40° C to

150°C at a rate of 3°C/min and under a shear frequency of 1.591 Hz. The T_g was also obtained from the maximum of the tanδ curve.

3.3 Results and Discussion

3.3.1 Experimental design

In this study, BA, MMA, and in some cases, AA, were used as the monomers. For the BA/MMA system, a 3^2 factorial design consisting of 10 runs (1 replicates) with two factors (NDM and AMA concentrations) and three levels (0, 0.2 and 0.4 phm) were carried out (see Table 3.1). (Note: NDM was CTA, and AMA was cross-linker.) For all these runs, the BA/MMA weight ratio was 90/10. An empirical model relating gel content with NDM and AMA concentrations was established. Table 3.1 summarizes the experimental design and final latex properties (i.e., gel content, M_w, M_n, and M_c) for 13 runs, which also includes three additional runs. Run 11 was carried out in order to validate the model's predictive power and also produce a latex with similar gel content as that from Run 1 of the factorial design; Runs 10 and run 12 were performed to expand the range of factorial design. They used 0.5 phm and 0.11 phm NDM, respectively, and resulted in two additional gel-free latexes.

Table 3.1: Experimental design and BA/MMA latex properties
(BA/MMA weight ratio: 90/10)

Latex ID	NDM (phm)	AMA (phm)	Gel content (wt%)	M_w	M_n	M_c	T_g^*
				($x10^{-3}$ g/mol)			(°C)
1	0.40	0.20	40	165	42	13.0	-
2	0.40	0	0	117	35	-	-39.2
3	0	0	64	296	90	65.0	-38.0
3R	0	0	67	291	71	-	-
4	0	0.20	91	107	51	32.3	-38.20
5	0.20	0.20	74	89	28	45.7	-
6	0.40	0.40	75	72	27	38.5	-
7	0.20	0.40	86	86	35	31.7	-
8	0	0.40	96	-	-	24.1	-37.0
9	0.20	0	0	275	54	-	-
10	0.50	0	0	88	35	-	-
11	0.20	0.10	42	230	73	15.5	-
12	0.11	0	0	586	73	-	-

Note: *T_g values in this table were obtained with DSC method.

A second experimental design included AA in the monomer system. A total of 6 runs involving three NDM levels (0, 0.2 and 0.4 phm) and two AA levels (2 and 4 phm) were completed. For all these runs, the total weight of monomer including AA and also the weight ratio of BA to the monomer mixture was fixed at the levels for the initial experimental design: the BA/(MMA+AA) weight ratio was set at 90/10, and the amount of AA was based on the total amount of monomers. The results from these runs are shown in Table 3.2.

Table 3.2: Influence of AA on BA/MMA/AA copolymer properties (BA/(MMA+AA) weight ratio: 90/10)

Latex ID	AA (wt%)	NDM (phm)	Gel content (wt%)	M_w (x10^{-3} g/mol)	M_n (x10^{-3} g/mol)	T_g* (˚C)
13	2	0.40	0	120	34	-38.0
14	4	0.40	0	126	38	-37.5
15	2	0.20	0	305	57	-37.7
16	4	0.20	0	349	68	-36.8
17	2	0	69	267	87	-
18	4	0	72	223	57	-

Note: *T_g values in this table were obtained with DSC method.

3.3.2 Empirical model building

An empirical quadratic model (Model A) was established based on the factorial design from Table 3.1 to relate the gel content (y) of the latexes to the concentrations of NDM (x_1) and AMA (x_2) used in the runs. x_1 and x_2 are the coded values (see Table 3.3), and their relations to the actual concentrations of NDM (X_1) and AMA (X_2) are shown in Equations 3-5 and 3-6. The units of X_1 and X_2 are phm (per hundreds parts of monomers).

$$x_1 = \frac{(X_1 - 0.2)}{0.2} \qquad (3-5)$$

$$x_2 = \frac{(X_2 - 0.2)}{0.2} \qquad (3-6)$$

Table 3.3: Experimental data for developing Model A

Latex ID	x_1	x_2	x_1x_2	x_1^2	x_2^2	y (wt%)
1	1	0	0	1	0	40
2	1	-1	-1	1	1	0
3	-1	-1	1	1	1	64
3R	-1	-1	1	1	1	67
4	-1	0	0	1	0	91
5	0	0	0	0	0	74
6	1	1	1	1	1	75
7	0	1	0	0	1	86
8	-1	1	-1	1	1	96
9	0	-1	0	0	1	0

Model A:

$$y = 0.6263 - 0.2356x_1 + 0.3127x_2 + 0.1209x_1x_2 + 0.0856x_1^2 - 0.1394x_2^2 \quad (3-7)$$

After statistical testing, it was found that Model A (see Equation 3-7) was adequate and also significant at $\alpha = 0.05$, but the coefficients of the last three terms in the model were not significant. Therefore, a simplified model (Model B, Equation 3-8) was developed by removing these terms. Model B was also found to be adequate and significant and was an improvement to Model A.

Model B:

$$y = 0.5893 - 0.2475x_1 + 0.3008x_2 \quad (3-8)$$

Using Model B, a new run (Run 11) was designed in order to produce a latex with gel content similar to the latex from Run 1, but using less cross-linker. The NDM and AMA concentrations for Run 11 were chosen as 0.20 and 0.10 phm, respectively. The gel content of the latex from Run 11 was 42 wt%, which compared well to the predicted gel content of 43.5 wt% using Model B.

3.3.3 Influence of CTA and cross-linker concentrations on latex particle size

During seeded semi-batch emulsion polymerization, secondary nucleation and particle coagulation may occur depending on polymerization conditions. These two phenomena may not only affect the polymerization rate but also the final latex properties such as composition, M_w and gel content.[22] In this study, we wanted to avoid secondary nucleation and particle coagulation, and therefore we monitored the particle growth during the polymerization process. It is known that secondary nucleation can be caused by several factors, but it is in particular, governed by the emulsifier concentration.[23,1] In the event of desorption of radicals from particles due to transfer to CTA reactions, new particles can also be nucleated. Such an effect is uncommon when NDM is used as CTA in the range used in this study.[11,24-25] Elevated levels of cross-linker, well beyond those used in this work, have also been reported to induce secondary particle nucleation.[26] Particle coagulation can be caused by low emulsifier concentrations, and can be influenced by CTA and cross-linker concentrations. Figure 3.2 shows a typical progression in the particle size distribution as demonstrated for Run 1.

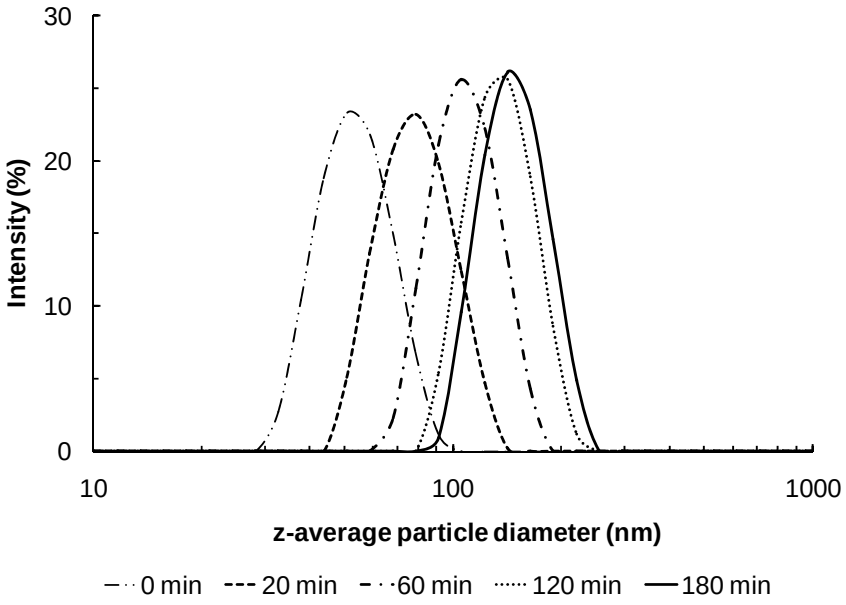

Figure 3.2: Latex particle size and size distribution change during polymerization (Run 1)

From Figure 3.2, we can see that the particle size distributions do not give any indication of secondary nucleation or particle coagulation. The increase in particle size with monomer feeding time (c.f. 20 min, 60 min, 120 min and 180 min) is also evident from the figure. After a reaction time of 180 min, monomer feeding was stopped and only the initiator solution was fed to the reactor until 210 min. At this point, the reaction mixture was allowed to consume the remaining monomer for an additional 50 min. Beyond 180 min, the particle size distribution remained unchanged. This is consistent with the fact that at 180 min, the monomer conversion was already very high and the particle size would not be expected to change further. All of the latexes produced in this study had average particle sizes around 148+/-3 nm and narrow particle size distributions (PDI<0.04). Thus, as expected, the CTA and cross-linker did not affect the number of particles under all of these conditions.

3.3.4 Influence of CTA and cross-linker concentration on monomer conversion

Latex samples withdrawn from the reactor were analyzed gravimetrically to calculate the overall monomer conversion (based on the total amount of monomer in the formulation) and the instantaneous monomer conversion (based on the total amount of monomer added up to the sampling time). The monomer conversion calculation is complicated, and the detailed procedure is provided in the Appendix of this thesis. Basically, the instantaneous and overall monomer conversions were calculated according to Equations 3-9 and 3-10.

$$x_{I,t} = \frac{W_{P,t}}{W_{TM,t}} \qquad (3-9)$$

$$x_{O,t} = \frac{W_{P,t}}{W_{TM}} \qquad (3-10)$$

In the above two equations, $x_{I,t}$ and $x_{O,t}$ are the instantaneous and overall monomer conversion at sampling time t, respectively; $W_{P,t}$ is the amount of polymer produced in the reactor up to sampling time t; $W_{TM,\ t}$ is the total amount of monomer added to the reactor up to the sampling time t; and W_{TM} is the total amount of monomer in the formulation, which is the same as the total amount of monomer added to the reactor up to the end of polymerization.

The instantaneous monomer conversion can be affected by many factors, such as the amounts of initiator and surfactant, monomer to initiator ratio, monomer mixture and initiator solution feeding rates, as well as the CTA and cross-linker concentrations. In this study, all factors, except for the CTA and cross-linker concentrations, were fixed. Figure

3.3 shows the instantaneous and total monomer conversions for Runs 1, 2, 3, 8 and 9, which covers the entire range of CTA and cross-linker concentrations. All runs in our factorial design gave nearly identical conversion profiles. Thus, the CTA and cross-linker concentrations did not appear to influence monomer conversion. This is consistent with the findings of Chauvet et al..[15] From Figure 3.3, it can also be seen that the instantaneous monomer conversion was high (greater than 90 wt%) for a large part of the time, which is typical of monomer-starved conditions, and the final overall monomer conversion was between 99.2 to 99.8 wt%, which gave the latexes a solid content of about 47 wt%. In addition, the instantaneous conversion was seen to slightly increase during the monomer feed period (i.e., from 20 to 180 min). As there was no secondary particle nucleation, as concluded from the particle size measurements, this increase was not caused by secondary nucleation. Rather, as Plessis et al.[11] observed, the growth in particle size likely led to a decrease in the rate of radical exit from the particles, and accordingly, the number of radicals per particle increased, so the instantaneous conversion increased as well.

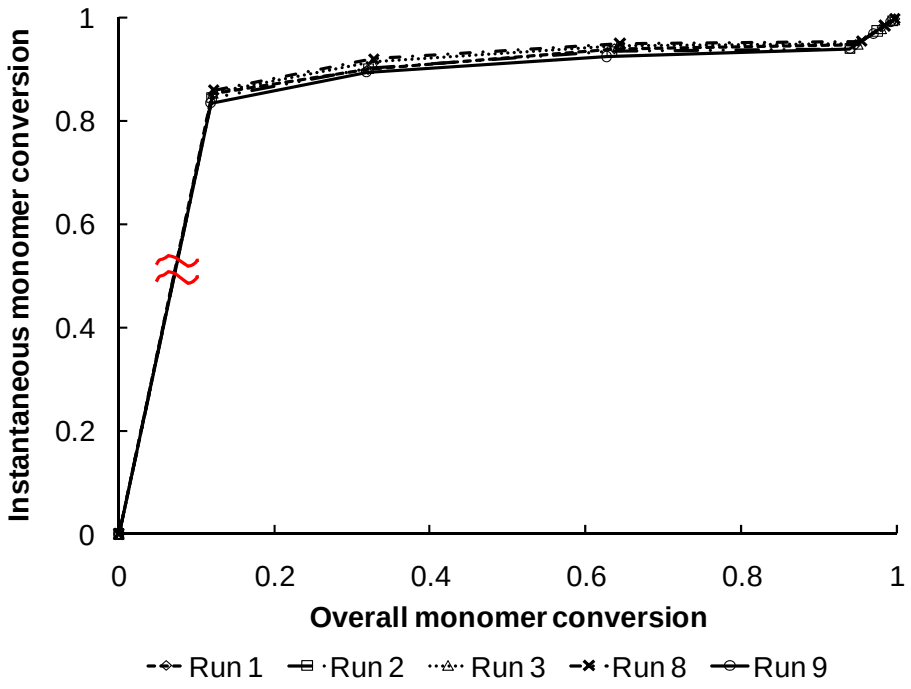

Figure 3.3: Evolution of instantaneous and overall monomer conversion

3.3.5 Latex polymer composition

In a conventional batch polymerization, due to the different monomer reactivity ratios (r_1 = 0.507 and r_2 = 2.375, where 1 represents BA and 2 represents MMA),[27] MMA will tend to polymerize faster thereby resulting in polymer composition drift. So in this study, we used a starved seeded semi-batch approach in order to achieve a homogeneous copolymer composition. The T_g was measured by DSC for several of the latexes. All the DSC results indicated the presence of a single T_g close to that calculated by the Fox Equation.[28] Figure 3.4 gives an example of a DSC thermogram for latexes 2 and 9. Only slight differences in T_g were measured from run to run (38.5+/-1.5°C). DMA measurements provided an even narrower range in T_g (+/-0.25°C). This confirms that the copolymer composition was indeed homogeneous.

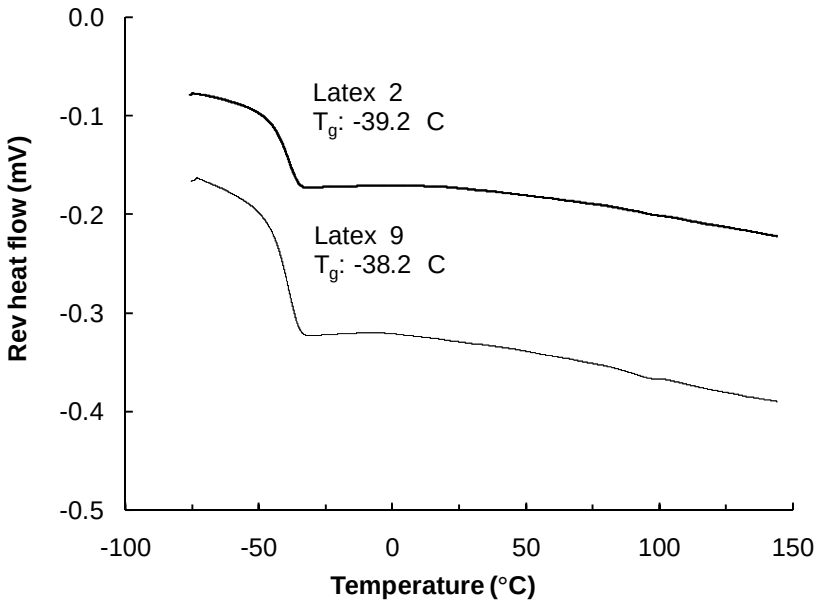

Figure 3.4: DSC thermograms for latex polymers from Run 2 and 9.

3.3. 6 Influence of CTA and cross-linker on polymer latex properties

By comparing latex 3 to latexes 2, 9, 10 and 12 in Table 3.1, it can be seen that adding the CTA (i.e., NDM) decreased the gel content to zero. In addition, with the increase in CTA concentration, M_w greatly decreased for the gel-free latexes. Fully expected, these phenomena resulted from an increase in chain transfer events, and therefore the kinetic chain length was significantly decreased.

By comparing latexes 3, 4 and 8 in Table 3.1, it can be seen that when no CTA was used, the gel content increased with the cross-linker (i.e., AMA) concentration, while the M_c of the gel polymers and the M_w of the sol polymers decreased. This phenomenon is well known for the emulsion polymerization of BA and BA-dominated comonomer systems.[12] When cross-linker was not used, gel formed by either inter- or intra-molecular chain transfer to polymer via back-biting, plus termination by

combination.[10,29] When cross-linker was used, gel also formed via another mechanism, propagation to the pendent double bond of the cross-linker unit in the polymer chain. In this case, the latter mechanism dominated the gel formation.

From Table 3.1, it can be seen that when the same amount of cross-linker (0.2 phm) was used, an increase in CTA concentration from 0 (latex 4) to 0.2 (latex 5) to 0.4 (latex 1) phm resulted in a decrease in gel content from 91 to 74 to 40 wt%, respectively. The tested M_c first increased from 32.3 to 45.7 kg/mol, and then decreased to 13.0 kg/mol. At the same time, the sol polymer molecular, M_w, first decreased from 107 to 89 kg/mol, and finally increased to 165 kg/mol as shown in Figure 3.5. It can be seen in Figure 3.5 that the molecular weight distribution (i.e., MWD) became broader with the increase in CTA concentration. Similar trends were found for latexes 7 and 6 as shown in Table 3.1.

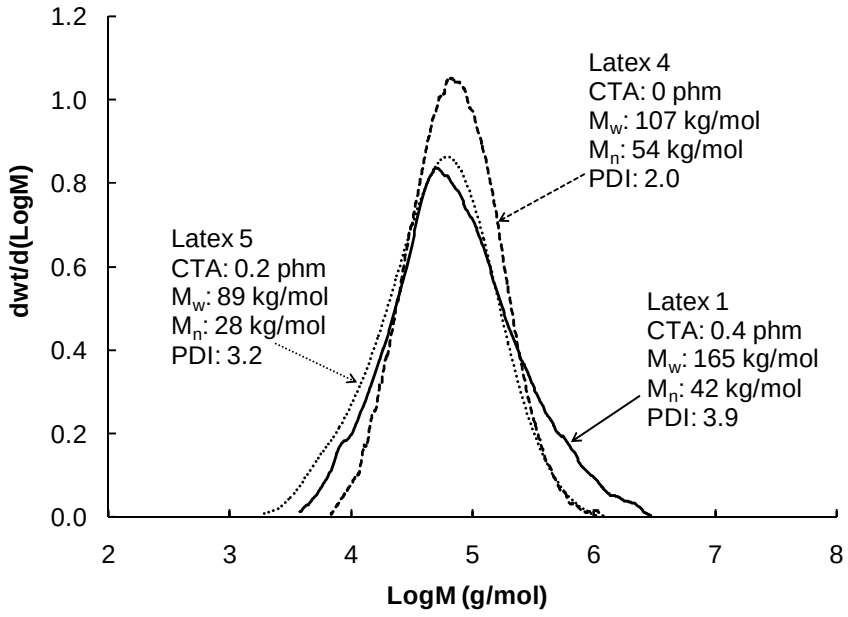

Figure 3.5: M_w change for latex 1, 4 and 5.

The seemingly contradictory changes in M_c and M_w warrant further discussion. Chauvet et al. reported on the evolution of gel content for the emulsion copolymerization of BA and AA under starved seeded semi-batch emulsion polymerization condition (i.e., conditions similar to that in this study).[15] They demonstrated that the gel contents were almost constant for most of the polymerization process (from ~20% overall monomer conversion to almost complete conversion of monomer) and only slightly increased during the cooking period when AMA and NDM were used separately or together. In addition, the gel content was increased by adding AMA. This implies that NDM and AMA can simultaneously affect the latex properties during whole polymerization process even though AMA has two non-symmetric double bonds. Hence, we can divide the polymerization process into two sub-processes: (1) the formation of polymers with kinetic chain length, which are here defined as "primary" polymers; and (2) the further growth of some of the primary polymer chains, either at the labile tertiary hydrogen points of the BA units via chain transfer to polymer (a.k.a. back-biting) or at the pendent double bonds of the cross-linker units. When cross-linker is used, the latter growth mechanism dominates. Larger primary polymer chains have a higher probability to engage in further chain growth; and once their sizes become sufficiently large after further growth, they become gel; otherwise they will remain as sol polymers.

Based on the above mechanism, one can surmise that at constant AMA concentration (0.2 phm), an increase in NDM from 0 to 0.2 phm resulted in the formation of much shorter primary polymer chains, so M_w decreased as expected. At the same time, the gel content decreased because the shortened primary polymer chains decreased the probability for primary polymers to transfer to gel by further growth. Finally, the

formation of a looser gel network was because NDM can also terminate some of the chain growth at the cross-linker points.

When the NDM was further increased to 0.4 phm, the primary polymer chains should become much smaller. As expected, this resulted in a decrease in the gel content, due to the reasons outlined earlier. However, the M_w increased, which contradicted our expectations. It is likely that small primary polymer chains, possessing cross-linker in their backbones, underwent further growth. However, some of these polymers did not reach the size of gel, so they were not gel but rather, highly branched sol polymers. This, in turn, resulted in higher than expected M_w. As for the change in M_c, this was possibly due to the imperfect structure of the gel formed under this condition. The formed gel in this case had many branches and very few cross-linking points, which implies that the actual M_c was very large. The formation of such a gel structure was possible because although chain growth could still occur at the pendent double bond points of the cross-linker, many of growing side chains were terminated by NDM and therefore became branches. The mechanical strength of this kind of gel is very weak, and it could easily break and collapse during swelling. The collapse causes significant solvent loss, which resulted in a lower swelling ratio. Thus, if calculated with Equation 3-2, the M_c would be smaller. In this case, the calculated M_c from the gel swelling model cannot describe the gel structure.

We can further confirm the explained M_w change by comparing latex 1 to latex 2. Latex 1 was produced with 0.4 phm CTA and 0.2 phm cross-linker; in contrast, latex 2 was produced with the same amount of CTA as that for latex 1, but without cross-linker. When no CTA was used, with the addition of cross-linker, we would expect the gel

content to increase, but M_w to decrease. However, by comparing latex 1 to 2, one can see that when 0.4 phm CTA was used, with the addition of 0.2 phm cross-linker, the gel content increased from 0 to 40%, and the M_w significantly increased too from 117 to 165 kg/mol. This is because at 0.4 phm CTA (i.e., NDM), the average chain length of the primary polymer were very small, so after further growth at the cross-linker points, some of them became gel and the others became branched sol polymers with larger molecular weight.

By comparing latex 5 with 6, and latex 1 with 11 (see Table 3.1), we can see that latexes with similar gel contents but different M_c and M_w could be produced by simultaneously increasing the concentration of CTA and cross-linker. At higher levels, the M_w and M_c were significantly lower, as shown in Figure 3.6 and Table 3.1. (Note: As we mentioned earlier, the tested M_c could not describe the gel structure for latex 1 and here, also for latex 11 due to its imperfect gel structure. Therefore, here we only compared the M_c of latexes 5 and 6).

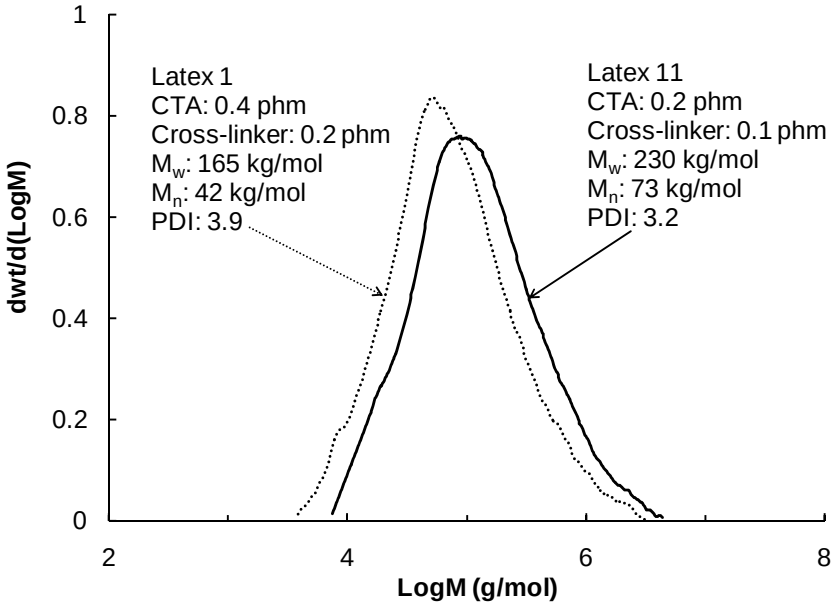

Figure 3.6: M_w of latexes with similar gel content (40 wt%)

The polymer property changes can also be explained via the polymerization process analysis mentioned earlier. At higher levels of NDM, the chain length of the primary polymer would be smaller, and correspondingly the M_w will be smaller; at higher levels of AMA, there would be more cross-linking points, so the M_c became smaller. Moreover, as the effect of increase CTA concentration on gel content can counterbalance that of increase cross-linker concentration, so the gel content could stay unchanged.

From the above results, we can see that to achieve similar gel contents with different M_w, and also very different M_c, we require latexes at fairly high gel contents (~70 wt%). In addition, in order to study the influence of M_c and M_w on polymer mechanical properties, it is better to make the difference in M_c and M_w more significant.

3.3.7 Influence of AA on BA/MMA/AA latex polymer properties

To study the influence of AA on latex polymer properties, we compared latexes from Table 3.1 to those in Table 3.2; specifically latex 2 with latexes 13 and 14, latex 9 with latexes 15 and 16, and latex 3 with latexes 17 and 18. We can see that changing the BA/MMM/AA weight ratio from 90/10/0 to 90/8/2 to 90/6/4, at 0.4 and 0.2 phm NDM, the gel content was 0 while the M_w and T_g slightly increased. At 0 phm NDM, the gel content slightly increased, and M_w decreased. The increase in gel content and decrease in M_w with the increase in AA concentration and decrease of MMA concentration was likely caused by an increase in back-biting reactions. It is known that when MMA copolymerizes with BA, it can decrease back-biting by lowering the rate of formation of six-membered transition rings, and therefore chain transfer to polymer is greatly lowered

and accordingly, leads to a lower gel content.[30] As the pendent group of AA is much smaller than that of MMA, it is likely that AA would not decrease back-biting as much as MMA. In addition, as AA has tertiary hydrogen similar as BA, increase the concentration of AA while decreasing that of MMA and keeping that of BA constant will also enhance inter-molecular chain transfer by backbiting, and accordingly, increase the gel content. Therefore, the gel content was increased with the increase in AA concentration and decrease in MMA concentration. Furthermore, as the pH of the reaction mixture was around 2.5 for all runs, and also the pKa of AA and poly(acrylic acid) are about 4,[31-32] it is unlikely that AA or poly(acrylic acid) underwent dissociation during the polymerization and caused the gel content and M_w changes.

3.3.8 Bulk properties of PSA film made from latexes 1 and 11 (hereafter referred to as PSAs 1 and 11)

DMA temperature sweep curves for PSA1 and 11, which have similar gel contents of ~40 wt%, are shown in Figures 3.7 and 3.8. Figures 3.7 and 3.8 show that the storage (G') and loss (G") moduli of these two PSAs were similar at temperatures below 10°C; and as the temperature increased, the G' and G" of PSA 11 became much larger than those of PSA 1. The significant increases in G' and G" were consistent with the much larger M_w for latex 11. The modulus increase also indicates that at high temperatures, PSA11 had a much higher cohesive strength than PSA1. In this study, we did not report the DMA data for the PSAs made from 17 and 18, which had similar gel contents of ~75 wt%, as the moduli of these two PSAs were beyond the testing limit of our DMA instrument, especially at the low temperature range.

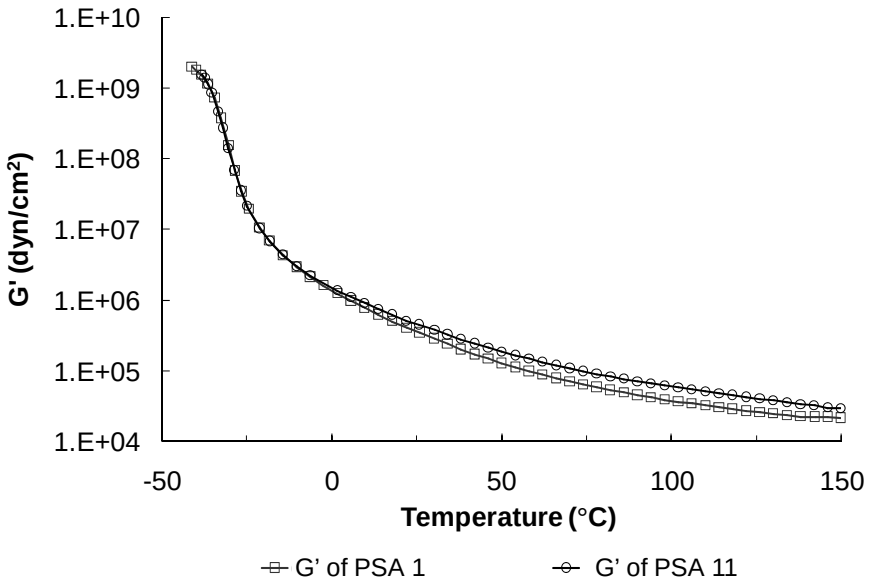

Figure 3.7: Storage modulus (G') of PSA 1 and 11.

(Note: 1 dyne/cm^2 = 0.1 Pa)

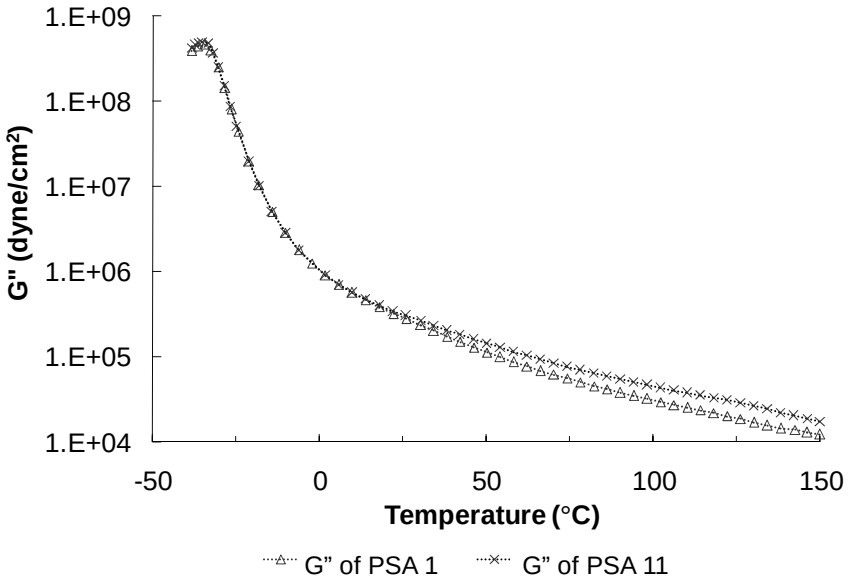

Figure 3.8: Loss modulus (G") of PSA 1 and 11.

3.3.9 PSA Performance

Henceforward the PSAs will be named after their latexes ID for the purpose of simplification. For example, the PSA made from latex 1 was referred to as PSA1.

Table 3.4 shows the M_w and M_e values for the BA/MMA gel-free latexes, and Figure 3.9 shows the performance of the PSA films made from these latexes.

Table 3.4: Polymer properties of gel-free BA/MMA latexes

Latex ID	NDM (phm)	M_w	M_n	M_e	M_w/M_e
		($x10^{-3}$ g/mol)			
10	0.50	88	35	23.7	3.7
2	0.40	117	35	22.6	5.2
9	0.20	275	54	21.2	13.0
12	0.11	586	73	21.3	27.5

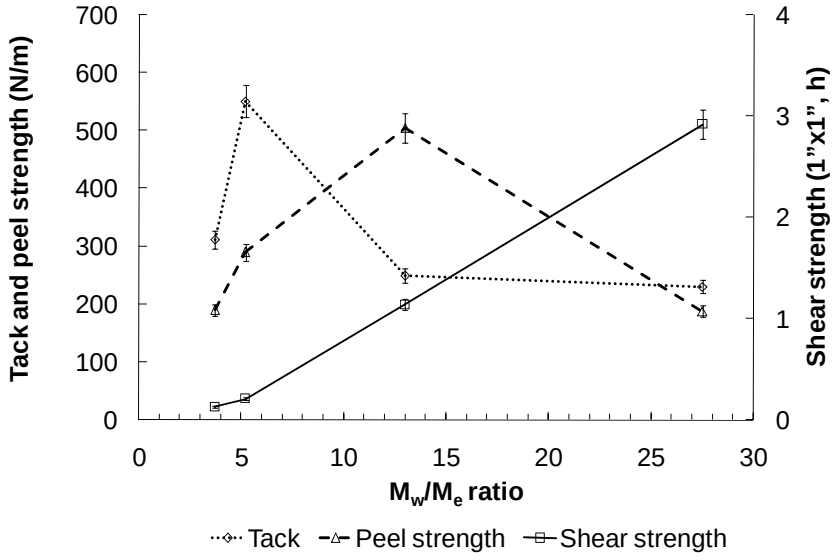

Figure 3.9: The performance of gel-free BA/MMA PSAs vs. their M_w/M_e ratio.

The values of M_e in Table 3.4 were obtained as follows: (1) Calculate the M_e of monodisperse copolymer of BA/MMA with weight ratio of 90/10 with Equation 3-11.

$$M_{e,copolymer,monodisperse} = W_{PBA} \times M_{e,monodisperse\ PBA} + W_{PMMA} \times M_{e,monodisperse\ PMMA} \quad (3-11)$$

where the M_e of monodisperse poly(butyl acrylate) (referred to as PBA) is 20773 g/moL,[6] M_e of monodisperse poly(methyl methacrylate) (referred to as PMMA) is about 10013 g/mol,[33] so

$$M_{e,copolymer,monodisperse} = 0.9 \times 20773 + 0.1 + 10013 = 19697 \frac{g}{mol} \quad (3-12)$$

(2) Calculate the M_e for our polydisperse polymers using the following plastic model: [34]

$$M_{e,polydisperse} = \frac{M_{e,monodisperse}}{\phi^{2.3}} \quad (3-13)$$

where ϕ is the weight fraction of polymer chains having size greater than the M_e of the monodisperse sample, and its values can be obtained with the sol polymer molecular distribution curves measured with GPC.

Figure 3.9 shows that tack greatly increased when the M_w/M_e ratio increased from 3.7 to 5.2, then greatly decreased when the M_w/M_e ratio changed to 13.0 and 27.5. Peel strength greatly increased when the M_w/M_e ratio increased from 3.7 to 5.2 to 13.0, and

then greatly decreased when the M_w/M_e further increased to 27.5. Shear strength increased with M_w/M_e. The change in PSA performance can be explained as follows. For gel-free PSAs, with the increase in M_w or M_w/M_e ratio, the deformability of the PSA would decrease, and at the same time, the cohesive strength would increase. As shear strength is mainly related to the cohesive strength of the PSA, it increased with the increase in the M_w/M_e ratio. As for tack and peel strength, it is known that their tests involve both a bonding and debonding procedure.[9,35-38] For a PSA film to have high tack and peel strength, it must stick well to the testing panel during the bonding process via deformation and flow, and also dissipate a lot of energy during the debonding process. Accordingly to Zosel, only when M_e is larger than 10 kg/mol, can fibrils be formed during the debonding process and therefore dissipate a significant amount of energy [9]. In addition, Lackout et al. reported that when M_w was low, fibrils only formed in the lateral direction during debonding, and in this case, only a small amount of energy was dissipated; however, with the growth in M_w, fibrils formed not only in this direction but also in the elongation direction, so in this case, a lot of energy was dissipated [39]. Based on this, it is likely that at a certain M_w/M_e ratio, an optimum condition can be reached under which the PSA film could adhere well to the testing panel during bonding and also a lot of energy could be dissipated during debonding. In Figure 3.9, one can see that the maximum tack occurred at a lower M_w/M_e ratio than the maximum peel strength. This is because the loop tack test uses a shorter bonding time and smaller contact force than the peel strength test. Therefore, in order to bond well during the loop tack test, the PSA must deform and flow better, which corresponds to a lower M_w/M_e value.

Given the information displayed in Figure 3.9 and the analysis regarding the deformability and cohesive strength of PSAs, we can conclude that any PSA having lower cohesive strength than that of PSA10 would give lower tack, peel strength and shear strength than those of PSA10. This was confirmed with a PSA reported by Tobing and Klein, which we named PSA10TK.[6] The M_w and M_e of PSA10TK were 97 and 24 kg/mol respectively, which are very similar to that of our PSA10. But PSA10TK was produced using BA/AA (97.5/2.5) and its T_g was ~-50°C, which was much lower than that of PSA10 (~-38°C). Therefore, the cohesive strength of PSA10TK should be much lower than that of PSA10. Figure 3.10 shows that PSA10TK did have lower tack, peel strength and shear strength than PSA 10. One should note that the shear strength of PSA10TK was reported to be "<< 0.1 min" with a contacting area of 1/2"x1/2". In this study, all the shear strength measurements were completed with a contact area of 1"x1", so the reported shear strength of PSA10TK was converted to a corresponding value at 1"x1" contact area using the following Equation.[40]

$$T = \frac{L^2 W \eta}{2tMg} \qquad (3-14)$$

where T is the shear strength, L is the length of contact area between PSA and testing panel, W is the width of the contact area, η is the zero shear viscosity of the PSA, t is the thickness of the PSA film, M is load for testing shear strength and g is the gravitational constant. When converting the shear strength from 1/2"x1/2" to 1"x1" using Equation 3-14, only L and W doubled, and all the other factors remained unchanged, so the shear strength at 1"x1" should be:

$$T_{1"\times1"} = 2^2 \times 2 \times T_{1/2"\times1/2"} \ll 8 \times 0.1min = 0.8\,\text{min} \qquad (3-15)$$

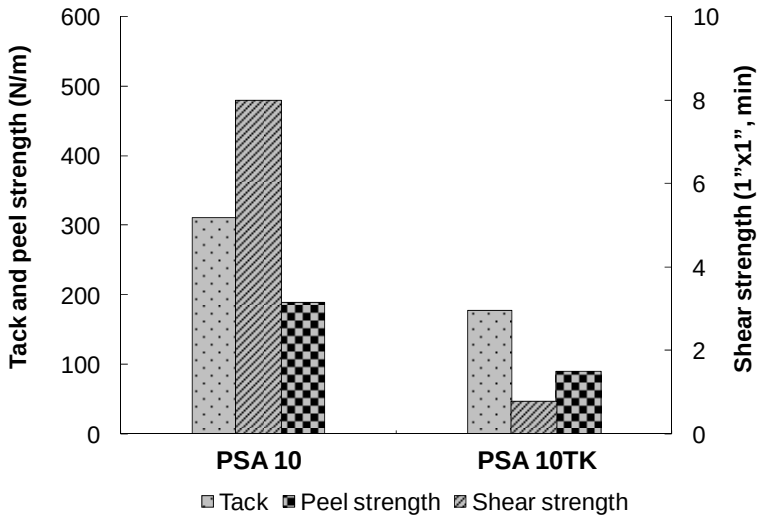

Figure 3.10: Performance of PSAs 10 and 10TK.

Figures 3.11 and 3.12 describe the influence of AA on the performance PSAs made from latexes produced with 0.4 and 0.2 phm NDM, respectively. (Note: PSA 2, 13 and 14 correspond to 0.4 phm NDM; and PSA 9, 15 and 16 correspond to 0.2 phm NDM) Figure 3.11 shows a decrease in tack and increases in peel strength and shear strength with increases in AA concentration. This behavior can best be explained by considering the PSA performance changes with M_w/M_e as shown in Figure 3.9. PSA 2, 13 and 14 had similar M_w of 117, 120 and 126 kg/mol, respectively; this places these PSAs in the M_w range between PSA 2 (i.e., M_w/M_e = 5.2) and the PSA 9 (i.e., M_w/M_e = 13) on Figure 3.9. According to Figure 3.11, the effect of increasing AA concentration resulted in the same PSA performance trend (i.e., decrease in tack, but increase in peel strength and shear strength) as in Figure 3.9 where the M_w/M_e ratio increased from 5.2 (PSA2) to 13.0

(PSA9). The AA concentration effect is due to the formation of strong hydrogen bonds, which increase the cohesive strength of the PSA. This is similar as the effect of increasing M_w/M_e on the cohesive strength of the BA/MMA PSAs. The PSA performance shown in Figure 3.12 differs from that in Figure 3.11 only with respect to the peel strength. The peel strength decreased with increasing AA concentration in Figure 3.12. This effect is also due to the formation of hydrogen bonds with AA, but as the M_w of PSA 9, 15 and 16 were 275, 305 and 349 kg/mol, respectively, this places these PSAs in the range of M_w/M_e ratio from 13.0 (PSA9) to 27.5 (PSA 12) (see Figure 3.9). Thus, with the increase in AA concentration (i.e., from PSA9 to 15 to 16), the peel strength decreased, which is the same trend as when increasing the M_w/M_e for BA/MMA PSAs in the range of 13.0 (PSA 9) to 27.5 (PSA 12) as shown in Figure 3.9.

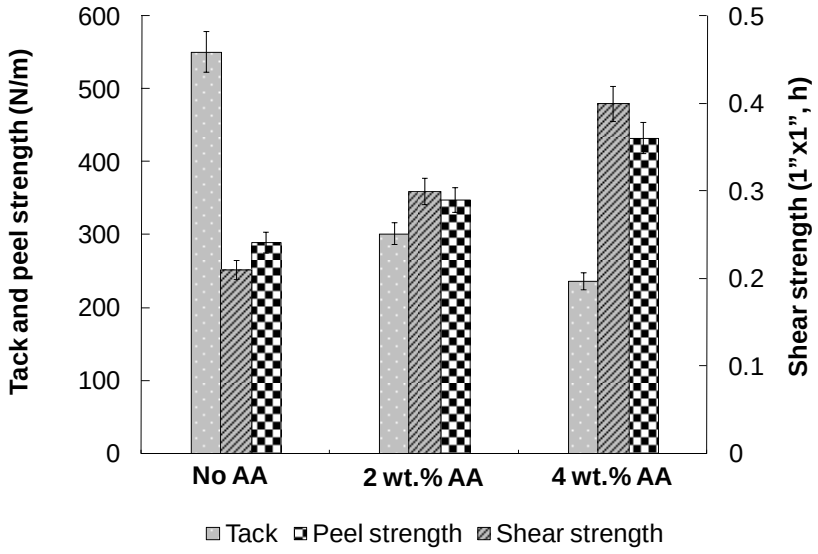

Figure 3.11: Influence of AA concentration on PSA performance at a CTA concentration of 0.4 phm.

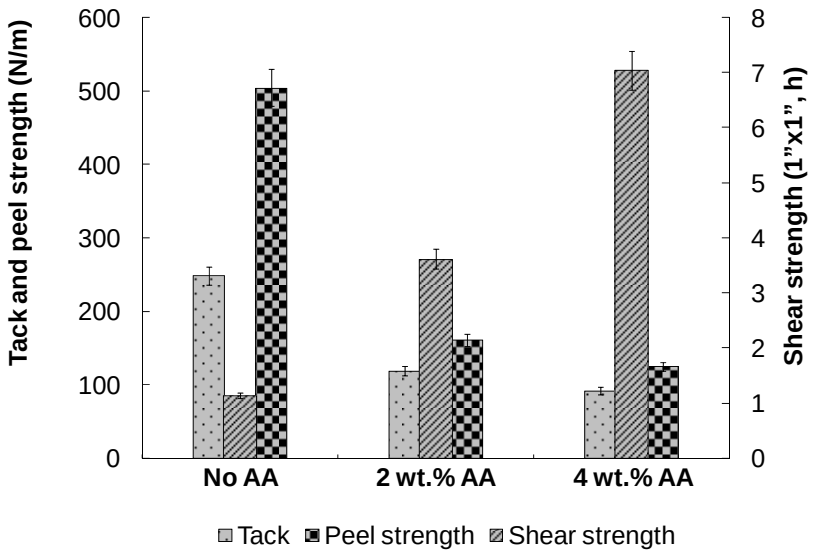

Figure 3.12: Influence of AA concentration on PSA performance at a CTA concentration of 0.2 phm.

Table 3.5 shows the performance of PSAs made from the gel-containing latexes produced in this study. Combining the polymer property data from Table 3.1 with the PSA performance data from Table 3.5, a number of observations can be made. First, comparing the PSAs made from latexes 3, 4 and 8 (NDM concentration = 0; AMA concentration = 0, 0.2 and 0.4 phm, respectively), we can see that with the increase in gel content, the shear strength greatly increased, and tack and peel strength slightly decreased. This is due to the increase in gel content which served to increase the cohesive strength of the PSA. It should be noted, however, that the elevated gel contents of PSA 4 and PSA 8 at a T_g of ~-38 °C made them impractical for use as PSAs. Second, comparing the PSAs produced from latexes 4, 5 and 1 (AMA concentration = 0.2 phm; NDM concentration = 0, 0.2 and 0.4 phm, respectively), we observed that an increase in gel content resulted in an increase in shear strength and a decrease in tack and peel strength.

The polymer materials from latexes 4 and 5 cannot be used as PSAs due to their high gel contents at a T_g of about -38°C. In the above mentioned two cases, the influence of gel content on PSA performance overshadows any effects due to M_w or M_c. Thus, to study the influence of M_c and M_w on PSA performance, it will be necessary to study PSAs with similar gel contents. Finally, comparing PSAs with similar gel contents and similar M_c, those from latexes 1 and 11, we observe a slight decrease in tack and peel strength and a significant increase in shear strength with an increase in M_w. This is consistent with the change in G' and G" moduli as shown in Figures 3.7 and 3.8 for PSA 1 and 11. These findings concur with the report that the shear strength is related to the modulus at high temperature (127°C), and the bigger the modulus, the larger the shear strength.[41] The fact that the increases in tack and peel strength are small is because tack and peel strength are proportional to the G" at debonding frequency/G' at bonding frequency,[38] and Figure 3.7 and 3.8 clearly show both G' and G" increased with M_w at the same magnitude. Latex 5 has similar gel content as latex 6, but larger M_c and M_w values (see Table 3.1), and from Table 3.5 we can see that the influence of M_c and M_w on PSA performance are not observable. This is because the polymer material from these two latexes no longer satisfied the Dahlquist contact criterion[42] due to combination of high gel content and high T_g. In a future study, we will modify the polymer composition to lower the T_g, and thus be able to use higher gel content latexes as PSAs.

Table 3.5: Performance of gel-containing BA/MMA PSAs

PSA ID	Gel content (wt%)	Tack (N/m)	Peel strength (N/m)	Shear strength
1	40	187	91	4.5 h
11	42	172	80	5.8 h
3	64	61	47	101.6 h
4	91	30	20	> 1 month
5	74	43	29	> 1 month
6	75	38	26	> 1 month
7	86	40	30	> 1 month
8	96	28	15	>1 month

3.4 Conclusions

The combined influence of CTA and cross-linker on various polymer micro-structural properties, such as gel content, M_c and M_w, was studied via starved seeded semi-batch emulsion polymerizations of BA/MMA. We showed that by combining CTA and cross-linker, latex polymers with unique micro-structural properties could be produced. For example: at the same cross-linker concentration, adding CTA led to a latex polymer with lower gel content, higher M_c and lower M_w; adding even more CTA resulted in a latex polymer with highly branched sol polymers having higher M_w and gel polymer with an imperfect network structure. The performance of the PSAs produced from these latexes was greatly affected by the gel content, which overshadowed the effects of M_w and M_c. Outside of PSA applications, these latexes may be very useful for a broad range of uses due to their unique microstructure. For example, these highly branched latex polymers might be added to linear polymers to improve their rheological behavior.[43]

Latexes with similar gel contents were produced by simultaneously increasing the CTA and cross-linker concentrations. At a moderate gel content range (~40 wt%), the latex produced at higher CTA and cross-linker levels had a lower M_w, and a similar M_c, which was due to the imperfect gel structure. The performance of PSA films cast from these latexes correlated well with DMA data. Under similar conditions (i.e., higher CTA and cross-linker levels) but at higher gel contents (~75 wt%), the latex had both a lower M_w and M_c. These higher gel content latex polymers could not be employed as PSAs due to combination of high gel content and high T_g. In addition, all the medium and high gel content PSAs produced in this study showed very low tack and peel strength. This is also due to the high T_g of these polymers. Therefore, the monomer mixture should be modified in future study so as to lower the T_g of the corresponding latex polymers, and accordingly generate adequate PSAs at medium or high gel content.

3.5 Acknowledgements

We thank the Natural Science and Engineering Research Council (NSERC) of Canada and Omnova Solutions Inc. for financial support.

3.6 References

1. Lovell P. A., El-Aasser M. S., Emulsion Polymerization and Emulsion Polymers 1997, New York, John Wiley & Sons.
2. Jovanovic R., Dubé M. A., Journal of Macromolecular Science. Polymer Reviews 2004, C44(1): 1-51.

3. El-Aasser M. S., Tang J. S., Wang X. R., Journal of Coatings Technology 2001, 73: 51-63.
4. Nakayama Y., Progress in Organic Coatings 2004, 51(4): 280-299.
5. Tobing S., Klein A., Sperling L. H., Journal of Applied Polymer Science 2001, 81(9): 2109-2117.
6. Tobing S. D., Klein A., Journal of Applied Polymer Science 2001, 79(12): 2230-2244.
7. Tobing S. D., Klein A., Journal of Applied Polymer Science 2001, 79(14): 2558-2564.
8. Zosel A., Ley G., Macromolecules 1993, 26(9): 2222-2227.
9. Zosel A., International Journal of Adhesion and Adhesives 1998, 18(4): 265-271.
10. Plessis C., Arzamendi G., Leiza J. R., Macromolecules 2000, 33(14): 5041-5047.
11. Plessis C., Arzamendi G., Leiza J. R., Journal of Polymer Science Part A: Polymer Chemistry 2001, 39(7): 1106-1119.
12. Bouvier-Fontes L., Pirri R., Asua J. M., Journal of Polymer Science Part A: Polymer Chemistry 2005, 43(20): 4684-4694.
13. Bouvier-Fontes L., Pirri R., Magnet S., Macromolecules 2005, 38(7): 2722-2728.
14. Shen H. Z., Zhang J. Y., Liu S. J., Journal of Applied Polymer Science 2008, 107(3): 1793-1802.
15. Chauvet J., Asua J. A., Leiza J. R., Polymer 2005, 46(23): 9555-9561.
16. Elizalde O., Arzamendi G., Leiza J. R., Industrial and Engineering Chemistry Research 2004, 43(23): 7401-7409.

17. Plessis C., Arzamendi G., Agnely M., Journal of Polymer Science Part A: Polymer Chemistry 2002, 40(16): 2878-2883.
18. Barudio I., Guillot J., Fevotte G., Journal of Polymer Science Part A: Polymer Chemistry 1998, 36(1): 157-168.
19. Former C., Castro J., Fellows C. M., Journal of Polymer Science Part A: Polymer Chemistry 2002, 39(20): 3335-3349.
20. Kajtna J., Golob J., Krajnc M., International Journal of Adhesion and Adhesives 2009, 29(2): 186-194.
21. Pressure Sensitive Tape Council, Test Methods for Pressure Sensitive Adhesive Tapes 2004, Northbrook, Illinois.
22. Odian G., Principles of Polymerization 2004, Willey, Hoboken, New Jersey.
23. Tang J. S., Ding T. H., Daniels E. S., Journal of Applied Polymer Science 2003, 88(1): 30-41.
24. Maxwell I. A., Morrison B. R., Napper D. H., Makromolekulare Chemie-Macromolecular Chemistry and Physics 1992, 193(2): 303-313.
25. Sayer C., Lima E. L., Pinto J. C., Journal of Polymer Science Part A: Polymer Chemistry 2000, 38(2): 367-375.
26. Bajpai S., Rai J. S. P., Nigam I., Journal of Applied Polymer Science 2009, 112(4): 2374-2382.
27. Dubé M. A., Penlidis A., Polymer 1995, 36(3): 587-598.
28. Robeson L., Polymer Blends: A Comprehensive Review 2007, Munich, Germany.
29. Plessis C., Arzamendi G., Leiza J. R., Macromolecules 2000, 33(1): 4-7.
30. Gonzalez I., Asua J. A., Leiza J. R., Polymer 2007, 48(9): 2542-2547.

31. Perrin D., Dempsey B., Serjeant E. P., pKa Predictions for Organic Acids and Bases 1981, Chapman & Hall, London.
32. Lee J. W., Kim S. Y., Kim S. S., Journal of Applied Polymer Science 1999, 73(1): 113-120.
33. Fetters L. J., Lohse D. J., Richter D., Macromolecules 1994, 27(17): 4639-4647.
34. Wool R. P. Polymer Interfaces, Structure, and Strength. Cincinnati 1995, Hanser Gardner Publications, Cincinnati.
35. Chang E. P., Journal of Adhesion 1991, 34(1-4): 189-200.
36. Chang E. P., Journal of Adhesion 1997, 60(1-4): 233-248.
37. Tse M. F., Jacob L., The Journal of Adhesion 1996, 56(1-4): 79-95.
38. Yang H. W. H, Chang E. P., Trends in Polymer Science 1997, 5(11): 380-384.
39. Lakrout H., Creton C., Ahn D. C., Macromolecules 2001, 34(21): 7448-7458.
40. Dahlquist C. A., Handbook of Pressure Sensitive Adhesives 1989, Van Nostrand Reinhold, New York.
41. Dale W. C., Paster M. D., Haynes J. K. Journal of Adhesion 1989, 31(1): 1-20.
42. Satas D., Handbook of Pressure Sensitive Adhesive Technology 1989, Van Nostrand Reinhold, New York.
43. Brigitte I. V., Albena L., Chemistry Reviews 2009, 109: 5924-5973.
44. Brandrup J., Immergut E.H., Grulke E.A., Polymer Handbook 1999, 4th Edition, John Wiley & Sons.

CHAPTER 4

THE INFLUENCE OF BUTYL ACRYLATE/METHYL METHACRYLATE/2-HYDROXY ETHYL METHACRYLATE/ACRYLIC ACID LATEX PROPERTIES ON PRESSURE SENSITIVE ADHESIVE PERFORMANCE

The Influence of Butyl Acrylate/Methyl Methacrylate/2-Hydroxy Ethyl Methacrylate/Acrylic Acid Latex Properties on Pressure Sensitive Adhesive Performance

Lili Qie and Marc A. Dubé*
Department of Chemical and Biological Engineering,
Centre for Catalysis Research and Innovation,
University of Ottawa, 161 Louis Pasteur Pvt., Ottawa, Ontario, Canada K1N 6N5

Abstract

Pressure sensitive adhesives (PSAs) were produced using latexes synthesized via a starved seeded semi-batch emulsion polymerization process with butyl acrylate (BA), methyl methacrylate (MMA), and sometimes additional monomers, 2-hydroxy ethyl methacrylate (HEMA) and/or acrylic acid (AA). For the BA/MMA comonomer latexes, the amount of cross-linker (allyl methacrylate), monomer emulsion and initiator solution feeding times, and the BA/MMA weight ratio were manipulated to vary the polymer properties. The performance of PSA films cast from these latexes was evaluated by tack, peel strength and shear strength. The effect of polymer properties on PSA performance was related to the viscoelastic properties of the PSAs. For BA/MMA latexes, it was not possible to greatly improve the peel strength even at great sacrifice of shear strength for PSAs with gel contents of ~60 wt% or higher. This was because the ratio of the loss modulus at debonding frequency to the storage modulus at bonding frequency did not vary significantly for the conditions studied. The addition of HEMA provided a

significant influence on latex polymer properties as well as PSA performance for both high (>60 wt%) and low (~20 wt%) gel contents. For some cases, tack, peel strength and shear strength were simultaneously and greatly improved by the addition of HEMA. Adding both AA and HEMA while decreasing the amount of emulsifier, also resulted in a PSA with much better performance (i.e., higher tack, peel strength and shear strength) than a BA/MMA PSA with similar gel content (~60 wt%).

4.1 Introduction

Pressure sensitive adhesives (PSAs) are viscoelastic materials. They are permanently tacky and can adhere to solid surfaces under light pressure and short contact time.[1] PSAs are widely used in many applications such as tape, label, protection film, and medical products.[2] Furthermore, they are broadly applied as assembling tools where precise positioning and instant adhesion are required.[3] PSAs can be produced via hot-melt, solution polymerization and emulsion polymerization techniques. Recently, the latter has attracted much interest due to its relatively more environmental friendly process. Hence, the focus of the current study is on latex-based PSAs.

PSA performance is usually evaluated by tack, peel strength and shear strength. Since each PSA application has its own unique performance requirements, much research has been carried out in order to understand what affects this performance. It is known that PSA performance is strongly related to its polymer properties such as composition, glass transition temperature (T_g), and microstructure (e.g., gel content, molecular weight of sol polymers (M_w))[4-19] as well as the work of adhesion (or surface interaction energy) between the PSA and its substrate.[20-23] It is very challenging to develop PSAs, especially

latex-based PSAs, suitable for applications that require high tack, peel strength and shear strength. The reason is that these PSAs often require high gel contents to provide them with high cohesive strength, and correspondingly high shear strength. However, tack and peel strength usually decrease with gel content. Therefore, high shear strength usually corresponds to low tack and peel strength.[1,16-17] This conundrum was encountered in a previous study where most of the high gel content (> ~60 wt%) polymer materials produced were unsuitable for use as PSAs due to their extremely high shear strength and low tack and peel strength.[24] Considering this, an approach for significantly improving tack and peel strength at small sacrifice of shear strength, or if possible increasing tack, peel strength and shear strength simultaneously, is needed.

To achieve the above goal, a starved seeded semi-batch emulsion polymerization process was employed, as it can provide improved process and polymer property control (i.e., polymerization rate, heat release rate, polymer composition and particle morphology), compared with batch polymerization.[25-28] The butyl acrylate (BA)/methyl methacrylate (MMA) copolymer system was selected due to its wide use in commercial PSA production. Cross-linker (allyl methacrylate, AMA) concentration, feeding rates, and BA/MMA weight ratio were varied to provide a range of properties. With these BA/MMA polymers, we studied if decreasing gel content, cross-linking density, and/or glass transition temperature (T_g) could significantly increase tack and peel strength at a small sacrifice of shear strength.

The effect of adding 2-hydroxy ethyl methacrylate (HEMA) to the BA/MMA monomer mixture on the polymerization process, latex polymer properties, and PSA performance was also studied. HEMA is widely used for making latex-based PSAs, as it

can help stabilize latex particles and improve surface properties.[29-31] In this study, it was desired to: (1) modify PSA bulk properties by introducing strong hydrogen bonds, changing T_g, etc., and (2) modify PSA surface properties by introducing polar hydroxyl groups at the surface of the PSA films. These PSA surface hydroxyl groups might form strong hydrogen bonds with the polar groups of a substrate. Hence the work of adhesion between the PSA and substrate could be greatly improved. Thus, with BA/MMA/HEMA PSAs, there is potential to improve tack, peel strength and shear strength simultaneously by manipulating PSA bulk and surface properties concurrently. The BA/MMA/HEMA PSA polymers were produced by manipulating the HEMA concentration while maintaining the BA/MMA weight ratio and by varying the concentration of chain transfer agent (1-dodecanethiol, NDM). Finally, in order to further improve the PSA surface properties, acrylic acid (AA) was also added to the recipe while reducing the emulsifier concentration.

4. 2 Experimental procedures

4.2.1 Materials

Butyl acrylate (BA, reagent grade), methyl methacrylate (MMA, reagent grade), acrylic acid (AA, reagent grade) , and 2-hydroxy methacrylate (HEMA, 97%) monomers, allyl methacrylate (AMA, reagent grade) cross-linker, 1-dodecanethiol (NDM, reagent grade) chain transfer agent, sodium dodecyl sulphate (SDS, reagent grade) surfactant, sodium bicarbonate ($NaHCO_3$) buffer, potassium persulfate (KPS, reagent grade) initiator and hydroquinone (HQ) inhibitor were all obtained from Sigma Aldrich and were used as supplied. Distilled deionized water (DI-H_2O) was used throughout the study. Ammonia

(30 wt% in H_2O) was obtained from British Drug House. Tetrahydrofuran (THF, HPLC grade from EMD Chemicals) solvent was used in the polymer characterization. Nitrogen gas (Linde Canada) was used to purge the reactor. PTFE porous membranes with pore size of 0.2 μm, for use in gel content measurements, were purchased from Cole-Parmer Canada.

4.2.2 Latex preparation

All runs were performed via a seeded semi-batch emulsion polymerization process. The seed was prepared batch-wise using the initial charge formulation as shown in Table 4.1. To prepare the seed, all the reactants except the initiator solution and monomer mixture were charged to a one-litre Mettler-Toledo LabMax™ reactor at room temperature. The stainless steel reactor vessel was equipped with an anchor stirring blade and various feed and sampling ports. The stirring speed was maintained at 250 rpm throughout the polymerization process. The temperature of the reactants was increased to 70^{o}C within 30 min, and the monomer mixture and initiator solution were added in two separate shots to the reactor to make the seed. The temperature was then raised to 75^{o}C within 5 min and the seed polymerization was continued for an additional 10 min. At this point, the initiator feed solution and monomer emulsion, as shown in Table 4.1, were added slowly to the reactor using two separate metering pumps. The feed times of the initiator solution and the monomer emulsion were manipulated to modify the polymer properties as reported in the Results and Discussion section. After the feeding was completed, the reaction was allowed to proceed for an additional 50 min to increase monomer conversion. The latex was then cooled to below 30^{o}C, then HQ was added to stop the

polymerization, and ammonia was added to adjust the pH to ~3.5. The amounts of CTA and cross-linker as well as the monomer composition for both the seed and feed steps were varied as reported in the Results and Discussion section.

Table 4.1: Formulation for latexes production

Ingredients	Initial charge (g)	Feeding (g)	
		Monomer emulsion	Initiator solution
H_2O	202/15[a]	89	90
Monomer mixture	12	338.4	-
NDM (CTA)	-	0 – 0.2 phm	-
AMA (cross-linker)	-	0 - 0.4 phm	-
KPS	0.40	-	0.90
SDS	0.45	6.7 or 4.25[b]	-
$NaHCO_3$	0.05	-	-

Note: (1) "phm" is the abbreviation for "parts per hundred parts monomer".
(2) [a]water used for making the initiator solution in the seed production stage.
(3) [b]4.25 g SDS used only in Run 14, all other runs were at 6.7 g SDS.

4.2.3 Characterization

Characterization of the polymer latex and PSA films was conducted according to methods outlined previously.[24] A standard gravimetric method was used to calculate the monomer conversion. Latex particle sizes were measured using a Dynamic Light Scattering (DLS) instrument (Malvern NanoS Zetasizer) with an angle of 176°. The reported diameter is an intensity-weighted average particle size. The polydispersity index values (PDI) given by the instrument reflect a narrower particle size distribution (PSD) with PDI values closer to 0.01. Latexes having a PDI smaller than 0.4 were considered to

have a narrow particle size distribution. The detection range of the instrument was 0.6 nm to 6 μm.

A modification of the method by Tobing and Klein[16] was used to measure gel content.[24] The THF solution remaining from the gel content test was concentrated, as necessary, and analyzed for sol polymer molecular weight using Gel Permeation Chromatography (GPC). The calibration curve included a set of 12 polystyrene standards (EasiCal from Polymer Laboratories) with a range of 162 to 6,035,000 g/mol. The universal calibration method was used based on the BA/MMA composition with the Mark-Houwink parameters, K and α, for BA and MMA are 1.1×10^{-4} dL/g and 0.708, and 1.28×10^{-4} dL/g and 0.690, respectively.[32]

Tack, peel strength and shear strength were measured according to the Pressure Sensitive Tape Council standards PSTC-6, PSTC-1 and PSTC-7, respectively.[33] Further details of these methods were given previously.[24]

The viscoelastic properties of the PSAs were characterized using a RDA III rheometer (TA Instruments) with 25 mm parallel plate geometry. The sample thickness was 1.7+/-0.2 mm. Three types of measurements were done: (1) room temperature frequency sweep. This test was carried out at 23°C, the frequency range was from 0.031848 to 80 Hz, and there were 5 data points within each decade of the log frequency; (2) frequency sweep at various temperatures. In order to get a frequency master curve, frequency sweeps were carried out at different temperatures including -35, -23, 0, 23, 50 and 80°C; for each temperature, the frequency sweep data were obtained at 0.05, 0.1, 0.2, 0.5, 1, 2, 5, 10, 20 and 50 Hz. The frequency master curve was built with the 23°C frequency sweep as reference; and (3) temperature sweep. The measurements were from -

40 to 160°C at a heating rate of 2°C/min and a shear frequency of 1.591 Hz. The tanδ curves from the temperature sweep tests also provided glass transition temperature (T_g) data. The T_g was also measured by differential scanning calorimetry (DSC) over the temperature range -80 to 80°C.

4.3 Results and Discussion

4.3.1 Effect of AMA cross-linker

To study the influence of cross-linker, three runs (Run 1, 2 and 3) were carried out at a BA/MMA weight ratio of 90/10. AMA was used as the cross-linker, and the monomer emulsion and initiator solution feeding times were 3 and 3.5 h, respectively. The AMA concentration, latex properties and PSA performance related to these three runs are shown in Table 4.2 (note that run number, latex ID and PSA ID have corresponding numbering, i.e., the latex from run 1 has a latex ID of 1 and the PSA film cast from that latex has a PSA ID of 1).

Table 4.2: Latexes and PSAs related to Run 1-3 (BA/MMA weight ratio: 90/10)

Latex ID	AMA (phm)	Gel content (wt%)	M_w ($x10^{-3}$ g/mol)	M_n ($x10^{-3}$ g/mol)
1	0	64	296	90
2	0.2	91	107	51
3	0.4	96	-	-
PSA ID	**Film thickness (μm)**	**Tack (N/m)**	**Peel strength (N/m)**	**Shear strength (1"x1")**
1	30	61	47	101.6 h
2	30	30	20	> 1 month
3	30	28	15	> 1 month

The three latexes had similar z-average particle diameters (~150 nm). In addition, the PSD of these latexes was very narrow with PDI < 0.04 with no apparent secondary peaks or shoulders at either the low or high particle size ranges. This is consistent with the assumption that neither secondary particle nucleation nor coagulation occurred during the polymerization.

All three runs were carried out under monomer-starved conditions with the instantaneous monomer conversion beyond 90 wt% for most of the polymerization process. The solids contents of these three latexes were each ~47 wt%. It was found that AMA did not significantly affect the polymerization rate.

Table 4.2 shows that with an increase in AMA concentration, the gel content increased and the M_w decreased. This phenomenon is well known.[34-35] While polymerizing a BA-rich monomer mixture in the absence of cross-linker, gel is formed by chain transfer mechanism, and it involves two steps: (1) branch radical formation via either intra-molecular chain transfer by backbiting or inter-molecular chain transfer to polymer, due to the presence of labile tertiary hydrogen in the BA unit of the polymer chains;[36-39] (2) gel formation through combination termination between the branched polymer radicals.[40] In the presence of cross-linker, the pendent double bonds of the cross-linker unit in the polymer chains can also result in the formation of branched radicals via propagation. The termination by combination of these branched radicals will also result in the formation of gel. This is the main gel formation mechanism.[41] Since the number of pendent double bonds increased with the AMA concentration, the gel content increased. In addition, as longer polymer chains have more pendent double

bonds, they are more likely to incorporate into gel polymer, and accordingly M_w decreases with the increase in gel content.

All three PSAs showed adhesive (as opposed to cohesive) failure during both tack and peel strength tests. Table 4.2 shows that with the increase in gel content, tack and peel strength decreased while shear strength increased. The increase in gel content led to higher cohesive strength and a larger shear strength. At the same time, the resulting lower deformability and flow ability of the PSA weakened the bonding between the PSA and substrate, causing lower tack and peel strength.[1] In all cases in Table 4.2, the tack and peel strength values of the PSAs were very low.

4.3.2 Effect of feeding time

In order to improve tack and peel strength, the monomer emulsion and initiator feeding times of Run 1 were reduced by 0.5 h each. Thus, Run 4 was identical to Run 1 except for the feeding times. Run 4 was also carried out under monomer-starved condition. All remaining runs were conducted using these shortened feeding times of 2.5 h for the monomer emulsion and 3 h for the initiator solution.

The polymer properties and PSA performance of Run 4 are shown in Table 4.3. By comparing the data of Run 4 to that of Run 1 (see Table 4.2), one observes a slight decrease in gel content from 64 wt% to 60 wt%, and a slight increase in M_w from 296,000 to 328,000 g/mol. The particle size and T_g were not significantly affected by the feeding times. The PSD of latex 4 was very narrow with a z-average diameter close to that of latex 1, i.e., ~150 nm. The T_g values obtained via DMA were -27°C and -28°C,

respectively for PSA 1 and 4. It was clear from the DMA results that latex copolymers with homogenous compositions similar to that of the monomer mixture were formed.

Table 4.4 shows the change in latex polymer properties during the polymerization process for Run 4. As the polymerization progressed, the gel content increased only slightly and the M_w decreased slightly. This further confirms that the polymerization was carried out under monomer-starved conditions with no secondary nucleation,[25] and is consistent with the gel content and M_w changes reported by other researchers.[36,41-42]

Table 4.3: Latexes and PSAs related to Run 4-6 (BA/MMA weight ratio was varied) and Run 14 (BA/MMA for initial charge, and BA/AA/HEMA for feeding)

Run ID	BA/MMA weight ratio (initial load & feeding)	T_g (°C)	Gel content (wt%)	M_w ($x10^{-3}$ g/mol)	M_n ($x10^{-3}$ g/mol)
4	90/10	-28	60	328	117
5	95/5	-33/-44[a]	63	315	92
6	98/2	-35	64	309	55
14	95/5 (initial load) 96/2/2[b] (feeding)	-45[a]	51	443	105

PSA ID	Film thickness (μm)	Tack (N/m)	Peel strength (N/m)	Shear strength (h)
4	30	65	57	73.9
4	60	141	135	31.9
5	33	93	60	22.2
14	33	223	216	41.8

Note: (1) [a]T_gs obtained via DSC method. Other T_g values were obtained with DMA method. It is known that the DMA method results in a higher T_g than the DSC method.[25] (2) [b]BA/AA/HEMA weight ratio of 96/2/2. Other weight ratios were for BA/MMA mixture.

Table 4.4: Polymer properties of latex samples taken during Run 4

Latex sample ID	Feeding time (min)	Gel content (wt%)	M_w ($x10^{-3}$ g/mol)	M_n ($x10^{-3}$ g/mol)
1#	20	53	401	120
2#	50	57	351	99
3#	150	60	325	102
4# (Final latex)	-	60	328	117

By comparing the performance of PSA 4 (Table 4.3) and PSA 1 (Table 4.2), one can see that at the same film thickness of 30 μm, PSA 4 had slightly higher tack and peel strength, but significantly lower shear strength compared with PSA 1. The significant decrease in shear strength from 101.6 h to 73.9 h was caused by not only the slightly lower gel content (60 wt% for PSA 4 and 64 wt% for PSA 1), but possibly due to the looser gel network. Previous researches have shown that when BA was polymerized via a starved seeded semi-batch emulsion polymerization process, decreasing the monomer feeding rate did not greatly affect gel content, but did significantly enhance intra-molecular polymer chain transfer and accordingly led to higher branching levels.[36,41] Since it is well known that termination by combination between these branched polymer radicals leads to gel polymer,[40] the cross-linking density should also increase with a decrease in monomer feeding rate.

Despite the slight improvements in tack and peel strength for PSA 4 compared to that of PSA 1, the results were still impractically low. Thus, given the known influence of film thickness on PSA performance,[1] PSA 4 was recast with a film thickness of 60 μm. Table 4.3, shows that the increase in film thickness led to increases in tack and peel

strength, but a significant decrease in the shear strength. All future PSA films were cast at a thickness of 60 μm, unless otherwise mentioned.

4.3.3 Influence of BA/MMA weight ratio

Since the tack and peel strength were not significantly improved by shortening the monomer feeding rate, the BA/MMA monomer weight ratio was manipulated to achieve this goal. Considering that the T_g of poly(butyl acrylate) (PBA, -45°C) is much lower than that of poly(methyl methacrylate) (PMMA, 105°C),[25] the BA/MMA weight ratio was adjusted to 95/5 and 98/2 for Runs 5 and 6, respectively. The polymerization conditions of these two runs were otherwise exactly the same as for Run 4.

The PSDs of latexes 5 and 6 were very narrow and did not show evidence of secondary nucleation or coagulation. The particle diameters of latexes 5 and 6 were similar to that of latex 4. The instantaneous monomer conversions for Runs 5 and 6 were monitored and no significant differences from that of Run 4 were detected, although it is well known that the polymerization reactivity ratio of MMA is almost 5 times of that of BA ($r_{BA} = 0.507$ and $r_{MMA} = 2.375$).[43] This is due to the fact that the BA/MMA weight ratio was changed only slightly and that monomer-starved conditions were used. In this case, polymerization rate was mainly controlled by the monomer feeding rate. This is consistent with the results of Elizalde et al. who studied the influence of BA/MMA weight ratio on polymerization rate under monomer-starved conditions. In their case, they examined a much broader BA/MMA weight ratio range and they observed only slight decreases in instantaneous monomer conversion from ~91% to ~88% to ~85%, when the

BA/MMA weight ratio was changed form 90/10 to 70/30 to 50/50 (Figure 6a of ref. 40).[44]

The polymer properties of the latexes form these three runs are shown in Table 4.3. As expected, increasing the amount of BA led to decreased T_g and slightly increased gel contents. The latter was likely due to increased backbiting related to the higher BA concentrations.[40]

The performance of PSA films 4, 5 and 6 is shown in Figure 4.1. Increasing the BA concentration led to increases in tack and peel strength and a significant decrease in shear strength. The decrease in shear strength was obviously due to the lower cohesive strength of the PSA related to its lower T_g.[1] To explain the change in peel strength with the increase in BA content, the viscoelastic properties of the three PSAs were measured. Figures 4.2 and 4.3 show the storage and loss moduli, respectively, obtained via frequency sweeps at 23°C for the three PSAs. One can observe that the storage modulus curves of PSAs 4, 5 and 6 (see Figure 4.2) were nearly parallel to each other as were the loss modulus curves (see Figure 4.3). This similarity in viscoelastic properties was likely caused by the similar polymer microstructures of these PSAs. As mentioned earlier, these PSAs had similar gel contents and M_w. Furthermore, it is likely that the M_c (molecular weight between the cross-linking points) were also similar, considering the minor composition differences between these three PSAs. Thus, similar polymer microstructures enabled the PSAs to store (G') and dissipate (G") energy similarly under the same dynamic force and the ratios of stored energy to dissipated energy were similar. In addition, Figures 4.2 and 4.3 show that the values of the modulus decreased with the increase of the amount of BA in the copolymer; this was due to the lower T_g.

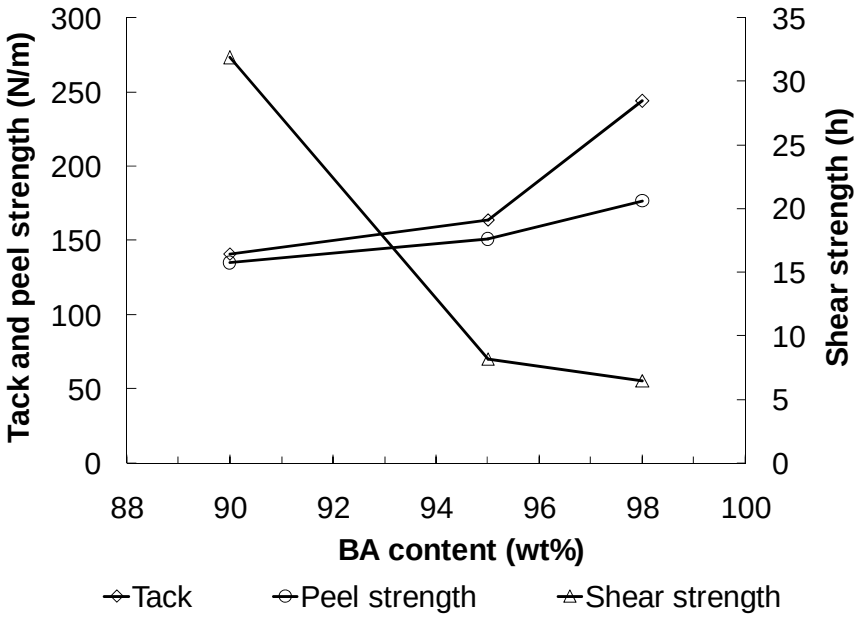

Figure 4.1: Performance of PSA films 4, 5, and 6. (PSA film thickness: 60 μm)

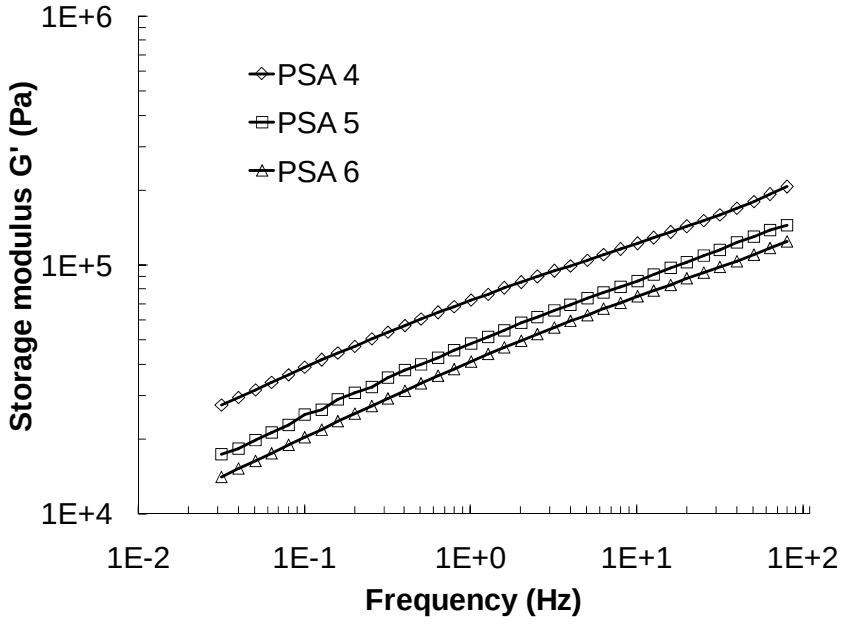

Figure 4.2: Storage modulus (G') vs. frequency at 23°C for PSA 4, 5 and 6.

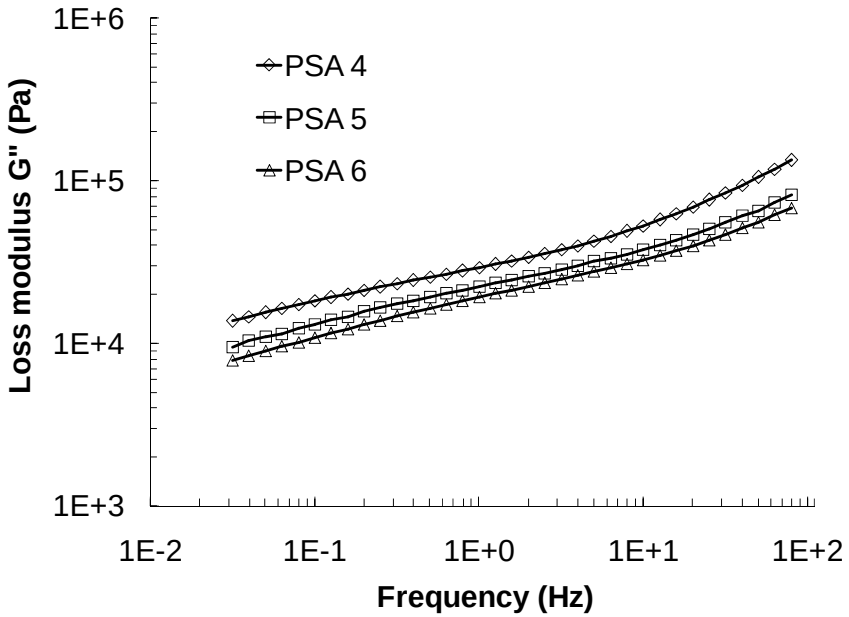

Figure 4.3: Loss modulus (G") vs. frequency at 23°C for PSA 4, 5 and 6.

Yang et al. reported that peel strength is proportional to the ratio of the loss modulus at debonding frequency (G" (ω_1)) to the storage modulus at bonding frequency (G' (ω_2)) as shown in Equation 4-1.[22] To get the exact values of the ratios, the debonding frequencies (ω_1) were calculated with Equation 4-2 reported by Tse.[45] The test conditions used in Tse's work were identical to ours except for the film thickness. Tse used a film thickness of 37 μm, and they reported a debonding frequency, ω_1, of 435 rad/s (or 69.3 Hz). In our case, the film thickness was 60 μm, so we corrected ω_1 for our peel strength test as shown in Equation 4-3. Similarly, bonding frequency, ω_2, was corrected for film thickness as shown in Equation 4-5. For ω_2, a value of 1 rad/s (or 0.16 Hz) for a standard peel test from the work of Yang was used.[22]

$$P \propto I \times G"(\omega_1)/G'(\omega_2) \qquad (4-1)$$

$$\omega_1 = \frac{2\pi(bonding\ rupture\ speed)}{(adhesive\ thickness)}\frac{rad}{s} \qquad (4-2)$$

$$\omega_1 = 435\frac{rad}{s} \times \frac{37\ nm}{60\ nm} \times 0.1592\frac{Hz}{(rad/s)} = 42.7Hz \qquad (4-3)$$

$$\omega_2 = 1\frac{rad}{s} \times \frac{37\ nm}{60\ nm} \times 0.1592\frac{Hz}{(rad/s)} = 0.0982Hz \qquad (4-4)$$

At bonding and debonding frequencies obtained above, the G”(ω_1) values for PSA 4, 5 and 6 were 96918, 61849, and 52207 Pa, respectively, the G’(ω_2) values were 38436, 24723, and 20083 Pa, respectively, and the G”(ω_1)/G’(ω_2) ratios were 2.52, 2.50 and 2.59, respectively. As the BA/MMA weight ratio changed from 90/10 to 95/5, the G”(ω_1)/G’(ω_2) values remained nearly constant, which is in agreement with the similar peel strength values of PSA 4 compared PSA 5. Further changes in the BA/MMA weight ratio to 98/2 resulted in a slight increase in the G”(ω_1)/G’(ω_2) ratio from 2.50 to 2.59, which corresponds to a slight increase in the peel strength of PSA 6 compared to that of PSA 5.

Lowering the T_g from PSA 4 to PSA 6 resulted in improved deformability and flow ability of the PSA. From Figure 4.1, we observe that the resulting changes in tack differ in magnitude from that in peel strength, with tack exhibiting larger changes. It is well known that tack and peel strength tests consist of both bonding and debonding processes. In addition, the bonding process of the tack test features a much shorter contact time and lower force compared to the peel strength test.[1] Therefore, the deformability and flow ability of the PSA should have a larger influence on tack than on peel strength, as observed in Figure 4.1.

4.3.4 Influence of HEMA in the absence of CTA and cross-linker

To study the influence of HEMA, three additional runs (Runs 7, 8 and 9) were carried out by adding HEMA to the recipe for Run 5. These three new runs had the same seed composition as in Run 5 but differed in the fed monomer emulsion mixtures with BA/MMA/HEMA weight ratios of 95/5/0, 95/5/1, 95/5/2 and 95/5/4, for Runs 5, 7, 8 and 9, respectively.

The PSDs of latexes 7, 8 and 9 were all very narrow, and did not present evidence of any secondary nucleation or coagulation; this was despite the hydrophilic nature of HEMA.[46] The z-average particle diameters of latexes 5, 7, 8 and 9 are shown in Table 4.5. The particle diameter was independent of the amount of HEMA in the monomer emulsion feed.

Table 4.5: Polymerization conditions and latex polymer properties for Run 5, 7-9
(No NDM; BA/MMA/HEMA weight ratio was varied)

Latex ID	5	7	8	9
BA/MMA/HEMA weight ratio				
Initial load	95/5/0	95/5/0	95/5/0	95/5/0
Monomer emulsion feeding	95/5/0	95/5/1	95/5/2	95/5/4
z-Ave. particle diameter (nm)	151	147	145	150
T_g (°C)	-33	-31	-30	-27
Gel content (wt%)	63	64	67	82
M_w ($x10^{-3}$ g/mol)	315	203	190	117
M_n ($x10^{-3}$ g/mol)	92	36	32	46

The monomer conversions for Runs 7, 8 and 9, were monitored throughout the feed process (i.e., at feed times of 50, 100, 150 and 180 min) in addition to the end of the polymerization. Both the instantaneous and overall monomer conversions were calculated using the gravimetric method reported previously[24] and compared to those of Run 5. The results showed that the monomer conversions did not significantly change with the change of HEMA concentration in the monomer mixture.

The insignificant influence of HEMA on the polymerization rate is due to the small amounts of HEMA added to the monomer mixture as well as the monomer-starved conditions used. The final monomer conversions for these four runs were all at or beyond 99.5%, and one can assume that the added HEMA for all these runs was fully polymerized given the higher reactivity ratio of HEMA compared to that of BA (r_{HEMA} = 4.497 and $r_{t\text{-}BA}$ = 0.212)[47] and MMA (r_{HEMA}*=0.98 and* r_{MMA}*= 0.82).*[48] (Note: Considering the structural similarity of n-BA (abbreviated as BA) to t-BA (tert-butyl acrylate), it is reasonable to assume that they have similar polymerization reactivities.)

It is of interest to know the distribution of HEMA in the latexes. This was accomplished using a temperature sweep in the DMA (dynamic mechanical analysis) for PSAs 5, 7, 8 and 9. The storage modulus (G') and tanδ curves of PSA 5 and 9 are shown in Figure 4.4 as examples. PSA 5 (BA/MMA/HEMA weight ratio: 95/5/0) exhibited only one tanδ peak at -33°C while PSA 9 (BA/MMA/HEMA ratio: 95/5/4) gave two tanδ peaks; one at -27 °C and a second, smaller one over a very broad temperature range (50 to 160°C). If homogenous copolymer was formed, the tanδ curve should exhibit only one peak at a low temperature (~-30°). We suspect that the broader peak for PSA 9 was due to the presence of a small amount of carboxyl groups which were formed during

polymerization via the oxidation of OH groups by the persulfate from the initiator. This well-known phenomenon has been reported previously.[49-50] Thus, during the temperature sweep, it is likely that the carboxyl groups reacted with the OH groups at high temperature (> 120°C), in essence slightly increasing the gel content and therefore the G' value. This would result in the broad tan δ peak.

To avoid this phenomenon, we proceeded with a series of frequency sweep measurements using the DMA, with the highest temperature of 80°C. With these measurements, a frequency sweep master curve was built for PSA 9 as shown in Figure 4.5, only one tanδ peak is evident in that figure which confirms that HEMA was randomly distributed in the copolymer of PSA 9.

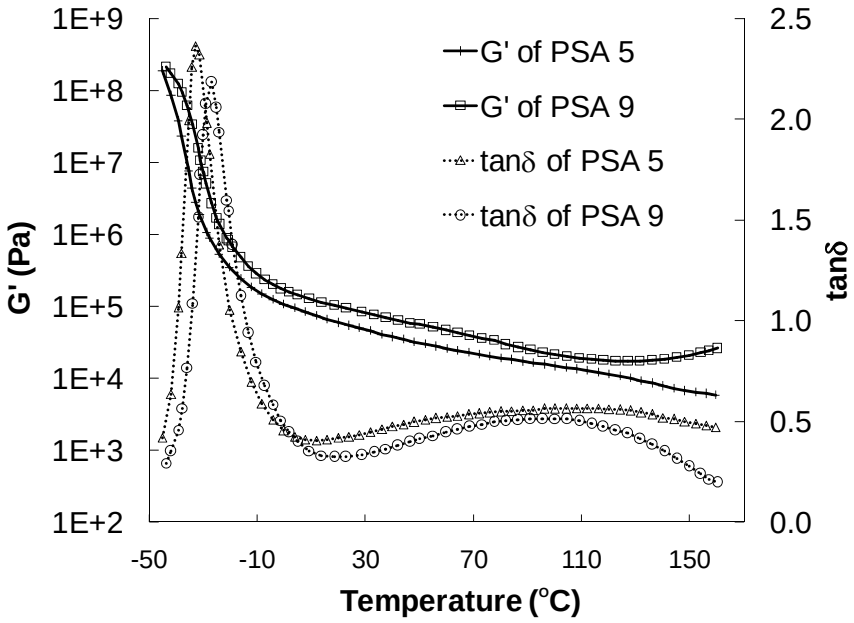

Figure 4.4: DMA temperature sweep curves of PSA 5 and 9.

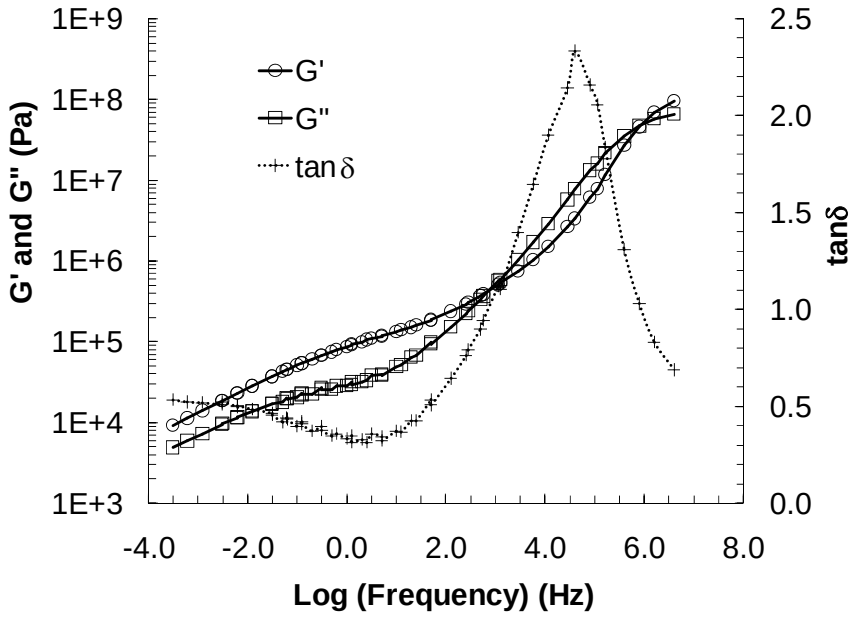

Figure 4.5: Frequency sweep master curve of PSA 9.

It is clear from the discussion above that the tanδ peak at the low temperature range of the temperature sweep curve represents the actual single T_g of the BA/MMA/HEMA copolymer. The T_g values listed in Table 4.5 for PSA 5, 7, 8 and 9, show an increase with HEMA content. This is consistent with the fact that the T_g of poly(HEMA) is 87°C,[51] while that of BA/MMA polymer (weight ratio: 95/5) was -33°C as shown in Table 4.5 for PSA 5.

Table 4.5 reports that an increase in HEMA resulted in an increase in gel content. As the polymerization rate was not significantly affected by adding HEMA, the possible reason for the increase in gel content might be related to the purity of HEMA. The HEMA used in this study contained ~3 wt% of diethylene glycol monomethacrylate (DEGM), which has two double bonds and is a side product arising from HEMA production. To estimate the influence of this impurity in HEMA on the gel content, gel

content vs. cross-linker concentration trend line was constructed with the data related to latexes 1, 2 and 3 shown in Table 4.2. The corresponding runs had longer feeding times compared to Runs 4, 7, 8 and 9. Considering the minor influence of shortening feeding times on gel content discussed earlier, the trend line could still be useful for predicting the gel content of HEMA-containing latexes.

The trend line shown in Figure 4.6 has the coded values of cross-linker AMA as the *x* axis. The coded values were obtained with Equation 4-5. In the equation, *x* is the coded amount of cross-linker while *X* is the actual amount in phm. Hereafter, we will use latex 9 as an example, and use the trend line to predict its gel content. As Run 9 had the impurity DEGM as a possible cross-linker, in order to use the trend line, we converted the amount of DEGM to the equivalent molar amount of AMA using Equation 4-6.

$$x = \frac{(X - 0.2\ phm)}{0.2\ phm} \qquad (4-5)$$

$$x_{AMA} = x_{DEGM} \times \frac{M_{AMA}\left(\frac{g}{mol}\right)}{M_{DEGM}\left(\frac{g}{mol}\right)} = x_{DEGM} \times \frac{126}{187} = 0.674 x_{DEGM} \qquad (4-6)$$

where x_{AMA} and x_{DEGM} are the coded amounts of AMA and DEGM.. M_{AMA} and M_{DEGM} are the molecular weights of AMA and DEGM, respectively.

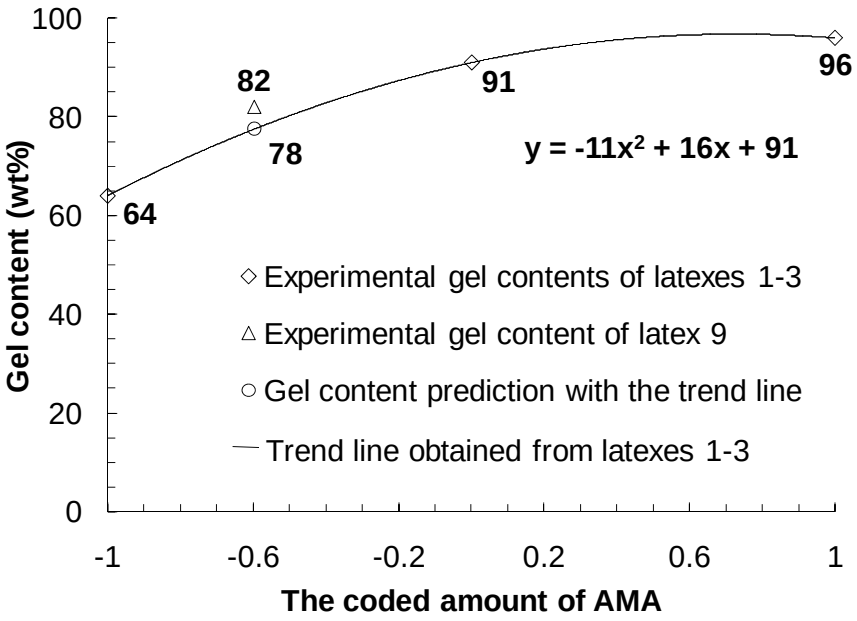

Figure 4.6: Gel content prediction for latex 9.

Seeing that there was ~4 wt% of HEMA in Run 9 and there was ~3 wt% of DEGM in the HEMA monomer, one can assume that there was ~0.12 phm DEGM in the monomer mixture. Using Equation 4-6, this amount of DEGM was implied ~0.081 phm AMA. Using the trend line, a predicted gel content of ~78 wt% for latex 9 was calculated, as shown in Figure 4.6. This predicted value is very close to the gel content value obtained from the experiment (~82 wt%) as shown in Figure 4.6. Thus, the gel content increase caused by increasing the amount of HEMA can be attributed mainly to the presence of DEGM impurity in HEMA.

4.3.5 Effect of HEMA when 0.2 phm NDM (CTA) was added

To further confirm the influence of HEMA on polymerization kinetics and latex polymer properties, Runs 10, 11, 12 and 13 were conducted. These runs corresponded to Runs 5,

7, 8 and 9, respectively, in terms of their recipes except that the new runs contained 0.2 phm NDM (CTA). The polymerization conditions and the latex polymer properties are shown in Table 4.6 for these runs.

Table 4.6: Polymerization conditions and latex polymer properties for Run 10-13 (0.2 phm NDM; BA/MMA/HEMA weight ratio was varied)

Latex ID	10	11	12	13
BA/MMA/HEMA weight ratio				
Initial load	95/5/0	95/5/0	95/5/0	95/5/0
Monomer emulsion feeding	95/5/0	95/5/1	95/5/2	95/5/4
z-Ave. particle diameter (nm)	149	146	147	151
T_g (°C)	-33	-32	-31	-28
Gel content (wt%)	0	2	5	21
M_w ($x10^{-3}$ g/mol)	223	264	234	189
M_n ($x10^{-3}$ g/mol)	43	31	38	32

For Runs 10-13, the instantaneous monomer conversion and the effect of HEMA provided no different observations from runs 5, 7, 8 and 9.

4.3.6 Effect of HEMA on PSA performance

Latexes 5, and 7-13 were cast as PSA films with thickness ~60 μm. Their performance as PSAs is shown in Figures 4.7 and 4.8.

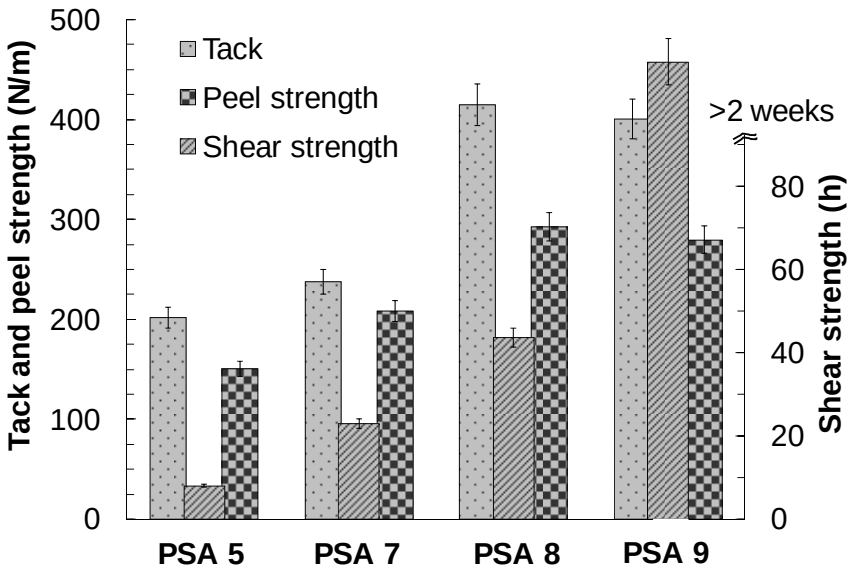

Figure 4.7: Performance of PSA film 5, 7, 8 and 9. (PSA film thickness: 60 μm)

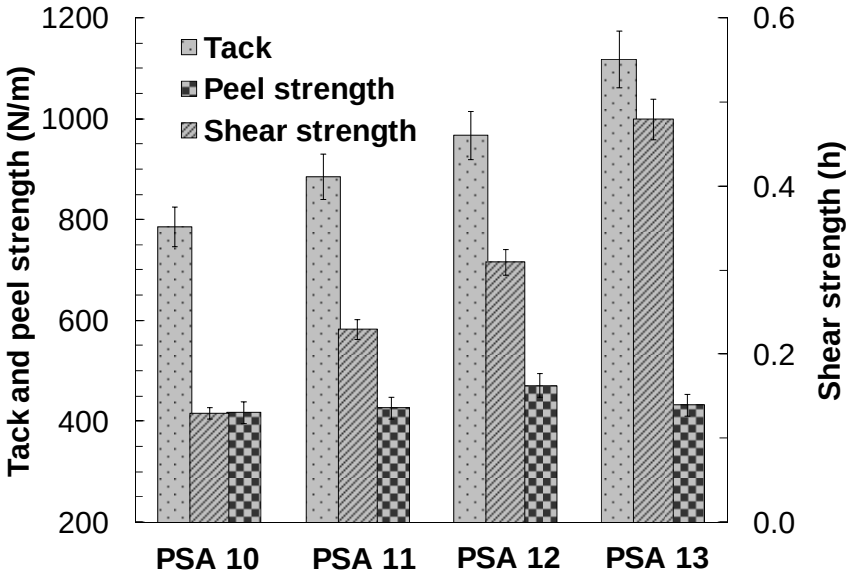

Figure 4.8: Performance of PSA film 10-13. (PSA film thickness: 60 μm)

To facilitate the discussion, hereafter we refer to the PSAs in Figure 4.7 as “high gel content PSAs” and that in Figure 4.8 are referred to as “low gel content PSAs”. The

high gel content PSAs all showed adhesive failure during tack and peel strength tests, while the low gel content PSAs all showed cohesive failure during these tests.

Figure 4.7 shows that for the high gel content PSAs, the shear strength increased with HEMA content. Obviously, this is because adding HEMA resulted in higher T_gs, higher gel contents, as well as stronger hydrogen bonds between the copolymer chains. The same trend for the influence of HEMA on shear strength is shown in Figure 4.8 for the low gel content PSAs. Figure 4.7 also shows that for the high gel content PSAs, tack first increased and then decreased with the increase of HEMA from 0 to ~ 4 phm, and the maximum was at ~2 phm HEMA. The same trend for the influence of HEMA on peel strength was observed.

Further insight into these tack and peel strength changes were obtained from the viscoelastic properties of these PSAs via frequency sweep tests at 23°C using DMA (see examples using PSA 5 and PSA 9 in Figures 4.9 and 4.10). In Figure 4.9, we observe that the storage modulus (G') increased with HEMA concentration. This was due to the stronger hydrogen bond, higher T_g, as well as the higher gel content related to the presence of HEMA. In addition, the shape of the G' curves stayed almost unchanged. The same behavior was observed for the loss modulus (G") in Figure 4.10. Given the similarity in shape of the G' and G" curves for these PSAs, it is likely that these PSAs had very similar G"(ω_1)/G'(ω_2) values. G"(ω_1 = 42.7 Hz)/G'(ω_2 = 0.0982 Hz) values of 2.50, 2.28, 2.19 and 1.80, were obtained for PSA 5, 7, 8 and 9, respectively. Thus, only a slight decrease in the G"/G' ratio with increasing HEMA content was noted.

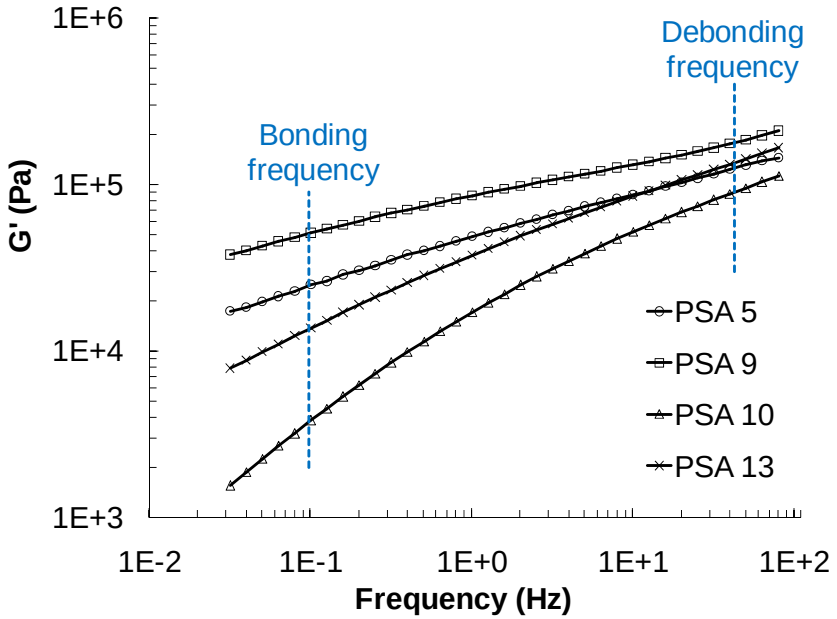

Figure 4.9: Storage modulus of high gel content (PSA 5 and 9) and low gel content (PSA 10 and 13) PSAs. (Bonding and debonding frequency corresponds to PSA film thickness of 60 μm)

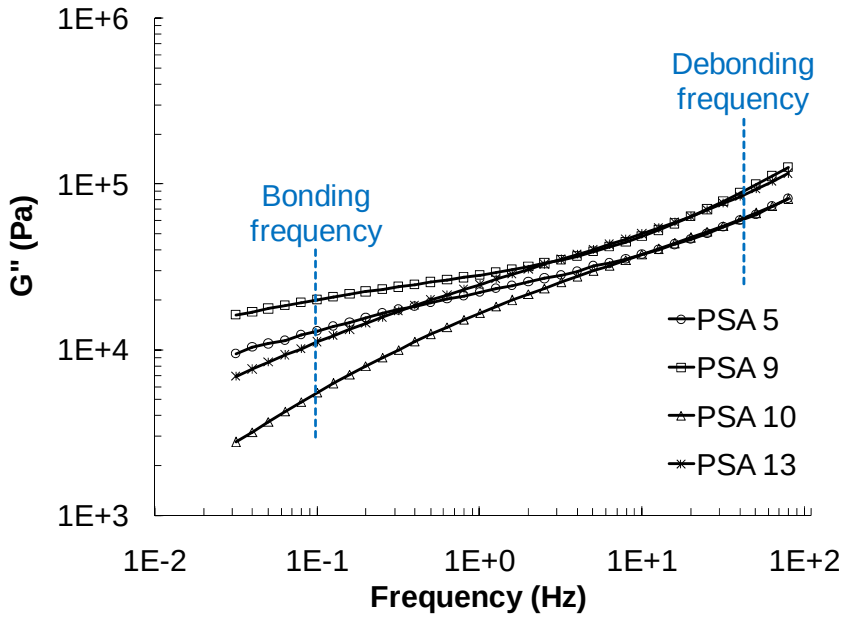

Figure 4.10: Loss modulus of high gel content (PSA 5 and 9) and low gel content (PSA 10 and 13) PSAs. (Bonding and debonding frequency corresponds to PSA film thickness of 60 μm)

It is well known that peel strength decreases with the decrease in G”(ω_1)/G’(ω_2), but at the same time it can be increased by improving the work of adhesion (a.k.a. surface interaction energy) between the PSA and the substrate.[22-23] Based on this knowledge and the observed slight decrease in G”(ω_1)/G’(ω_2) with the increase in HEMA concentration, we hypothesize that the reason for the increase in peel strength when HEMA was increased from 0 to 2 phm was that the work of adhesion between the PSA and the testing panel was increased. It is well known that introducing polar groups such as carboxyl and hydroxyl groups into a PSA could increase the work of adhesion between the PSA and a substrate with polar groups such as stainless steel. This is because the polar groups in the adhesive can rearrange and thereafter orient to the interface between the adhesive and the polar substrate so as to minimize interfacial free energy during adhesion. At the same time, hydrogen bonds can form between the polar groups in the PSA and those in the substrate. Hence, work of adhesion can be greatly increased.[20-21,52-53] Li et al. reported an increase in work of adhesion by ~9 times in some cases for EHA (2-ethyl hexyl acrylate)/AA (acrylic acid) (EHA/AA weight ratio: 90/10) PSAs after orientation of the carboxyl groups. In addition, the work of adhesion increased ~3 times by adding ~10 wt% AA in poly(EHA) PSAs.[21] Flanigan et al. found that even with about 3-4 mol% acrylic acid in P(AA-BA-AA) block polymer could increase the effective work of adhesion by a factor of 18 compared to a P(MMA-BA-MMA) block polymer.[20]

As HEMA contains polar hydroxyl groups and also some of the hydroxyl groups were likely oxidized by the initiator to polar carboxyl groups, by introducing more HEMA to the PSA, the work of adhesion was enhanced. Consequently, higher peel strength was observed when 0 – 2 phm HEMA was added, while the G”(ω_1)/G’(ω_2) did

not change much. As for the more or less constant peel strength when HEMA was increased from about 2 phm to about 4 phm, the reason might be that the positive effect on the peel strength caused by improving the work of adhesion could no longer counterbalance the negative effect caused by the decrease in G"(ω_1)/G'(ω_2). Taking into account that the change in tack with the increase of HEMA is very similar to that in peel strength as mentioned earlier, it is reasonable to hypothesize that the above explanation for the change in peel strength should also apply to the change in tack.

Figure 4.8 shows that for the low gel content BA/MMA/HEMA PSAs, tack increased with HEMA concentration; however, the peel strength remained more or less constant. This trend differs from what was observed for the high gel content PSAs. We therefore referred to the viscoelastic properties for these low gel content BA/MMA/HEMA PSAs via frequency sweeps at 23°C using DMA. The G' and G" curves of PSAs 10 and 13 are shown in Figures 4.9 and 4.10 as examples. It was found that the change in G' curves with the increase in HEMA content for the low gel content PSAs was very different from that for the high gel content PSAs. These low gel content PSAs showed a much steeper increase in G' in the lower frequency range (near or below the bonding frequency) than in the higher frequency range (near or above the debonding frequency), with the increase in HEMA content (see, for example, Table 4.7). Consequently, the shape of the G' curves of these low gel content PSAs were no longer similar. The same changes in the G" curves for the low gel content PSAs were observed.

Table 4.7: G' and G" changes by adding ~4 phm HEMA

Modulus ratio	High debonding Frequency (42.7 Hz)	Low bonding Frequency (0.1 Hz)
High gel content PSAs (5 & 9)		
G'_{PSA9}/G'_{PSA5}	1.42	2.03
G''_{PSA9}/G''_{PSA5}	1.47	1.55
Low gel content PSAs (10 & 13)		
G'_{PSA13}/G'_{PSA10}	1.50	3.60
G''_{PSA13}/G''_{PSA10}	1.40	2.00

The differences in behavior between the low and high gel content PSAs can be explained as follows: (1) According to Chang,[50] the debonding frequency lies in the transition region. This is also the case for our PSAs. For example, one can confirm this by referring to the frequency sweep master curve of PSA 9 (see Figure 4.5). Therefore, the polymer chains in both the high and low gel content PSAs were still in a somewhat densely packed state at frequencies beyond or near the debonding frequency (~42.7 Hz). In contrast, the bonding frequency usually occurs at the plateau region for standard tack and peel strength tests.[1,54] Under our PSA testing conditions, the bonding frequency was found to be around the beginning of the viscous flow region. Hence, at frequencies below or near the bonding frequency, the packing states of the polymer chains in high and low gel content PSAs were different. For the low gel content PSAs, the free volume between the polymer chains was much larger; however, the polymer chains in the high gel content PSAs could not separate as much due to the existence of the gel network. (2) By adding HEMA to the PSA copolymer, the G' and G" were increased (compare 5 to 9, and 10 to 13 in Figures 4.9 and 4.10, respectively) due to a higher T_g. The increased T_g led to a

shift of the transition zone to a slightly lower frequency range according to the time-temperature superposition principle.[1,55] Consequently, at the same debonding frequency, which lies in the transition zone as mentioned earlier, the PSA with the larger amount of HEMA showed higher G' and G" values (compare PSAs 9 to 5 and 13 to 10, respectively). This was also the case for the frequencies still in the transition zone but greater than the debonding frequency (see Figures 4.9 and 4.10).

The modulus change by adding HEMA can also be explained by referring to the packing state of the polymer chains. Adding HEMA might be able to make the PSA polymer chains stay closer, due to the interaction between the hydroxyl groups and formation of hydrogen bonds. In addition, the effect of adding HEMA should be more significant for the loosely packed state of polymer chains than the densely packed, as in the latter, the polymer chains are already very close to each other. Since the polymer chains of the high gel content PSAs were in a somewhat densely packed state at both the high and low frequency ranges due to the existence of gel, the contribution of HEMA to polymer chain packing should be similar in both ranges. Consequently, nearly parallel modulus curves were obtained for these PSAs (e.g., PSA 5 and 9 in Figures 4.9 and 4.10). As for the low gel content PSAs, the contribution of HEMA to chain packing should be significantly larger in the low frequency range considering the loosely packed state of the polymer chains at lower frequencies and the somewhat densely packed state at higher frequencies. As a result, the modulus difference was significantly larger in the low frequency range, and therefore the modulus curves did not remain parallel (e.g., PSA 10 and 13 as shown in Figures 4.9 and 4.10). The influence of the polymer chain packing state on the modulus can be further confirmed as follows: From Figures 4.9 and 4.10, one

can see that at the high frequency range, the modulus of PSA 5 (BA/MMA/HEMA weight ratio: 95/5/0; gel content: ~60 wt.%; T_g: -33°C) was smaller than that of PSA 13 (BA/MMA/HEMA: 95/5/4; gel content: ~20%; T_g: -28°C). This was because at the high frequency range, the polymer chains of both PSAs were in a somewhat densely packed state, so the influence of gel content on polymer chain packing was not significant. Instead, HEMA played a bigger role on affecting the modulus, since it increased the T_g. In contrast, we can see that in the low frequency range, the modulus of PSA 5 was higher than that of PSA 13. This was because in this frequency range, the polymer chains in PSA 13 were much more loosely packed compared to those in PSA 5 due to its significantly lower gel content. In this case, gel content had a much more significant influence on the modulus than the T_g, which is related to the HEMA content. For the low gel content PSAs, the significant difference in shape of the modulus curves between the PSAs result in very different G" (ω_1 = 42.7 Hz)/G' (ω_2 = 0.0982 Hz) ratios: 16.70, 11.52, 6.42 and 5.80, respectively, for PSA 10, 11, 12 and 13. A significant decrease in the ratios with increasing HEMA content is evident.

As the frequency sweep tests were carried out with a strain of about 1%, the obtained viscoelastic properties represent the linear region of the PSA deformation. However, as the low gel content PSAs all showed cohesive failure during the tack and peel strength tests, the tack and peel strength of these PSAs should definitely be correlated with the viscoelastic properties from the non-linear region, where large strains were involved. It is known that the viscoelastic properties measured in these two regions are different. In addition, these PSAs might have experienced very different strains during the tack and peel tests. However, since we did not have the actual strain exhibited

by the PSAs during the tack and peel strength tests, we did not carry out frequency tests for the non-linear region. In any case, results from the linear region allow us to conclude that decreases in the $G''(\omega_1)/G'(\omega_2)$ ratio with increasing HEMA content were much larger for the low gel content PSAs compared to their high gel counterparts. Therefore, the expected increase in peel strength caused by the increased work of adhesion between the PSA and the testing panel due to the additional amounts of HEMA were roughly balanced by the negative effect on peel strength caused by the decrease in $G''(\omega_1)/G'(\omega_2)$. Thus, the peel strengths of these low gel content PSAs were similar.

The increase in tack with HEMA content for the low gel content PSAs might be due to the improved work of adhesion caused by the presence of HEMA. The slight decrease in tack (at ~4 phm HEMA) observed for the high gel content PSAs was not evident in this case due to the much better deformability of the low gel content PSAs compared with those of the high gel content ones. In addition, by comparing Figures 4.8 and 4.1, we can see that for both the low gel content BA/MMA/HEMA PSAs (PSA 10, 11, 12 and 13) and the PSAs with various BA/MMA weight ratios (PSA 3, 4 and 5), the increase in tack was more significant than that in the peel strength. This phenomenon was explained earlier for PSAs 3, 4, and 5. The same explanation should be applied here for the low gel content BA/MMA/HEMA PSAs. However, in this case, better bonding between the PSA and the testing panel was caused by introducing polar hydroxyl and carboxyl groups in the PSAs; while in the former case it was due to better deformation and flow ability of the PSA.

4.3.7 Effect of HEMA on latex viscosity and emulsifier migration during PSA film formation

While filtering the latexes, it was observed that it took a much longer time to filter latexes containing more HEMA. This implies that the viscosity of the latex increased with HEMA content. The reason might be that at high solid contents such as 47%, the latex particles with average particle diameter around 150 nm are densely packed,[56] so that the polar hydroxyl groups on the particle surface can interact with each other, and therefore increase viscosity.

It is well known that ionic emulsifier (e.g., SDS) can migrate from the bulk latex to the surface during the PSA film drying process.[57] Therefore, increasing viscosity by adding HEMA might decrease the emulsifier migration. Considering the negative influence of emulsifier on the work of adhesion, and accordingly, on tack and peel strength,[58] the PSA performance might also be improved by adding HEMA.

4.3.8 Effect of addition of AA and HEMA plus reduction of emulsifier concentration

We have noted above that the addition of HEMA led to a simultaneous increase in tack, peel strength and shear strength for high gel content PSAs. This was due to improvements to the PSAs' surface properties and increases in their cohesive strength. To confirm this idea, and also to produce PSAs with even better performance, we manipulated the PSA bulk and surface properties by adding both AA and HEMA in the monomer mixture and at the same time, greatly decreasing the emulsifier concentration.

The experiment, run 14, was identical to run 5 except for the monomer emulsion feed composition of BA/AA/HEMA (weight ratio: 96/2/2), SDS (4.25 g) and NDM (0.05

phm) (see Table 4.1 and 4.3) concentrations. The addition of NDM was done to produce a latex with a similar gel content to that of latex 5, in anticipation of the influence of adding AA[24] and HEMA (as discussed earlier) to the BA/MMA monomer mixture. Table 4.3 shows that latex 14 had a similar T_g (-45°C), slightly lower gel content (51 wt%), and higher M_w (443 kg/mol), compared to those of latex 5 (-44°C, 63 wt%, and 315 kg/mol, respectively).

The adhesive performance of PSA 14 was compared to PSA 5; both films were cast with a film thickness of ~33 μm. The tack, peel strength and shear strength of PSA 14 were all significantly larger than those of PSA 5 (see Table 4.3, i.e., 223 vs. 93 N/m for tack, 216 vs. 60 N/m for peel strength, and 41.8 vs. 22.2 for shear strength). The increase in peel strength was much bigger (i.e., 3.6 times) than that resulting from the addition of HEMA alone (see Figure 4.7, i.e. 1.9 times by comparing PSA 8 with PSA5). (Note: In Figure 4.7, the PSA performance was obtained at a film thickness of 60 μm instead of 33 μm). Furthermore, PSA 14 showed similar adhesive performance at a smaller film thickness of 33 μm compared to PSA 8 at a film thickness of 60 μm (i.e., 216 vs. 293 N/m for peel strength and 41.8 vs. 43.7 h for shear strength).

The PSA performance differences between PSAs 14 and 5 can be explained via their viscoelastic properties, shown in Figure 4.11. The bonding (ω_2) and debonding (ω_1) frequencies were corrected according to Equation 4-2 with a film thickness of 33 μm instead of 60 μm. The G”(ω_1 =78 Hz) for PSA 14 and 5 were 119292 and 80954 Pa, respectively, the G’($\omega_2 = 0.179$ Hz) for PSA 14 and 5 were 41214 and 29508, respectively, and the G”(ω_1)/ G’(ω_2) were 2.89 and 2.74, respectively. The slightly higher G”(ω_1)/ G’(ω_2) for PSA 14 was due to its lower gel content. The tack and peel strength

increases of PSA 14 compared to PSA 5 were attributed mainly to the improved surface properties of PSA 14 due to the reduction in emulsifier concentration and the addition of AA and HEMA. The increase in shear strength is consistent with the formation of hydrogen bonds in PSA 14, which resulted higher modulus as shown in Figure 4.11.

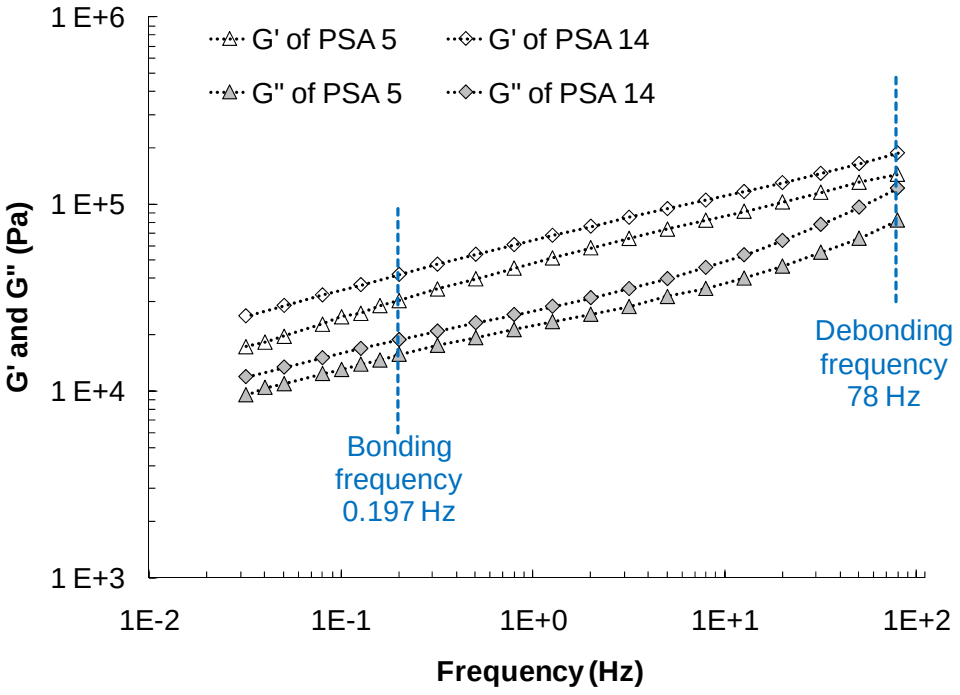

Figure 4.11: Viscoelastic properties of PSAs 5 and 14. (Bonding and debonding frequency corresponds to PSA film thickness of 33 μm)

4.4 Conclusions

In a study of BA/MMA based PSAs, it was found that it was not possible to greatly improve peel strength even at the great sacrifice of shear strength either by using less cross-linker, by shortening monomer feed time, or by changing the BA/MMA monomer weight ratio from 90/10 to 95/5 to 98/2. This was confirmed with similar

$G''(\omega_1)/G'(\omega_2)$ ratios when the BA content was increased, and the similar $G''(\omega_1)/G'(\omega_2)$ values were likely due to the similar polymer microstructures of these PSAs including gel content, M_w and possibly M_c, as well as the narrow changes in T_gs.

Adding HEMA to the BA/MMA polymer appeared to be an interesting option. We found that for high gel content BA/MMA/HEMA PSAs, increases in HEMA content increased tack and peel strength as well as shear strength, for most cases. The reasons might be: (1) The $G''(\omega_1)/G'(\omega_2)$ ratios did not decrease much with the increase in HEMA. This was due to the somewhat densely packed state of the PSA polymer chains at both bonding and debonding frequencies caused by the presence of high amounts of gel. (2) At the same time, the work of adhesion between the PSAs and the testing panels was increased by adding HEMA. This work of adhesion increase was due to the presence of polar hydroxyl and carboxyl groups, which formed via oxidation of the primary hydroxyl groups of HEMA by the initiator. Furthermore, adding HEMA might also have decreased the amount of emulsifier on the PSA surface, due to the higher viscosity, and therefore, the work of adhesion could also have been increased. For low gel content BA/MMA/HEMA PSAs, the peel strength was not significantly affected by the change in the amount of HEMA. The reason was that with the increase of HEMA, the $G''(\omega_1)/G'(\omega_2)$ ratio greatly decreased as the PSA polymer chains were much more loosely packed at the bonding frequency than at the debonding frequency. Therefore, at the bonding frequency, the influence of HEMA on polymer chain packing and correspondingly modulus is more significant than at higher frequencies. As a result, the negative influence of the $G''(\omega_1)/G'(\omega_2)$ ratio on peel strength could no longer be counterbalanced by the positive influence caused by an increase in the work of adhesion.

Improvements to the PSA's surface properties through the addition of AA and HEMA (and greatly decreasing the emulsifier concentration) resulted in a PSA with improved shear strength as well as tack and peel strength. This was even accomplished using a much lower film thickness (33 vs. 60 μm).

In summary, we can forecast that it is possible to simultaneously increase tack, peel strength and shear strength for high gel content PSAs, which are very important commercially. In order to achieve this, we should improve the PSA surface properties and increase the PSA cohesive strength simultaneously. For example, we can introduce monomers with polar groups and similar or even higher T_g (compared to that of the copolymer before adding the polar monomer) in the monomer mixture, and also decrease the amount of emulsifiers.

4.5 Acknowledgements

We thank the Natural Science and Engineering Research Council (NSERC) of Canada and Omnova Solutions Inc. for financial support.

4.6 References

1. István B., Pressure-Sensitive Adhesives and Applications 2004, Marcel Dekker Inc., New York.
2. Jovanovic R, Dubé M. A., Journal of Macromolecular Science. Polymer Review 2004, C44(1): 1-51.
3. Satas D., Handbook of Pressure Sensitive Adhesive Technology 1989, Van Nostrand Reinhold, New York.

4. Elizalde O., Vicente M., Leiza J. R., Polymer Reaction Engineering 2002, 10(4): 265-283.
5. Elizalde O., Vicente M., Plessis C., Journal of Coating Technology and Research 2004, 1(1): 45-51.
6. Gower M. D., Shanks R. A., Macromolecular Chemistry and Physics 2004, 205(16): 2139-2150.
7. Gower M. D., Shanks R. A., Journal of Applied Polymer Science 2004, 93(6): 2909-2917.
8. Gower M. D., Shanks R. A., Macromolecular Chemistry and Physics 2005, 206(10): 1015-1027.
9. Gower M. D., Shanks R. A., Journal of Polymer Science Part B: Polymer Physics 2006, 44(8): 1237-1252.
10. Jovanovic R., McKenna T. F., Dubé M. A., Macromolecular Materials and Engineering 2004, 289(5): 467-474.
11. Jovanovic R., Ouzineb K., McKenna T. F., Dubé M. A., Macromolecular Symposia 2004, 206: 43-56.
12. Jovanovic R., Dubé M. A., Industrial and Engineering Chemistry Research 2005, 44(17): 6668-6675.
13. Jovanovic R., Dubé M. A., The Canadian Journal of Chemical Engineering 2007, 85(3): 341-349.
14. Tobing S. D., Klein A., Sperling L. H., Journal of Applied Polymer Science 2001, 81(9): 2109-2117.

15. Tobing S. D., Klein A., Journal of Applied Polymer Science 2001, 79(14): 2558-2564.
16. Tobing S. D., Klein A., Journal of Applied Polymer Science 2001, 79(12): 2230-2244.
17. Zosel A., Ley G., Macromolecules 1993, 26(9): 2222-2227.
18. Zosel A., International Journal of Adhesion and Adhesives 1998, 18(4): 265-271.
19. Kajtna J, Golob J., Krajnc M., International Journal of Adhesion and Adhesives 2009, 29(2): 186-194.
20. Flanigan C M., Crosby A. J., Shull K. R., Macromolecules 1999, 32(21): 7251-7262.
21 Li L. H., Tirrell M., Korba G. A., Journal of Adhesion 2001, 76(4): 307-334.
22. Yang H. W. H., Chang E. P., Trends in Polymer Science 1997, 5(11): 380-384.
23. Zosel A., Colloid and Polymer Science 1985, 263(7): 541-553.
24. Qie L., Dubé M. A., European Polymer Journal 2010, 46(6):1225-1236.
25. Lovell P. A., El-Aasser M. S., Emulsion Polymerization and Emulsion Polymers 1997, John Wiley and Sons, New York.
26. Šebenik U., Golob J., Krajnc M., Polymer International 2003, 52(5):740-748.
27. Šebenik U., Krajnc M., Colloids and Surfaces A: Physicochemical and Engineering Aspects 2004, 233: 51-62.
28. Sajjadi S., Journal of Applied Polymer Science 2001, 82(10): 2472-2477.
29. Fillatrault T. D., Lewandowski K. M., Anderson K.S., 2008, Patent No.: US0200587A1

30. Lewandowski K.M., Filiatrault T. D., Anderson K. S., 2010, Patent No.: US7645827.
31. Yang J., Lu Y., Kropp J., 2000, Patent No.: US006013722A
32. Brandrup J., Immergut E. H., Grulke E. A., Polymer Handbook 1999, John Wiley and Sons, New York.
33. Sensitive Tape Council, Test Methods for Pressure Sensitive Adhesive Tapes 2004, Northbrook Illinois.
34. Bouvier-Fontes L., Pirri R., Arzamendi G., Macromolecular Symposia 2004, 206: 149-164.
35. Bouvier-Fontes L., Pirri R., Asua J. A., Macromolecules 2005, 38(4): 1164-1171.
36. Plessis C., Arzamendi G., Leiza J. R., Macromolecules 2000, 33(14): 5041-5047.
37. Plessis C., Arzamendi G., Leiza J. R., Macromolecules 2000, 33(1): 4-7.
38. Farcet C., Belleney J., Charleux B., Macromolecules 2002, 35(13): 4912-4918.
39. Ahmad N. M., Heatley F., Lovell P. A., Macromolecules 1998, 31(9): 2822-2827.
40 Gonzalez I., Asua J. A., Leiza J. R., Polymer 2007, 48(9): 2542-2547.
41. Bouvier-Fontes L., Pirri R., Asua J. M., Journal of Polymer Science Part A: Polymer Chemistry 2005, 43(20): 4684-4694.
42. Chauvet J., Asua J. A., Leiza J. R., Polymer 2005, 46(23): 9555-9561.
43. Dubé M. A., Penlidis A., Polymer 1995, 36(3): 587-598.
44. Elizalde O., Arzamendi G., Leiza J. R., Industrial and Engineering Chemistry Research 2004, 43(23): 7401-7409.
45. Tse M. F., Journal of Adhesion Science and Technology 1989, 3(7): 551-570.
46. Pedraza E. P., Soucek M. D., Polymer 2005, 46(24): 11174-11185.

47. He J., Wang Y. F., Lin Q. F., Journal of Macromolecular Science Part A: Pure an Applied Chemistry 2009, 46(4): 405-411.
48. Hooda S., Goyal A. K., Journal of the Indian Chemical Society 2008, 85(8): 818-824.
49. Khan A. K., Ray B. C., Maiti J., Pigment and Resin Technology 2009, 38(3): 159-164.
50. Martin-Rodriguez A., Cabrerizo-Vilchez M. A., Hidalgo-Alvarez R., Colloids an Surfaces A: Physicochemical and Engineering Aspects 1996, 108(2-3): 263-271.
51. Caykara T., Ozyurek C., Kantoglu M., Polymer Degradation and Stability 2003, 80(2): 339-343.
52. Mahdavi H., Taghizadeh S. M., Iranian Polymer Journal 2005, 14(4): 379-385.
53. Oshibe Y., Ohmura H., Yamamoto T., Journal of Adhesion 1994, 47(1-3): 3-16.
54. Chang E. P., Journal of Adhesion 1997, 60(1-4): 233-248.
55. Ferry J. D., Viscoelastic Properties of Polymers 1980, John Wiley and Sons, New York.
56. Horsky J., Quadrat O., Porsch B., Colloids an Surfaces A: Physicochemical and Engineering Aspects 2001, 180(1-2): 75-85.
57. Keddie J. L., Materials Science and Engineering, R 1997, 21(3): 101-170.
58. Zosel A., Schuler B., Journal of Adhesion 1999, 70(1-2): 179-195.

CHAPTER 5

MANIPULATING LATEX POLYMER MICROSTRUCTURE USING CHAIN TRANSFER AGENT AND CROSS-LINKER TO MODIFY PSA PERFORMANCE AND VISCOELASTICITY

Manipulating Latex Polymer Microstructure using Chain Transfer Agent and Cross-linker to Modify PSA Performance and Viscoelasticity

Lili Qie and Marc A. Dubé*
Department of Chemical and Biological Engineering,
Centre for Catalysis Research and Innovation,
University of Ottawa, 161 Louis Pasteur Pvt., Ottawa, Ontario, Canada K1N 6N5

Abstract

Two series of butyl acrylate (BA)/acrylic acid (AA)/2-hydroxy ethyl methacrylate (HEMA) latexes were produced via starved seeded semi-batch emulsion polymerization. The first series, five latexes with gel contents ranging from 0 to 75 wt%, were generated by varying the amount of chain transfer agent (CTA, n-dodecyl mercaptan) in the absence of cross-linker. The second series, two latexes with gel contents of 49 and 74 wt%, were obtained by manipulating the amount of CTA in the presence of a constant cross-linker (allyl methacrylate) concentration. Latexes with similar gel contents, one from each series, were compared with respect to their microstructure, viscoelastic properties and PSA performance. It was found that at similar gel contents, latexes obtained in the absence of cross-linker had larger sol polymer molecular weight (M_w) and molecular weight between cross-linking points (M_c), compared to the latexes generated using both CTA and cross-linker. The different microstructures of latexes with similar gel contents resulted in significantly different viscoelastic properties and shear strength of the pressure-sensitive adhesive (PSA) films cast from the latexes.

5.1 Introduction

Pressure sensitive adhesives (PSAs) are viscoelastic materials. They are permanently tacky and can stick to a substrate under light, finger pressure. Commercial PSAs can be produced via hot-melt techniques, solution polymerization and emulsion polymerization;[1] the latter, being considered more environmental friendly, was used to produce the PSAs in this study.

The performance of PSAs is typically evaluated by tack, peel strength and shear strength. Tack reflects the adhesive's capability to deform and adhere quickly. Peel strength shows its ability to resist removal by peeling. Shear strength measures its ability to resist flow under shear forces and is mostly related to the cohesive strength of the PSA.[2] To achieve desirable performance, commercial PSAs are commonly produced using at least two monomers. One monomer, such as butyl acrylate (BA) and 2-ethyl hexyl acrylate (EHA), will yield a polymer with a low glass transition temperature (T_g) (e.g., <-40°C), and therefore impart good deformability and flow ability to the PSA. In contrast, the other monomer, such as methyl methacrylate (MMA), methacrylic acid (MAA), and acrylic acid (AA), will lead to a polymer with a high T_g (e.g., >100°C), and accordingly endow the PSA with sufficient cohesive strength. In this study, BA/AA/2-hydroxy ethyl methacrylate (HEMA) was chosen as the monomer mixture as a result of a previous study.[3] A starved, seeded semi-batch emulsion polymerization approach was employed in order to ensure homogeneous polymer composition and also constant polymer properties over the course of the polymerization.[4-6]

PSA performance has been shown to depend on PSAs' bulk properties (i.e., PSAs' mechanical properties and viscoelastic properties).[3,7-15] PSAs' bulk properties are affected by the PSAs' T_g, composition, morphology and microstructure (e.g., gel content, molecular weight between cross-linking points (M_c), molecular weight of sol polymers (M_w) and molecular weight between entanglement points (M_e)).[3,9,16-19]

Due to the importance of polymer microstructure, much work has been done to manipulate it by varying polymerization conditions in a seeded semi-batch emulsion polymerization process (e.g., polymerization temperature, monomer composition, and chain transfer agent (CTA), cross-linker and emulsifier concentrations).[5,20-24] The most effective of these are the CTA and cross-linker concentrations. However, most studies have reported on the individual effect of using either CTA or cross-linker. It is not possible to decouple gel content and M_w under these conditions. For example, when cross-linker is added, high gel content latexes can be produced, and for these latexes, M_w always decreases with increasing gel content.[5,24] When CTA is used, gel-free to medium gel content latexes can be obtained. In addition, for these latexes, M_w increases with gel content.[6,20,24]

There are few reports on the effect of simultaneously using CTA and cross-linker to manipulate polymer microstructure. Interesting phenomena, different from that observed while using CTA and cross-linker individually, have been reported.[5,24] For example, Chauvet et al. found that in the presence of a constant amount of cross-linker, adding less CTA could yield a latex with a higher gel content together with a higher M_w over a narrow, high gel content range (i.e., 71 to 88 wt%).[5] In a previous study, we also simultaneously manipulated CTA and cross-linker concentrations to produce latexes, but

over a broader gel content range (40 - 96 wt%).[24] In addition, we provided estimates of M_c, which is a main parameter for describing polymer microstructure, besides gel content and M_w. It was shown, at a constant amount of cross-linker (allyl methacrylate (AMA)), that an increase in the amount of CTA resulted in a lower gel content and looser gel network. However, the M_w was shown to first decrease and then increase with decreasing gel content. Another key finding was that latex with similar gel contents but different M_c and M_w could be produced by changing the CTA and cross-linker concentrations simultaneously. Based on the above two studies, one can forecast that latexes with novel (or unique) microstructures can be produced by using CTA and cross-linker simultaneously. It is of importance to study these novel microstructures by comparing to those generated by using either only CTA or cross-linker, since this will provide very useful information regarding how to improve PSA performance via polymer microstructure optimization. .

In this study, we report on four important concepts: (1) The influence of CTA and cross-linker on the polymerization process and latex properties. (2) A comparison of the microstructures of latexes produced using CTA and cross-linker simultaneously to the microstructures of latexes produced via varying the amount of CTA in the absence of cross-linker. To achieve a consistent comparison, the latexes generated from both techniques should have similar gel contents. This is because microstructure (i.e., M_c and M_w) also depends on gel content.[24] (3) A study of the viscoelastic properties and performance of the PSAs produced from both techniques. Many studies did not provide viscoelastic property measurements for the PSAs, although they are important for discerning the nature of the PSA microstructure and can give insight into PSA

performance. (4) Our attempts to relate the microstructure, viscoelastic properties and PSA performance to each other.

5.2 Experimental

5.2.1 Materials Butyl acrylate (BA), acrylic acid (AA), 2-hydroxyl methacrylate (HEMA), and methyl methacrylate (MMA) monomers, allyl methacrylate (AMA) cross-linker, 1-dodecanethiol (NDM) chain transfer agent (CTA), sodium dodecyl sulphate (SDS) surfactant, sodium bicarbonate ($NaHCO_3$) buffer, potassium persulfate (KPS) initiator and hydroquinone (HQ) inhibitor were all obtained from Sigma Aldrich and were used as supplied. All the above materials were reagent grade except HEMA, which had a purity of 97 wt%. Distilled deionized water (DI-H_2O) was used throughout the study. Ammonia (30 wt% in H_2O for pH control) was obtained from British Drug House. All solvents used in the polymer characterization such as tetrahydrofuran (THF, HPLC grade, EMD Chemicals) and toluene (99.8%, Fisher Scientific), were also used as supplied by the manufacturer. Nitrogen gas (Linde Canada) was used to purge the reactor. PTFE porous membranes with pore size of 0.2 μm, for use in gel content measurements, were purchased from Cole-Parmer Canada.

5.2.2 Polymerization procedure

A seeded semi-batch emulsion polymerization process was adopted to produce all the latexes in this study. It included three stages: a batch stage to produce seed latexes, a continuous feeding stage to grow latex particles, and a cook stage to react the remaining monomers. The polymerization formulation is shown in Table 5.1. The amounts of CTA

and cross-linker were varied as reported in Table 5.2. To start the polymerization, all the initial charge except for the initiator solution and monomers was added to a one-litre Mettler-Toledo LabMax™ reactor at room temperature. The reactor vessel was made of stainless steel, and equipped with an anchor stirring blade as well as several feeding and sampling ports. The stirring speed was maintained at 250 rpm throughout the polymerization process. The reactor temperature was then increased to 70°C within 30 min, then the monomer mixture and initiator solution were added. The temperature was immediately raised to 75˚C within 5 min, and maintained at 75˚C for 10 min for the seed latex production stage. Next, the monomer emulsion and initiator solution (see Table 5.1) were fed to the reactor using two separate metering pumps at constant rates and feeding times of 2.5 and 3 h, respectively. At the completion of the feed stage, the polymerization was continued for an additional 50 min in order to react the remaining monomers (i.e., the cook stage). The latex was then cooled to below 30°C and HQ was added to quench the polymerization. The latex was then separated into two roughly equal portions. One portion had its pH adjusted to ~3.0 and the other to ~5.5 with ammonia. The solids content of the latexes were adjusted to ~45 wt% by adding DI-H_2O, in order to modify the latex viscosity and therefore produce good PSA films.

Table 5.1: Polymerization formulations for Run 1-7

Ingredients	Initial charge	Feeding (g)	
	(g)	Monomer emulsion	Initiator solution
H_2O	202/15*	89	90
KPS	0.4	-	0.90
BA	11.58	324.48	-
AA	-	6.76	-
HEMA	-	6.76	-
MMA	0.42	-	-
NDM (CTA)	-	0-0.4 phm**	-
AMA (cross-linker)	-	0-0.2 phm**	-
SDS	0.45	4.25	-
$NaHCO_3$	0.05	-	-

Note: (1) *Water used for initiator solution in seed production stage.

(2) **phm = parts per hundred parts monomer

Table 5.2: CTA (NDM) and cross-linker (AMA) concentrations for producing latexes 1-7 as well as the polymer microstructure of latexes 1-7.

Latex ID	NDM (phm)	AMA (phm)	Gel content (wt%)	M_w	M_n	M_c	M_e	x^{**} (wt%)
				(x 10^{-3} g/mol)				
1	0.20	0	0	252	48	-	26	
2	0.15	0	13	470	66	-	22	
3	0.10	0	36	656	78	-	22	4
4	0.05	0	51	443	105	82	21	2
5	0	0	75	217	70	59	21	2
6	0.40	0.20	49	113	28	38	27	24
7	0.20	0.20	74	87	42	20	23	16

Note: x^{**} refers to the weight ratio of sol polymers with size smaller than M_e to the total sol polymers.

During the polymerization process, samples were taken at feed times of 0, 20, 50, 100, 150, and 180 min, as well as at the end of the polymerization. These samples were used to monitor particle growth as well as monomer conversion. The final latex was characterized as discussed below.

5.2.3 Characterization

The polymerization rate during the polymerization process was evaluated by both the instantaneous and overall monomer conversions, which were measured according to a standard gravimetric method.[24]

Latex particle size and size distribution (PSD) were measured with a Dynamic Light Scattering (DLS) instrument (Malvern NanoS Zetasizer). Gel content was tested with a modification of the membrane method by Tobing and Klein.[24] M_w was measured using gel permeation chromatography (GPC); the sol polymer was obtained from the THF solution resulting from the gel content measurement. The GPC calibration curve was generated from 12 polystyrene standards (EasiCal from Polymer Laboratories; range = 162 to 6,035,000 g/mol). The Mark-Houwink parameters of the polymers from Run 1 through 7, K and α, for the universal calibration method were chosen as those of the polyBA, considering the very high BA concentration in the copolymer (96 wt%). The K and α for polyBA are 1.1×10^{-4} dL/g and 0.708 respectively.[33]

M_c was tested in accordance with the method reported previously.[24] In the M_c calculation for polymers from Run 1-7, the polymer density (ρ_p = 1.06 g/cm^3) and solubility parameter (δ_1 = 8.9 (cal/cm^3)$^{1/2}$) of polyBA were used as the latexes were composed of 96 wt% BA. M_e was calculated with a previously reported method (ref. 24)

using the value of monodisperse polyBA, M_e = 208 kg/mol, for the calculations. The T_g was measured with a differential scanning calorimeter (Model Q1000 from TA Instruments) with a temperature sweep range of -80 to 80°C in order to avoid promoting reaction between AA and HEMA at elevated temperatures.

PSA performance including loop tack, peel strength and shear strength were evaluated according to the Pressure Sensitive Tape Council standards PSTC-6, PSTC-1 and PSTC-7, respectively.[25] The PSA film thickness was measured as ~33 μm. Further details on the measurement methods are reported elsewhere.[24] In addition, shear strength was also measured using a modified method based on PSTC-7. In this case, the contact area was changed to ½" x ½", and the other testing conditions, such as temperature and shear force, were kept the same.

The PSA viscoelastic properties were characterized using dynamic mechanical analysis (DMA) with a RDA III rheometer (TA Instruments). The geometry used was a pair of 25-mm parallel plates, and the sample thickness was 1.8+/-0.2 mm. The PSA samples were prepared as follows: First, a certain amount of latexes were put in home-made silicon release paper dishes (3.5 cm x 3.5 cm). Then, the latexes were dried for 4 weeks to obtain PSA films with constant weight as well as a thickness of about 0.6 mm. Finally, three of these films were pressed together with the DMA plates to form one PSA sample with a thickness of ~1.8 mm. The frequency sweep tests were performed at 23 and 83°C over a frequency range of about 80 to 0.02 Hz, under a compression mode and with a strain of 1%. A frequency master curve was built using the time-temperature superposition method and with the data at 23^{o}C as the reference.

5.3. Results and discussion

5.3.1 Influence of CTA and cross-linker on the polymerization process and latex properties

The polymerization formulations of Runs 1-7 are shown in Tables 5.1 and 5.2. Runs 1-5 employed only CTA (NDM, 0.2 to 0 phm), while Runs 6 and 7 used CTA (NDM) and cross-linker (AMA) simultaneously.

It was observed that for all runs, particle size increased over the course of the feeding stage of the polymerization, and the particle size remained essentially constant thereafter, until the end of the cooking stage. In addition, no secondary nucleation or coagulation was detected during the entire polymerization process. The final latexes of all runs had z-average particle diameters of ~143+/-3 nm. No significant influence of CTA and cross-linker on particle growth was observed. This is consistent with previous studies.[5,24] Figure 5.1 shows an example of the particle growth trajectory for runs 1 (NDM = 0.2 phm), 4 (NDM = 0.05 phm), and 6 (NDM = 0.4 phm; AMA = 0.2 phm). The particle size was seen to change with polymerization time in a similar manner for all runs. It is noted that the latex samples at feed times of 50 and 100 min from Run 1 appear to have a broader PSD compared to that from Runs 4 and 6. This difference however, is within experimental error judging from the change in PSD from the replicate analyses of samples from Run 4.

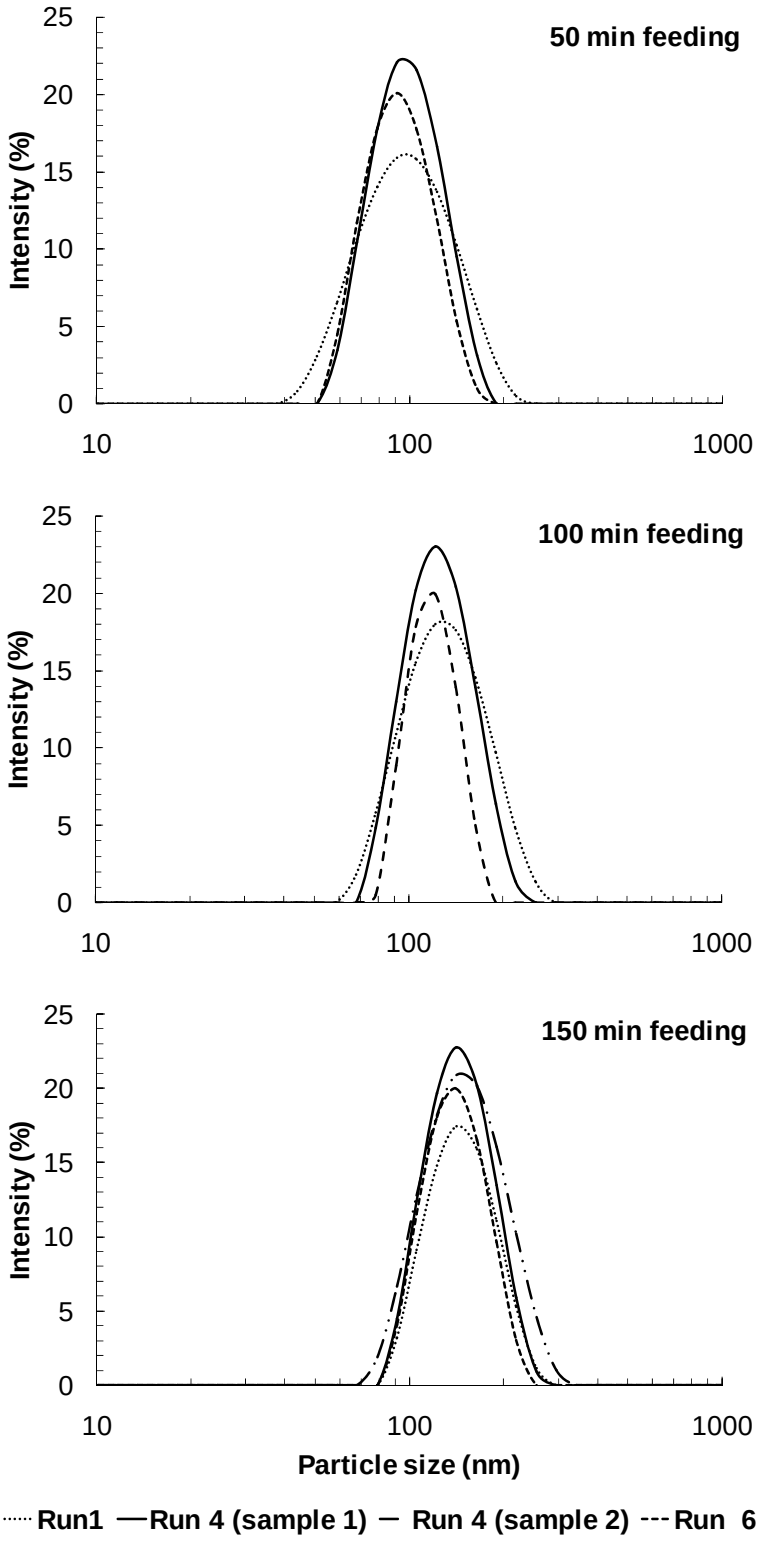

Figure 5.1: Particle growth trajectories for Run 1, 4 and 6.

The instantaneous vs. overall monomer conversion curves of all the runs were almost identical. Conversion profiles for Runs 3 through 5 (as examples) are shown in Figure 5.2. It is clear that CTA and cross-linker had no significant influence on polymerization rate, as reported elsewhere.[5,24] In addition, all runs were carried out under monomer-starved conditions, i.e., the instantaneous monomer conversion was > 90 wt% for most of the polymerization process. Thus, a homogeneous polymer composition was achieved for all runs. This was confirmed by DSC measurements which exhibited only a single peak (T_g of about -45°C) for the polymer sample tested.

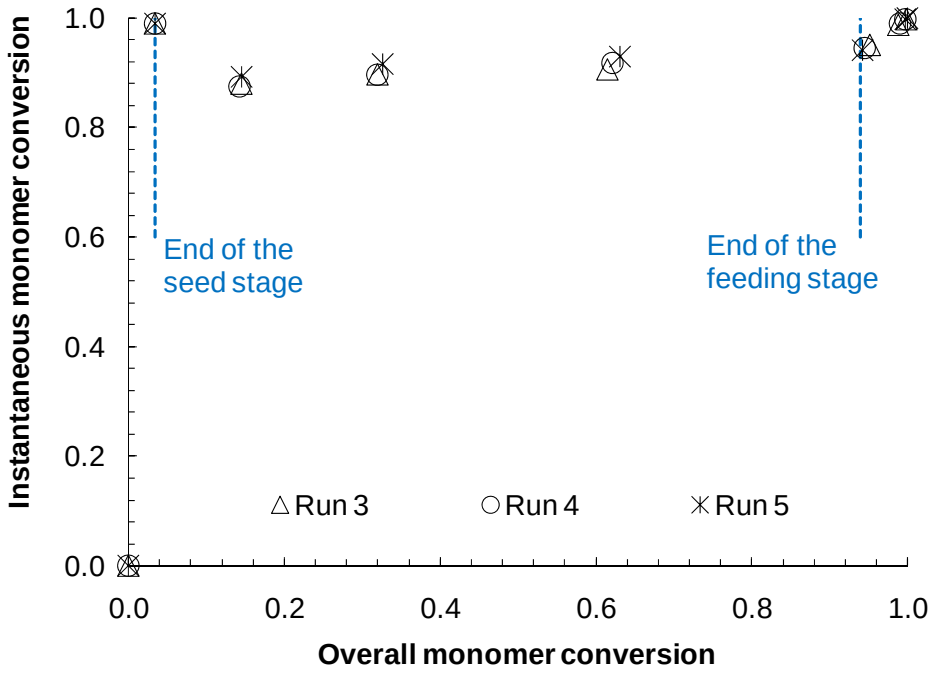

Figure 5.2: Instantaneous vs. overall monomer conversion for Runs 3 through 5.

Polymer microstructure results for the latexes from Runs 1 through 7 are shown in Table 5.2. (Note: The latexes were named according to their run number.) One should

recall that latexes 1 through 5 were produced with varying CTA levels with no cross-linker added, whereas latexes 6 and 7 were produced using both CTA and cross-linker. The result was a series of latexes with markedly different microstructures.

As noted in a previous study, during a polymerization process there are principally two kinds of reactions which control the polymer microstructure. One is the formation of primary polymer chains.[24] The average primary polymer chain size is usually defined as kinetic chain length, and it decreases with an increase in CTA concentration. The second reaction type is the formation of either branched sol polymers or gel polymers. In the absence of cross-linker, some of the primary polymer chains could undergo further growth at the labile tertiary hydrogen sites from the BA units. This growth is initiated by inter-molecular chain transfer at the tertiary hydrogen sites followed by propagation with monomer to produce branched polymer radicals. In the presence of cross-linker, some of the primary polymer chains can also grow into branched polymer radicals via another path, which is usually the dominant one. In this case, the branch growth begins at the pendent double bond sites from the cross-linker unit. In both cases, once formed, these branched polymer radicals can then terminate either by chain transfer to CTA or by combining with each other. The resulting polymers will be gel polymers if their size is sufficiently large. In general, larger primary polymer chains have a greater probability to become gel polymer since they are more likely to undergo further growth due to the presence of more tertiary hydrogen and pendent double bonds in their chains. In contrast, if the resulting polymers are not large enough, they will become sol polymers. In addition, sol polymers can arise from another source, the ungrown primary polymer chains.

The effect of CTA on the polymer microstructure is shown in Table 5.2. In the absence of cross-linker, the decrease in CTA concentration from 0.2 to 0 phm (Runs 1-5) resulted in an increase in gel content from 0 to 75 wt%, as well as a decrease in M_c. This was because less CTA led to the generation of larger primary polymer chains and a correspondingly higher probability for these chains to grow into gel polymers. In contrast, the M_w first increased from 252 kg/mol (i.e., at 0.2 phm NDM, gel content: 0 wt%) to a maximum of 656 kg/mol (i.e., at 0.1 phm NDM, gel content: 36 wt%) then decreased to 217 kg/mol (i.e., at 0 phm NDM, gel content: 75 wt%). This change in M_w can be explained as follows. In the CTA concentration range 0.2 to 0.1 phm, most of the primary polymers became sol polymers, accounting for the low gel content of the latexes. Since the primary polymers became larger with the decrease in CTA concentration, the sol polymer also became larger (i.e., larger M_w). In contrast, when the CTA concentration is smaller than 0.1 phm, most of the primary polymers, especially the larger ones, became gel polymers, accounting for the high gel content; while the other, smaller ones became sol polymers. As with the decrease in CTA concentration, more larger primary polymers became gel polymers, resulting in higher gel content, therefore the sol polymers became smaller (i.e., smaller M_w).

The influence of the cross-linker can be seen by comparing the latex microstructure of Runs 7 and 1, which employed the same amount of CTA (NDM, 0.2 phm), but a different amount of cross-linker (Run 1: 0 phm AMA; Run 7: 0.2 phm AMA). From Table 5.2, one can observe that the addition of 0.2 phm AMA significantly increased the gel content from 0 to 74 wt%. At the same time, the M_w greatly decreased from 252 to 87 kg/mol. These changes, caused by adding cross-linker at identical CTA

concentrations, were similar as those reported changes resulted by adding cross-linker in the absence of CTA.[4-5,23-24] Thus, the addition of cross-linker significantly increased the opportunity for primary polymer chains, especially the larger ones, to engage in further growth due to the introduction of double bonds. Most of these primary polymer chains grew into gel polymers, and therefore the gel content greatly increased and M_w decreased.

Comparing Run 6 to Run 7 allows us to observe the effect of CTA on the polymer microstructure in the presence of the same amount of cross-linker (AMA: 0.2 phm). From Table 5.2, one can observe that increasing the amount of CTA from 0.2 (Run 7) to 0.4 phm (Run 6) led to a decrease in gel content from 74 to 49 wt%, an increase in M_c from 20 to 38 kg/mol, and an increase in M_w from 87 to 113 kg/mol. With a smaller amount of CTA, the average size of the primary polymer chains in Run 7 was relatively larger than that in Run 6. Due to their larger average size, most of the primary polymer chains in Run 7 (i.e., the larger ones) underwent further growth and eventually became gel polymers, while a small amount of these chains (i.e., the smaller ones) became sol polymers. In contrast, because the primary polymers in Run 6 were significantly smaller, the majority of the chains did not become gel polymer even after multiple further growths at the pendent double bonds and then termination. Instead they grew into highly branched polymers and became sol polymer together with those ingrown small primary polymer chains. Thus, the M_w of latex 6 was larger than that of latex 7. This presence of branched sol polymers was also reflected in the breadth of the molecular weight distribution (MWD): polydispersity index (PDI) for latex 6 = 4.0 and PDI for latex 7 = 2.1.

The larger M_c of the gel of latex 6 can be explained as follows. During the polymerization, the branched polymer radicals generated via further growth of primary

polymers could be terminated with other branched polymer radicals. In this case, the double bonds from which the branched radicals grew became cross-linking points, if the resulted polymer is sufficiently large as gel polymer. The branched polymer radicals could also be terminated by chain transfer to CTA, and in this case, the corresponding double bonds connected to the branched radicals will turn into branching points. As Run 6 used more CTA, more double bonds became branching points instead of cross-linking points. Accordingly, the M_c of the gel of latex 6 was larger than that of latex 7.

Comparing Run 4 to Run 6 and Run 5 to Run 7, one can see that latexes with similar gel contents but much smaller M_w and M_c can be produced by simultaneously increasing the CTA and cross-linker concentrations (see Table 5.2). The MWD of the sol polymers of these latexes are shown in Figure 5.3. To explain these microstructural changes, one can refer to the polymerization process analysis explained earlier. At higher CTA concentrations, the average size of the primary polymer chains would be much smaller and this would lead to a much smaller $M_{w.}$ At higher cross-linker concentrations, more pendent double bonds would be present in the primary polymer chains. As a result, there would be more cross-linking points in the final latex polymers and hence, M_c would be lower. If one increases the concentrations of CTA and cross-linker simultaneously, the effect of increasing the CTA concentration could counterbalance that of increasing the cross-linker concentration with respect to the gel content under appropriate conditions. Therefore, latexes with similar gel contents could be produced.

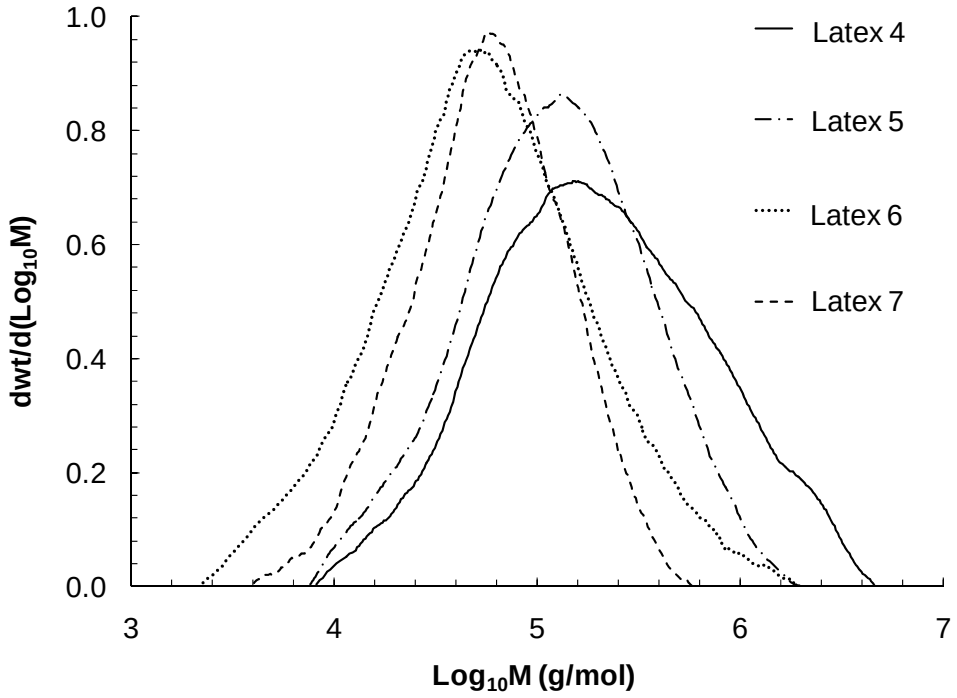

Figure 5.3: Molecular weight distribution of the sol polymers of latex 4 through 7.

5.3.2 Influence of latex pH and PSA microstructure on PSA viscoelastic properties

As mentioned earlier in the experimental part, latexes 1-7 were all divided into two portions, with the pH of one portion adjusted to 3 and the other to 5.5. The PSAs obtained from these latexes are referred to according to the run number and pH of the latex (A: pH = ~3.0, B: pH = ~5.5). The viscoelastic properties of these PSAs were measured via frequency sweeps using DMA. It was found that increasing the latex pH from 3 to 5.5 did not significantly affect the viscoelastic properties of the corresponding PSAs. Hereafter, for the purpose of consistency, the viscoelastic properties were reported only for the PSAs made from latexes with pH of 5.5.

The frequency sweep master curves built by using data at 23°C as the reference are shown in Figures 5.4 through 5.6. The tested range was from about 10^{2} to 10^{-3} Hz because PSA performance is related to the viscoelastic properties exhibited in this range.[11-12]

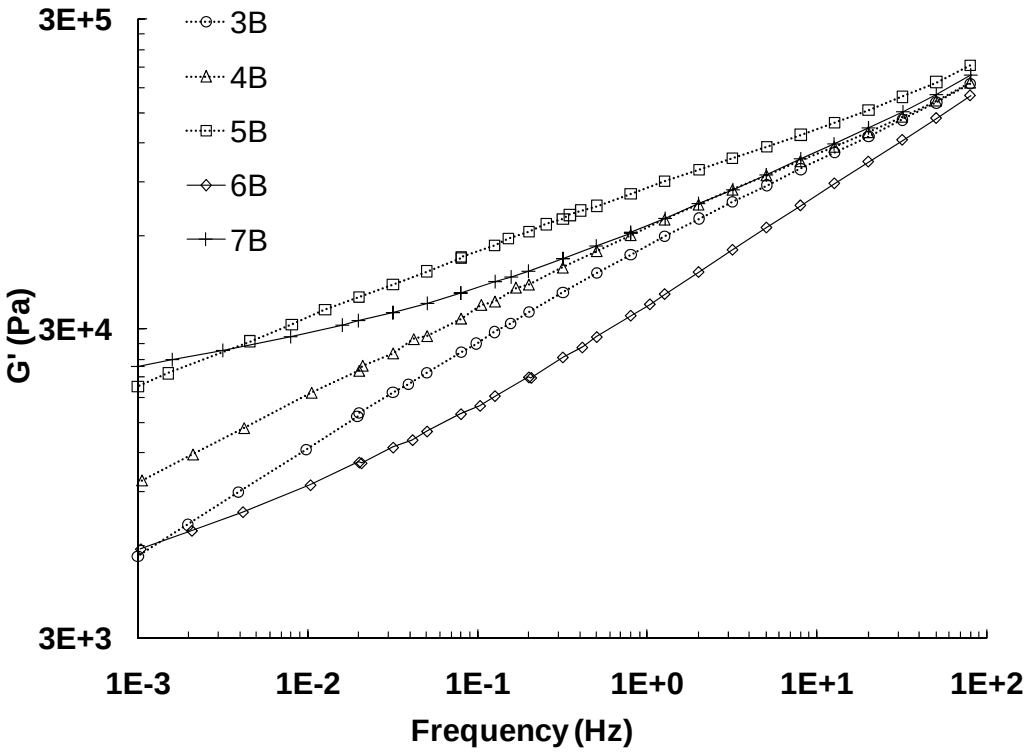

Figure 5.4: Storage moduli of PSAs 3B through 7B.

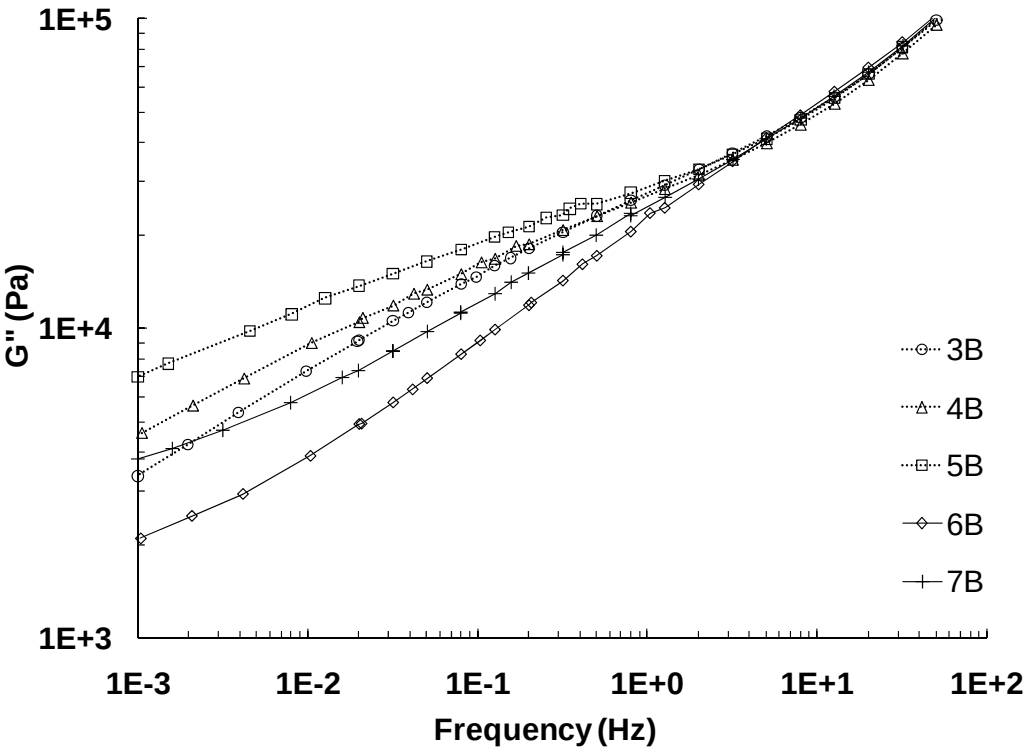

Figure 5.5: Loss moduli of PSAs 3B through 7B.

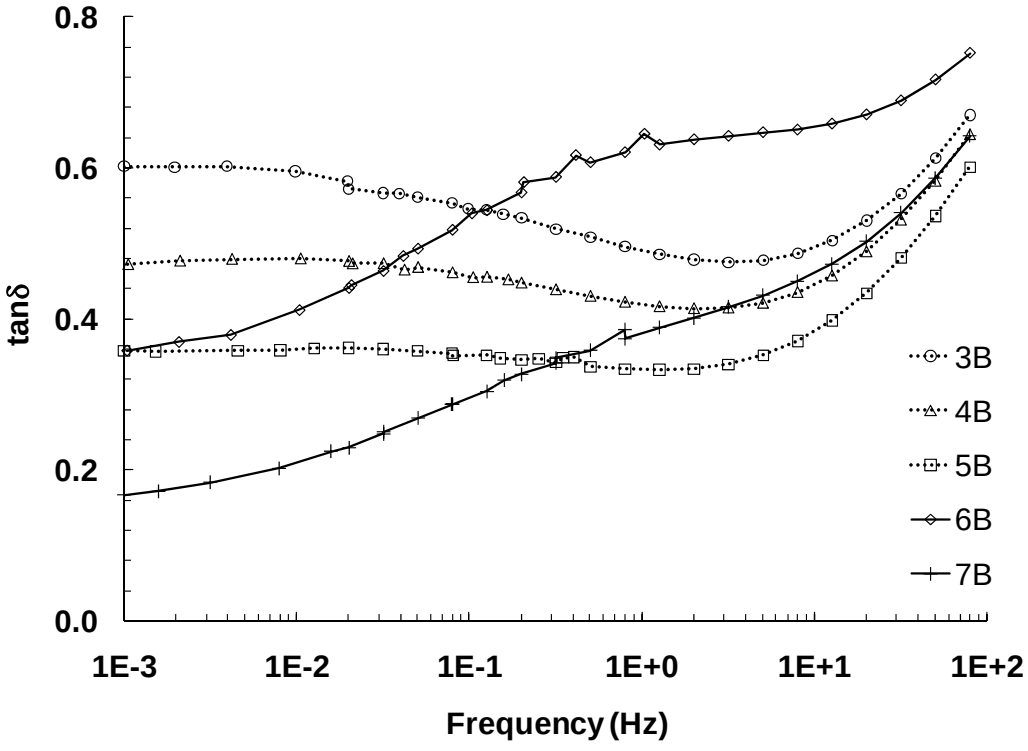

Figure 5.6: tanδ of PSAs 3B through 7B.

When analyzing viscoelastic data, it is important to be aware of the following five general principles related to PSAs and the DMA testing method. First of all, higher frequencies correspond to shorter times when a dynamic force is used. Secondly, PSA polymers typically contain many movable units of greatly varying sizes. These can be classified by increasing size as: the chemical bonds in the polymer chains, small polymer chain segments either at the end or middle of sol and gel polymer chains, large sol and gel polymer chain segments or even very small whole polymer chains (all $<M_e$), and very large polymer segments of sol and gel polymers or some whole polymer chains (all $>M_e$). Each movable unit has its own relaxation time (τ), and the size order shown above corresponds to increasing relaxation times. In addition, for similar size segments (e.g., small end and middle chain segments), those with higher flexibility (i.e., the chain end segments) correspond to a smaller τ.

Thirdly, the strain experienced by a PSA polymer (γ) is the sum of the individual strains (γ_i) of all of the moving units:

$$\gamma = \sum_i \gamma_i(\tau, t, T, \sigma) \tag{5-1}$$

where τ is the relaxation time, t is the time the force acts on the PSA, T is the temperature, and σ is the force exerted on the PSA. From Eq. 5-1, one can note that under different conditions, the contributions of each moving unit to the total strain may vary. At constant temperature, if a certain force is exerted on a PSA, the much smaller moving unit ($\tau << t$) can reach an equilibrium state within a much shorter period of time but with a

resulting, much smaller equilibrium strain and a correspondingly smaller contribution to the total strain. For a much larger moving unit ($\tau >> t$), its strain contribution will be negligible because it does not have sufficient time to move and thereafter develop a strain. Therefore, the main contribution to strain arises from the moving units which have relaxation times (τ) close to *t*.

The fourth principle concerns the various zones of the viscoelastic curve. In the plateau zone (i.e., ~80 to 0.3 Hz for PSA 5B), large polymer chain segments and very small whole polymer chains (all $<M_e$) have τ comparable to *t*. In the terminal region (e.g., ~0.3 Hz to 0.001 Hz for PSA 5B), very larger chain segments in either gel or sol polymer (all $>M_e$) and most of the whole polymer chains, have τ comparable to *t*. We hypothesize that in general, the above mentioned proximity of the τ of a certain moving unit to the *t* at a certain frequency applies even for PSAs without a plateau region but similar T_g. For example, if a PSA has a very large amount of very small sol polymers, it might not show a plateau zone due to lack of sufficient entanglements between polymer chains. However, the very small sol polymers ($<M_e$) in this PSA should still have τ close to *t* in the plateau region.

The fifth and last principle is that PSA is a viscoelastic material and under a dynamic shear force it will show the characteristics of both a solid (elasticity) and a liquid (viscous flow). The storage modulus (G') corresponds to the former and measures the energy stored and recovered, while the loss modulus (G") corresponds to the latter and measures the energy dissipated or lost.

With Figures 5.4 through 5.6, we can compare PSAs 3B, 4B and 5B, which had increasing gel contents, and were all cast with latexes produced in the absence of cross-

linker. At any given frequency, the moduli increased with gel content, and the magnitude of the increase was larger at lower frequencies, except for G" at the very early stage of the plateau zone. This phenomenon of moduli change with gel content is well known.[16] This arises because, with an increase in gel content, the PSA has a greater capacity to resist deformation by shear forces. The larger moduli differences at lower frequencies (i.e., 1 x 10^{-3} Hz) compared to that at higher frequencies (i.e., 80 Hz) are related to the disentanglement of the polymer chains at the lower frequency range, which lies in the terminal flow region. A PSA containing less gel undergoes greater disentanglement compared to PSAs with higher gel contents. Hence, its resistance to deformation decreases much more than the higher gel content PSA. As mentioned earlier, G" exhibited unique behavior in the range of ~80 to 10 Hz, where the G" of these PSAs were very similar, and did not exhibit influence from the polymer microstructure. This phenomenon was probably associated with the well known delayed behavior of G" compared with that of G'.[16] In the very early stage of the plateau region (i.e., 80 to 10 Hz), G' already shows the influence of polymer microstructure, while the G" does not and still behaves as in the glass transition zone. Figure 5.6 shows that the tanδ of PSA 3B through 5B increased with a decrease in gel content, and the magnitude of the increase was greater at lower frequencies. The larger tanδ of the lower gel content PSAs was due to its more liquid-like behavior. The much larger tanδ differences at lower frequencies also relate to polymer chain disentanglement which occurred in this region. Comparing PSAs 6B and 7B (see Figures 5.4-5.6), which were generated from latexes produced with both CTA and cross-linker, one can observe the same influences of gel content on moduli and tanδ.

The viscoelastic properties of PSAs with similar gel contents, but different M_c and M_w, have not been reported previously. From Figures 5.4 and 5.5, one can observe that at similar gel contents, the PSAs produced in the absence of cross-linker (i.e., PSA 4B or 5B) showed much larger G' and G" than their respective counterparts (6B or 7B) in almost the entire studied range. The much larger G' and G" was likely due to better entanglement between the microgels by sol polymers in PSAs 4B and 6B. The enhanced entanglements in PSA 4B and 5B, respectively, compared to their counterparts, can be concluded from the following facts: (1) The M_c and M_w of PSA 4B and 5B are respectively much larger than those of PSA 6B and 7B. (2) For PSA 7B, the M_c is smaller than M_e, so the connection between the microgels by sol polymers is almost impossible in this PSA.[27] (3) In PSA 6B, a larger amount of the sol polymers are hyper-branched, and according to Dealy and Larson, these types of polymer chains generally cannot provide good entanglement because of the short segments between branch points.[28] The better entanglement in PSA 4B and 5B led to enhanced cohesive strength and accordingly, larger moduli. In addition, from Table 5.2 and Figure 5.3, one can see that the amount of very small sol polymers (i.e., $< M_e$) in PSA 4B and 5B was very low (i.e., ~2 wt% of the total sol polymers), but much larger in PSA 6B and 7B (i.e., from ~16 wt% to 24 wt% of the total sol polymer). These small sol polymers cannot entangle with other polymer chains. Besides, they act like plasticizers and greatly decrease a PSA's capability to resist deformation. Hence, smaller amounts of very small sol polymers also contributed to the larger moduli of PSAs produced in the absence of cross-linker. The slightly lower G' of PSA 5B, compared to that of PSA 7B at the lower frequency end (i.e., ~0.001Hz) is related to the disentanglement in this terminal flow region. Since there

are more entanglement points in PSA 5B than 7B if no disentanglement occurred as we explained earlier, the loss of entanglement points should be larger for PSA 5B than 7B when disentanglement occurs. Hence, around the lower frequency, the deformation resistance of PSA 5B decreased to the same level of that of PSA 7B, and led to a similar G' at around 0.001 Hz.

From Figure 5.6, one can see that the tanδ curves of PSAs produced by using both CTA and cross-linker (i.e., PSA 6B and 7B) were very different from that produced in the absence of cross-linker (i.e., PSA 3B-5B). First, the tanδ of PSAs 3B-5B all showed a noticeable minimum point (i.e., ~5 Hz), but those of PSAs 6B and 7B did not. The minimum point is often used to identify the midpoint of the plateau zone, a zone which only exists for polymer materials having good entanglements and capable of recoverable stretching. The absence of this minimum point in PSA 6B and 7B further confirmed the presence of fewer entanglements between polymer chains in the PSAs produced by using CTA and cross-linker simultaneously. Secondly, the tanδ curves of PSAs produced using both CTA and cross-linker (i.e., PSA 6B and 7B) were very different from those of PSAs produced in the absence of cross-linker (i.e., PSA 4B and 5B). At the higher frequency range (i.e., ~80 to 0.3 Hz), the tanδ value of PSA 4B and 5B are much smaller than their respective similar gel content counterparts, PSA 6B and 7B. This range roughly corresponds to the plateau zone. In this range, larger polymer chain segments or very small sol polymers (all $<M_e$) have τ similar to t, therefore the strain mainly resulted by their movement. Specifically, for PSA 4B and 5B, the strain was almost totally due to the large polymer chain segments, while for PSA 6B and 7B, a large portion of the strain was due to the very small sol polymers. The reason is that there are significant amounts of

very small sol polymers in PSA 6B and 7B (see Table 5.2). The movement of very large polymer chains ($<M_e$) does not involve disentanglement of polymer chains and therefore movement between whole polymer chains. As a result, most of the exerted energy on the PSAs is recoverable, leading to smaller tanδ for PSAs produced in the absence of cross-linker (i.e., PSA 4B and 5B). In contrast, the movement of very small sol polymer ($<M_e$) will cause relative movement between whole polymer chains, thereby leading to unrecoverable strain and correspondingly larger tanδ for PSAs produced by using both CTA and cross-linker (i.e., PSA 6B and 7B). In the lower frequency region (i.e., ~0.7 to 0.001 Hz), the PSAs produced in the absence of cross-linker (i.e., PSA 4B and 5B) showed higher tanδ than their similar gel content counterparts. This trend is different from what was observed in the higher frequency range. The low frequency range roughly falls in the terminal flow region and disentanglement between polymer chains related to movement of very large polymer chain segments ($>M_e$) could occur. As the M_w and M_c of PSAs produced in the absence of cross-linker (e.g., PSA 4B and 5B) were much larger than their counterparts (i.e., PSA 6B and 7B), PSA 4B and 5B should have experienced greater disentanglement. It is known that disentanglement could dissipate a significant amount of energy. Consequently, in the lower frequency range, the tanδ (the ratio of dissipated energy to stored energy) was larger for the PSAs produced in the absence of cross-linker than their respective similar gel content counterparts.

5.3.3 PSA performance

Latexes 1-5 (pH of 3.0) were cast as PSA films with thicknesses of ~33 μm. Their tack, peel strength and shear strength are shown in Figure 5.7. (Note: PSAs are referred to according to the run number and pH of the latex; A: pH = 3.0, B: pH = 5.5.)

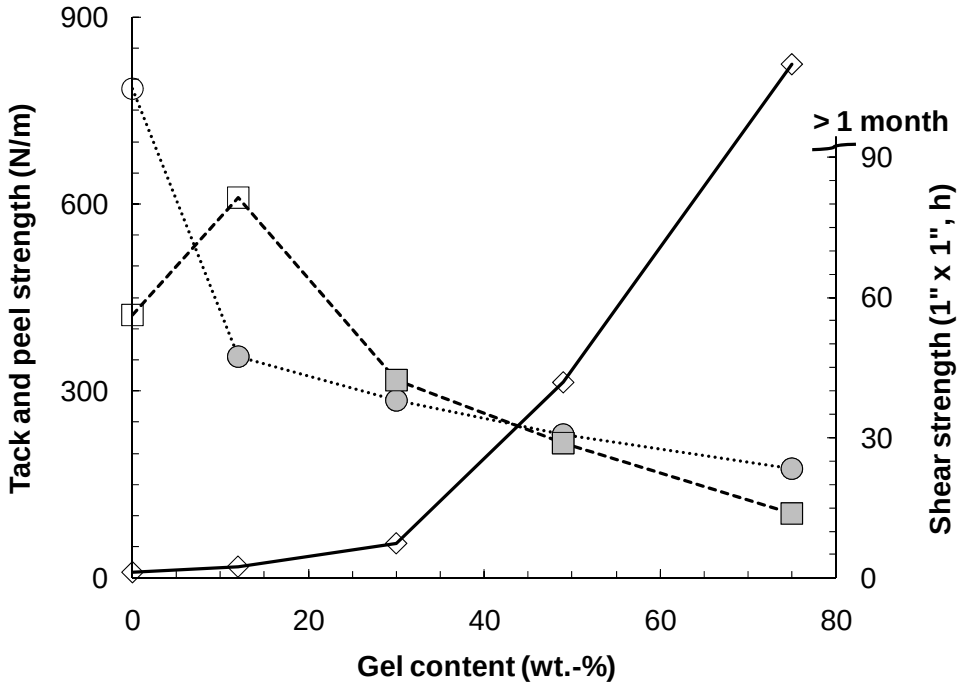

Figure 5.7: Performance of PSA films 1A through 5A.
(Circle: tack; square: peel strength; diamond: shear strength.
For tack and peel strength tests: open symbols refer to cohesive failure while solid symbols refer to adhesive failure).

The tack test showed cohesive failure at a gel content of zero and adhesive failure at larger gel contents (see Figure 5.7). Tack decreased with increasing gel content. Peel strength tests showed cohesive failure at gel contents of 0 and 13 wt%, and adhesive failure at larger gel contents (see Figure 5.7). With the increase in gel content, peel

strength showed an initial increase to a maximum at 13 wt% gel content followed by a decrease. Shear strength increased with gel content. Similar PSA performance with gel content has been reported previously.[29] Higher gel content endows a PSA with lower deformation and flow ability as well as higher cohesive strength. It is known that a PSA's shear strength is mainly affected by its cohesive strength and that higher cohesive strength usually results in larger shear strengths.

Peel strength testing involves both a bonding and a debonding process. It is a function of how well the PSA wets the substrate during the bonding process and how much energy is dissipated during the debonding process. All things being equal (e.g., composition and T_g), a lower gel content endows a PSA with enhanced ability for deformation and flow, and therefore improved wetting during the bonding process. The amount of energy dissipated during the debonding process is primarily affected by the strain experienced by the PSA, which is related to fibril formation and growth; the larger the strain, the larger the amount of energy dissipated.

Among PSAs 1A to 5A, PSA 2A (gel content: 13 wt%) resulted in a maximum peel strength, which implies that this PSA should have experienced a maximum strain during debonding compared to the other PSAs. To confirm this, hereafter we will analyze the strains in light of the following concepts: (1) Fibril formation is associated with elongation of PSA polymers in the tensile direction;[8-9] (2) Higher gel contents and tighter gel networks decrease fibril length.[18] First of all, PSA 2A had a much larger M_w (~$20M_e$, see Table 5.2) compared to that of PSA 1A (~$10M_e$, see Table 5.2; gel content = 0 wt%) as well as a very loose gel structure. M_c could not be measured for PSA 2A, as its swollen gel was very fragile and broke during testing. The gel in PSA 2A would not be

expected to affect fibril formation and growth considering its low concentration and very loose microstructure. Hence, the higher M_w/M_e ratio of PSA 2A should have led to longer fibrils (larger strain) compared to PSA 1A, and accordingly a larger strain. Additional evidence that maximum strain occurred with PSA 2A can be ascertained by comparing PSAs 3A, 4A and 5A. With increasing gel content (from 3A to 5A, see Table 5.2) the gel network became tighter, and beyond a certain gel content (say, >36 wt%), M_w became smaller. This should result in shorter fibrils and smaller strains with increasing gel content. PSA 2A showed higher peel strength than PSA 1A, despite the lower gel content and consequently better wetting during the bonding process of the latter. This was because the positive effect of larger strain during debonding on peel strength dominated the negative effect of less wetting during bonding. Comparing PSAs from 2A through 5A, with the increase in gel content, wetting of the substrate became worse and the dissipated energy also decreased due to the reduction of strain. Therefore, the peel strength decreased with increasing gel content (see Figure 5.7).

Tack testing also involves both a bonding and a debonding process. However, compared to the peel strength test, the tack test features a much shorter contact time and a much smaller applied pressure during the bonding process. Hence, the wetting capability of a PSA affects tack more than peel strength and as expected, tack decreased with gel content (see Figure 5.7). No maximum in tack was observed simply because the energy dissipation effect was not as strong for PSA 2A as in the case of the peel strength test.

To study the influence of polymer microstructure on PSA performance at similar gel contents, PSA 4B was compared to PSA 6B and PSA 5B was compared to PSA 7B as shown in Figure 5.8. It can be seen that PSAs with much larger M_c and M_w (i.e., PSA 4B

or 5B) showed similar tack and peel strength, as well as much larger shear strength, compared to their similar gel counterparts with smaller M_c and M_w (i.e., PSA 6B or 7B). During shear strength testing with a contact area of 1" x 1", both PSAs 5B and 7B did not show any signs of falling even beyond 1 month. Hence, a contact area of ½" x ½" was also used. In addition, with Figure 5.9, one can compare PSA 3B, which was produced in the absence of cross-linker, with PSA 6B, which was produced with both CTA and cross-linker. With lower gel content but significantly larger M_w, PSA 3B (gel content: 36 wt%, M_w: 656 kg/mol) showed not only higher shear strength but also larger tack and peel strength, compared with 6B (gel content: 49 wt%, M_w: kg/mol).

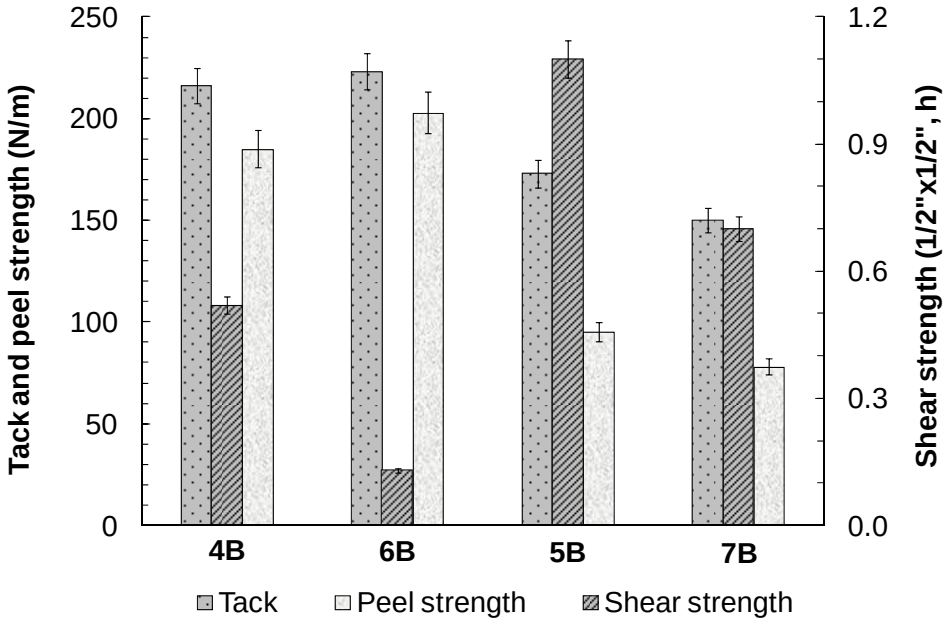

Figure 5.8: Performance of PSAs 4B through 7B.

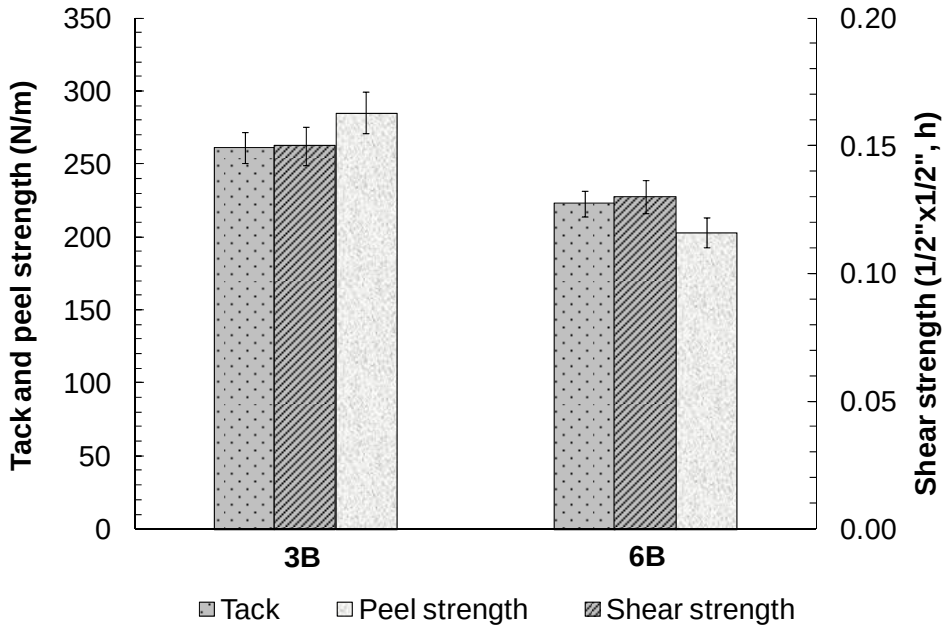

Figure 5.9: Performance of PSA 3B and 6B

Peel strength behavior can be described using Yang and Chang's theory,[30] which describes that peel strength is proportional to G" (debonding frequency, ω_1)/G' (bonding frequency, ω_2):

$$P \propto I \times G"(\omega_1)/G'(\omega_2) \quad (5\text{-}2)$$

where P is peel strength, I is the surface interaction energy between a PSA and substrate, and ω_1 and ω_2 are the debonding and bonding frequency, respectively. Because ω_1 and ω_2 change with film thickness,[30,31] they were corrected for the film thickness used in our study (33 μm) as shown below in Eqs. 5-3 to 5-5. The G"(ω_1)/G'(ω_2) ratios are shown in Table 5.3 for PSAs 3B through 7B.

$$\omega = \frac{2\pi(\text{bonding rupture speed})}{(\text{adhesive thickness})} \frac{\text{rad}}{\text{s}} \tag{5-3}$$

$$\omega_1 = 435 \frac{\text{rad}}{\text{s}} \times \frac{37\ \mu\text{m}}{33\ \mu\text{m}} \times 0.1592 \frac{\text{Hz}}{(\text{rad/s})} = 78\ \text{Hz} \tag{5-4}$$

$$\omega_2 = 1 \frac{\text{rad}}{\text{s}} \times \frac{37\ \mu\text{m}}{33\ \mu\text{m}} \times 0.1592 \frac{\text{Hz}}{(\text{rad/s})} = 0.179\ \text{Hz} \tag{5-5}$$

In Eq. 5-4, 435 rad/s and 37 nm are the reported debonding frequency and film thickness,[31] respectively. 0.1592 is the factor for transfer 1 rad/s to Hz, and 78 Hz and 33 μm are the calculated debonding frequency for our test and the thickness of PSA films produced in this study, respectively. In Eq. 5-5, 1 rad/s and 0.179 Hz are the reported bonding frequency (ref. 30) and the calculated bonding frequency, respectively, for the tests in this study.

Table 5.3 shows the G"(ω_1) and G'(ω_2) data for PSA 3B-7B. Combining Tables 5.2 and 3, one can see that for PSAs with similar gel contents, those with larger M_c and M_w had significantly smaller G"(ω_1)/G'(ω_2) than their counterparts with smaller M_c and M_w (i.e., PSA 4B vs. PSA 6B and PSA 5B vs. PSA 7B). At first glance, the G"(ω_1)/G'(ω_2) and peel strength results shown above appear to contradict Yang and Chang's theory (see Eqn. 5-2), but one should keep in mind that the theory did not consider that PSAs might experience different strains during debonding. The PSAs' viscoelastic data for developing Chang's theory were all obtained at the same and very small strain (i.e., ~1%). However, it is known that PSA could experience very large strain

during the debonding process with either cohesive or adhesive failure, and the strain depends on the PSAs' polymer properties.[7-9,17-18] For example, under proper debonding conditions (e.g., depending on debonding rate or temperature), most commercial PSAs, which could be either cross-linked or not, could experience cavitation at the PSA surface and concurrently, vertical growth of fibrillation in the bulk.[7-8,32] These fibrillations can lead to very large strain, and therefore significant energy could be dissipated during debonding. Hence, Chang's theory might not apply to PSAs which experienced very different strains during the debonding process.

Table 5.3: Viscoelastic properties of PSA 3B-7B.

PSA ID	3B	4B	5B	6B	7B
G"(ω_1=78 Hz) kPa	122.8	119.3	126.2	126.1	125.1
G'(ω_2=0.179 Hz) kPa	32.7	41.2	60.5	20.2	45.1
G"(ω_1)/G'(ω_2)	3.75	2.89	2.09	6.26	2.77
G'(0.002 Hz) kPa	7.0	11.6	22.5	6.7	24.3
G"(0.002 Hz) kPa	4.2	5.5	8.0	2.5	4.3
G*(0.002 Hz) kPa	8.2	12.9	23.9	7.1	24.7
J(0.002 Hz) x 10^5 Pa^{-1}	12.2	7.8	4.2	14.1	4.1

In this study, the strains experienced by the PSAs during debonding were not measured due to equipment limitations. However, it could be predicted that at similar gel contents, the PSAs with larger M_c and M_w would experience larger strains compared with their counterparts with smaller M_c and M_w. It is well known that the formation of fibrillar

structures is associated with elongation of PSA polymers in the tensile direction.[8-9,18] The much larger M_c and M_w of PSAs 4B and 5B, compared with their respective counterparts PSAs 6B and 7B, certainly favor larger elongation, and accordingly the formation of longer fibrils. In fact, we stretched the similar gel content PSAs manually, and found that the PSAs with much smaller M_c and M_w (i.e., PSA 6B or 7B) broke easily and at very small strains. Those with larger M_c and M_w (i.e., PSA 4B or 5B) showed very large strains at break. In addition, Zosel et al. found that fibrillation length decreases with increasing cross-link density, and more importantly, fibrillation will be completely inhibited when M_c is smaller than M_e.[18] Therefore, PSA 7B could not form fibrils (see Table 5.2). It is likely that PSA 5B could not form fibrils neither, considering its very high gel content and also the negative influence of gel content on fibrillation. Judging by the much larger elongation capability of PSA 5B, compared to 7B, we could assume that PSA 5B experienced larger strain than PSA 7B, even though fibrils were not formed in both cases.

Table 5.3 also shows that the PSAs with larger M_c and M_w exhibited much larger storage modulus around the bonding frequency (i.e., $G'(\omega_2)$), compared with their counterparts with smaller M_c and M_w (i.e., PSAs 4B vs. 6B, and PSAs 5B vs. 7B). Hence the former PSAs cannot wet the substrate as well as the latter ones. The negative effect of less wetting on tack and peel strength could be counterbalanced by the positive effect of the larger strains. A good example of this arises from the comparison of PSA 4B to PSA 6B. Figure 5.8 showed that at a similar gel content of 50 wt%, the PSA with larger M_c and M_w (i.e., PSA 4B) showed similar tack and peel strength as its counterparts with smaller M_c and M_w (e.g., PSA 6B) (see Figure 5.8). At a similar gel content of 75 wt%,

PSA 5B (larger M_c and M_w) and PSA 7B (smaller M_c and M_w) also showed similar tack and peel strength (see Figure 5.8). In addition, the above reasoning could also explain the larger peel strength of PSA 3B (36 wt%, M_w 656 kg/mol) compared to that of PSA 6B (gel content: 49 wt%, M_w: 113 kg/mol) (see Figure 5.9). Only in this case, the positive effect of larger strain dominated the negative effect of less wetting.

The PSA viscoelastic properties are useful when considering shear strength differences. Chang reported that shear strength usually increases with G' at 0.01 rad/s (~0.002 Hz).[12] Figure 5.4 and Table 5.3 show that at this frequency, the G' of PSA 4B was significantly larger than that of PSA 6B, while the G' of PSA 5B was slightly lower than that of PSA 7B. At similar gel contents, the much larger shear strength of PSAs with larger M_c and M_w could be explained by Chang's theory (e.g., PSA 4B vs. 6B, gel content: 50 wt%); while this was not the case for greatly differing gel contents (e.g., PSA 5B vs. 7B, gel content: 75 wt%). As G' only relates to the storage energy, it could not fully describe a PSA's resistance to deformation. Creep compliance *J(t)* should be a better indicator for predicting shear strength, as it considers both *G'* and *G"*:

$$J(t) = \frac{1}{G' \times \sqrt{1+tan^2\delta}} = \frac{1}{\sqrt{G'^2+G"^2}} = \frac{1}{G^*} \quad (5\text{-}6)$$

From Eq. 5-6, one observes that the smaller is *J(t),* the larger will be the PSA's capability to resist shear force and accordingly, the larger the shear strength measurement. For example, Table 5.3 shows that at a gel content of 50 wt%, PSA 4B had a much smaller *J(t)* than 6B and Figure 5.8 shows the larger shear strength for PSA 4B. However, at a gel content of 75 wt%, PSA 5B had a very close *J(t)* to that of 7B, which

still could not explain the much larger shear strength of PSA 5B. This suggests that the use of a single frequency may not be the best choice. Thus, the G' and G" between different PSAs were compared over a wide frequency range from the plateau region to the terminal flow region (i.e., 80 to 0.001 Hz) as suggested in a previous study.[11] In Figures 5.4 and 5.5, we note that at similar gel contents, the PSAs with much larger M_c and M_w (i.e., PSA 4B or 5B) yielded a much larger G' and G" in practically the entire region. This was due to the larger number of entanglements possessed by these PSAs produced in the absence of cross-linker. Accordingly, much longer times would be needed to separate the entanglements if a constant shear force was applied and larger shear strengths would result. In addition, the larger shear strength of PSA 3B compared to that of PSA 6B (see Figure 5.9), is consistent with its larger *J(t)* at a single frequency (~0.002 Hz) and also larger G' and G" over a broader region (i.e., 80 to 0.001 Hz).

5.3.4 Additional results and Discussion shown in Appendix

The influence of latex pH on PSA performance was also studied. In addition, for each PSA produced in this study, the shear strength were measured with two different contact areas (i.e., ½" x ½" and 1"x1"). Results of these two effects can be found in the Appendix of this thesis.

5.4 Conclusion

Using CTA and cross-linker simultaneously, as opposed to manipulating one concentration at a time, allows one to expand the range of latex microstructural possibilities. At similar gel contents, the latexes produced by varying the amount of CTA

in the absence of cross-linker showed significantly larger M_c and M_w as well as a much smaller amount of very small sol polymer (e.g., $<M_e$), compared with their counterparts obtained by using both CTA and cross-linker. The larger M_c and M_w led to improved entanglements between the polymer chains in the corresponding PSAs. Accordingly, these PSAs showed an enhanced capability to resist deformation, as reflected by their much larger modulus (i.e., G' and G") in almost the entire studied frequency range. Consequently, at similar gel content, PSAs with larger M_c and M_w exhibited much larger shear strengths than those with smaller M_c and M_w. The tack and peel strength of the above mentioned similar gel content PSAs were very close, despite their very different viscoelastic properties. During tack and peel strength tests, the PSAs with larger M_c and M_w could not wet the substrate as well as their similar gel content counterparts with smaller M_c and M_w, due to their larger elastic moduli at the bonding frequency ($G'(\omega_2)$). Meanwhile, they could have experienced much larger strains during the debonding process, due to their improved capability for elongation. This negative effect of less wetting on tack and peel strength counterbalanced by the positive effect of larger strain, therefore resulted in similar tack and peel strength readings. In summary, at similar gel contents, shear strength could be significantly improved at no sacrifice to tack and peel strength by improving the entanglement between polymer chains in the PSAs.

5.5 Acknowledgements

The authors thank the Natural Science and Engineering Research Council (NSERC) of Canada and Omnova Solutions Inc. for financial support.

5.6 References

1. Jovanovic R., Dubé, M. A., Journal of Macromolecular Science. Polymer Review 2004, C44(1): 1-51.
2. Benedek I., Pressure-Sensitive Adhesives and Applications 2004, 2nd edition, Marcel Dekker, Inc., New York.
3. Qie L., Dubé M. A., International Journal of Adhesion and Adhesives 2010, 30: 654-664.
4. Bouvier-Fontes L., Pirri R., Asua J. A., Macromolecules 2005, 38: 1164-1171.
5. Chauvet J., Asua J. A., Leiza J. R., Polymer 2005, 46 : 9555-9561.
6. Plessis C., Arzamendi G., Leiza J. R., Journal of Polymer Science Part A: Polymer Chemistry 2001, 39: 1106-1119.
7. Verdier C, Piau J. M., Benyahia L., Journal of Adhesion 1998 68: 93-116.
8. Lakrout H., P. Sergot P., C. Creton C., Journal of Adhesion 1999, 69: 307-359.
9. Deplace F., Carelli C., Mariot S., Journal of Adhesion 2009, 85: 18-54.
10. Zosel A., Colloid and Polymer Science 1985, 263: 541-553.
11. Chang E. P., Journal of Ahesion 1997, 60: 233-248.
12. Chang E. P., Journal of Adhesion 1991, 34: 189-200.
13. Christensen S. F., Flint S. C., Journal of Adhesion 2000, 72: 177-207.
14. Gibert F. X., Allal A., Marin G., Journal of Adhesion Science and Technology 1999, 13: 1029-1044.
15. Yarusso D. J., J. Adhesion 1999, 70, p. 299.
16. Ferry J. D., Viscoelastic Properties of Polymers 1980, 3rd edition, John Wiley & Sons, Inc., New York.

17. Lindner A.; Lestriez B.; Mariot S. J., Journal of Adhesion 2006, 82: 267-310.

18. Zosel A., International Journal of Adhesion and Adhesives 1998, 18: 265-271.

19. Zosel A., Ley G., Macromolecules 1993, 26: 2222-2227.

20. Shen H. Z., Zhang J. Y., S. Liu S. J., Journal of Applied Polymer Science. 2008, 107: 1793-1802.

21. Plessis C., Arzamendi G., Leiza J. R., Macromolecules 2000, 33: 5041-5047.

22. Gower M. D., Shanks R. A., Journal of Applied Polymer Science 2004, 93: 2909-2917.

23. Bouvier-Fontes L., Pirri R., Asua J. M., Journal of Polymer Science Part A: Polymer Chemistry 2005, 43: 4684-4694.

24. Qie L., Dubé M. A, European Polymer Journal 2010, 46: 1225-1236.

25. Pressure Sensitive Tape Council, Test Methods for Pressure Sensitive Adhesive Tapes 2004, Northbrook, Illinois.

26. Bouvier-Fontes L., Pirri L. R., Magnet S., Macromolecules 2005, 38: 2722-2728.

27. Tobing S. D., Klein A., Journal of Applied Polymer Science 2001, 79: 2230-2244.

28. Dealy J. M., Larson R. G., Structure and Rheology of Molten Polymers: From Structure to Flow Behavior and Back Again 2006, 1st edition, Hanser Gardner Publications, München, German.

29. Yarusso D. J., Ma J., Rivard R. J., Proceeding of the 22nd Annual Meeting of the Adhesion Scociety 1999, Panama City Beach, 72.

30. Yang H. W. H., Chang E. P., Trends in Polymer Science 1997, 5: 380-384.

31. Tse M. F., Journal of Adhesion Science and Technology 1989, 3: 551-570.

32. Benyahia L., Verdier C., Piau J. M., Journal of Adhesion 1997, 62: 45-73.

33. Brandrup J., Immergut E.H., Grulke E.A., Polymer Handbook 1999, 4th Edition, John Wiley & Sons.

CHAPTER 6

INFLUENCE OF POLYMER MICROSTRUCTURE OF LATEX-BASED PRESSURE SENSITIVE ADHESIVES ON THE PERFORMANCE OF POST-TREATED PSAS

Influence of Polymer Microstructure of Latex-based Pressure Sensitive Adhesives on the Performance of Post-treated PSAs

Lili Qie and Marc A. Dubé*
Department of Chemical and Biological Engineering,
Centre for Catalysis Research and Innovation,
University of Ottawa, 161 Louis Pasteur Pvt., Ottawa, Ontario, Canada K1N 6N5

Abstract

Latex-based butyl acrylate (BA)/acrylic acid (AA)/2-hydroxyethyl methacrylate (HEMA) pressure sensitive adhesive (PSA) films with various microstructures were heated in order to improve their performance. The treated PSA films showed significantly better performance than original latex-based PSA films with similar polymer microstructures. The effect of the heat treatment depended on the polymer microstructure of the untreated PSA films. Decreasing the amount of very small sol polymers (i.e., $<2M_e$) or very large sol polymers (i.e., $>20M_e$) in the untreated PSA films led to treated PSA films with significantly better performance. In addition, simultaneously increasing the size of the sol polymer (M_w) as well as the size of the chain segments between cross-linking points (M_c) of the gel polymer in the original PSAs resulted in treated PSA films with better performance.

6.1 Introduction

Pressure sensitive adhesives (PSAs) are viscoelastic materials. They can stick to a substrate even if only a very small force is exerted upon them. PSA performance is generally evaluated by tack, peel strength and shear strength. Tack measures how well a PSA can bond to a substrate under very short contact time and very small contact force. Peel strength evaluates how strong a PSA can bond to a substrate by peeling it off the substrate. Shear strength characterizes its capability to resist deformation under shear force. In general, an increase in shear strength corresponds to a decrease in tack and peel strength. The reason is that to increase shear strength, the cohesive strength of the PSA must be improved; however, this will lower the PSA's capability to deform and flow, and accordingly, the PSA's capability to wet the substrate.

According to their method of production, PSAs can be classified into three categories: solvent-based, hot melt, and water-based PSAs. Solvent-based PSA films are made by casting a polymer solution, hot melt PSAs by casting melt polymers, and water-based PSAs by casting latexes generated via emulsion or suspension polymerization. It is well known that solvent-based PSAs tend to have much better performance than latex-based PSAs (e.g., much larger shear strength at similar tack and peel strength levels). This is because the gel network is continuous in solvent-based PSAs but discontinuous in latex-based PSAs.[1] Due to their better performance, solvent-based PSAs are widely used in some applications where large shear strengths are needed.

Since the production and use of latex-based PSAs is more environmentally friendly than that of solvent-based PSAs, significant effort has been made in order to improve the performance of latex-based PSAs so that they can replace their solvent-based

counterparts in some applications. The commonly used method for improving the performance of latex-based PSAs is to produce PSAs with functional groups and then post-treat these PSAs to encourage the reaction of these functional groups and transform the discrete gel into a continuous gel structure. Most efforts have been focused on the optimization of the functional groups to simplify the post-treatment process.[2-8] The performance of the post-treated PSA is also related to the polymer microstructure of the original latex-based PSA. To our knowledge, only two such studies have been reported.[1,9] In these two publications, Tobing et al.[1,9] studied the influence of M_w (weight-average molecular weight of sol polymers) and M_c (molecular weight between two adjacent cross-linking points) of the original latex-based PSAs on the performance of treated PSAs. It was found that for gel-free latex-based PSAs, if M_w was larger than $2M_e$, then a continuous gel network could form in its corresponding treated PSAs. As for gel-containing PSAs, if they had M_w larger than $2M_e$ but smaller or close to $20M_e$ as well as M_c larger than M_e, then their discrete microgels could become a continuous gel network by post-treatment. Under the above two conditions, the treated PSAs showed significantly larger shear strength than the untreated PSAs with similar polymer microstructure. However, up to now, the performance of the post-treated PSAs has not been improved to the same level as that of the solvent-based PSAs with similar polymer properties. Therefore more research is still needed to improve the performance of latex-based PSAs via post-treatment.

This study focuses on improving the performance of post-treated latex-based PSA films by optimizing the polymer properties of the original PSAs. M_w is only an average number and cannot reflect the entire molecular weight distribution of sol polymers. Thus,

the influence of the amount of very small sol polymers and very large sol polymers was studied. In addition, similar gel content PSAs with different M_c and M_w were used to study if simultaneously increasing M_c and M_w could lead to the formation of a more perfect gel network in the treated PSAs, and accordingly, larger shear strengths for the treated PSAs.

6.2 Experimental methods

6.2.1 Materials

Butyl acrylate (BA), acrylic acid (AA), 2-hydroxyl methacrylate (HEMA), and methyl methacrylate (MMA) monomers, allyl methacrylate (AMA) cross-linker, 1-dodecanethiol (NDM) chain transfer agent (CTA), sodium dodecyl sulphate (SDS) surfactant, sodium bicarbonate ($NaHCO_3$) buffer, potassium persulfate (KPS) initiator and hydroquinone (HQ) inhibitor were all obtained from Sigma Aldrich and were used as supplied. All the above materials were reagent grade except HEMA, which had a purity of 97 wt%. Distilled deionized (DDI) water was used throughout the study. Ammonia (30 wt% in H_2O for pH control) was obtained from British Drug House. All solvents used in the polymer characterization such as tetrahydrofuran (THF, HPLC grade, EMD Chemicals), toluene (99.8%, Fisher Scientific) and di-iodomethane (99%, Sigma-Aldrich), were also used as supplied by the manufacturer. Nitrogen gas (Linde Canada) was used to purge the reactor. PTFE porous membranes with pore size of 0.2 μm, for use in gel content measurements, were purchased from Cole-Parmer Canada.

6.2.2 Latex preparation

All the BA/AA/HEMA (weight ratio: 96/2/2) latexes used for making PSA films were produced via a starved seeded semi-batch emulsion polymerization approach. The polymerization process included three stages: a short batch stage to make seed latexes, a long feeding stage to further grow the latex particles, and a short cook stage to fully react the remaining monomers in the latexes. The detailed polymerization process and recipes with respect to production of these latexes were provided in Chapter 5. The microstructure of the latex polymers was controlled by varying the amount of CTA and cross-linker used during the feeding stage of the polymerization process. After polymerization, hydroquinone was added to the latex to stop the reaction. A certain amount of ammonia and DDI-water was added to adjust the pH to ~5.5 and a solids content of ~45 wt%.

6.2.3 Preparation of original and post-treated PSA films

To prepare the original PSA films, two steps were taken. First, latexes were coated on a 50 μm thick Mylar sheet with a 30# Meyer rod to make PSA films with thicknesses of ~33μm. Then the films were dried and conditioned (24 h at 23^{o}C and relative humidity of 50%) before being tested. To prepare the post-treated PSA films, the conditioned films were heated via two steps: (1) heating at 90^{o}C for 10 min in order to remove the remaining water in the PSAs; (2) heating at a higher temperature (e.g., 120 or 126^{o}C) in order for the carboxyl and hydroxyl groups from AA and HEMA units to react. These two temperatures were chosen because it was found that at lower temperatures (e.g., 100^{o}C) the reaction was very slow, while at higher temperatures (e.g., 140^{o}C) visible

shrinkage of the backing material of the PSA film (i.e., Mylar sheet) was observed. The post-treated PSA films were also conditioned (24 h at 23^{o}C and relative humidity of 50%) prior to testing.

6.2.4 Characterization Methods

A contact angle method was used to measure the surface tension of the PSA films with VCA Optima contact angle equipment from AST Products Inc. DDI water and di-iodomethane were used as the testing liquids with known surface tensions.

The PSA film surfaces were imaged by atomic force microscopy (AFM) in tapping mode using a Multimode Scanning Probe Microscope (Veeco Instruments) and silicon cantilevers (Vistaprobes from NanoScience Instruments). The tip of the cantilever had a pyramidal geometry and the tip radius was 10 nm. The cantilevers had a resonant frequency of 300 kHz with a spring constant of 40 N/m. Height and phase images were taken in air at ambient temperature. The scan speed was about 0.9 Hz and the scanned area was about 5 μm x 5 μm.

The detailed testing procedures for gel content, M_c, M_w and M_e measurement were described previously in Chapter 5. The tack, peel strength and shear strength were measured according to the Pressure Sensitive Tape Council standards PSTC-6, PSTC-1 and PSATC-7, respectively.[10] Details of the testing procedures were also provided previously.[11] In this study, the shear strength was measured using two contact areas: 1" x 1" and ½" x ½", because it was found that with a contact area of 1" x 1", most of the heated PSAs showed shear strengths too large to be measured within a reasonable time period (e.g., >1 month).

6.3 Results and Discussion

The goal of this study was to improve the performance of post-treated latex-based PSAs by optimizing the polymer microstructure of the original PSAs. For this purpose, a series of BA/AA/HEMA latexes with a variety of polymer microstructures was produced for the preparation of PSA films. The polymer properties of these latexes are shown in Table 6.1. These latexes were produced via two different techniques: one by varying the amount of CTA in the absence of cross-linker; the other by using CTA and cross-linker simultaneously. From Table 6.1, one can see that some of these latexes had very interesting microstructures (e.g., similar gel content but different M_c and M_w). The reasons for the formation of such unique latex polymer microstructures were provided previously in Chapter 5. In this study, the PSA films were named as follows: (1) the original PSA films were named after their latex ID followed by a "B", which identifies that the latex had a pH of ~5.5. "B" was added in order to be consistent with the naming method used previously in Chapter 5; (2) the post-treated PSA films were named after their respective latex ID and pH as well as the heating condition. For example, PSA 5B-H126/11 refers to the PSA film cast from latex 5 with a pH of ~5.5 and heated at 126^{o}C for 11 min.

Table 6.1: Polymer properties of BA/AA/HEMA (weight ratio: 96/2/2) latexes

Latex ID	Gel content (wt%)	M_w	M_n	M_c	M_e
		($x10^{-3}$ g/mol)			
1B[a]	0	252	48	-	26
2B[a]	13	470	66	-	22
3B[a]	36	656	78	-	22
4B[a]	51	443	105	82	21
5B[a]	75	217	70	59	21
6B[b]	49	113	28	38	27
7B[b]	74	87	42	20	23

Note: (1) [a]Latexes 1B through 5B were generated by varying the amount of CTA in the absence of cross-linker (2) [b]Latexes 6B and 7B were produced by using both CTA and cross-linker.

A schematic representation of the latex-based PSA film formation process as well as the polymer microstructures of the original and treated PSA films is shown in Figure 6.1. The polymer microstructure of a solvent-based PSA film is also provided in Figure 6.1. From Figure 6.1, one can see that the solvent-based PSA film has a continuous gel structure (see image a). The latex-based PSA films are formed by casting the latexes (see image b for the polymer microstructure of latexes). The water in the latexes will evaporate and at the same time, some sol polymers of one latex particle will diffuse across the particle boundary. Then, if the latex polymer microstructure is appropriate (i.e., $M_w > 2M_e$ and $M_c \geq M_e$), the diffused sol polymers will entangle with the sol polymer or gel polymers from another particle.[1,9] Meanwhile, the latex particles will deform and the particle boundary will disappear gradually, and finally latex-based PSA films will form (see image c). From image "c" of Figure 6.1, one can see that in latex-based PSA films,

the gel is discrete, and the small microgel polymers are connected together by the sol polymer chains via entanglement. Actually, this is the best scenario, and in some cases, the microgels cannot be entangled together. The discrete gel structure is the cause for the lower shear strength of latex-based PSA films, compared with that of solvent-based PSA films. If the latex-based PSA polymer contains certain functional groups, then by post-treating the PSA film, some entanglement points can be transformed into cross-linking points (see image d). As a result, the discrete gel structure will be turned into a more continuous gel network and the shear strength will be greatly improved. Meanwhile, from image “d” of Figure 6.1, one can see that the continuous gel structure in the treated PSAs is not necessarily uniform. Weak points often exist around the edge of the original microgels in the treated PSAs if the microgels were not originally connected via a sufficient number of cross-linking points. The presence of these weak points can lead to a decrease in the cohesive strength of the treated PSA films, and thus a decrease in shear strength. In order to improve the performance of the treated PSA films, these weak points in their continuous gel network must be eliminated. The way to achieve this is to optimize the polymer properties of the untreated PSA films, so that the microgels will be very well entangled and consequently in the treated PSA films the original microgels will be connected via a sufficient number of cross-linking points.

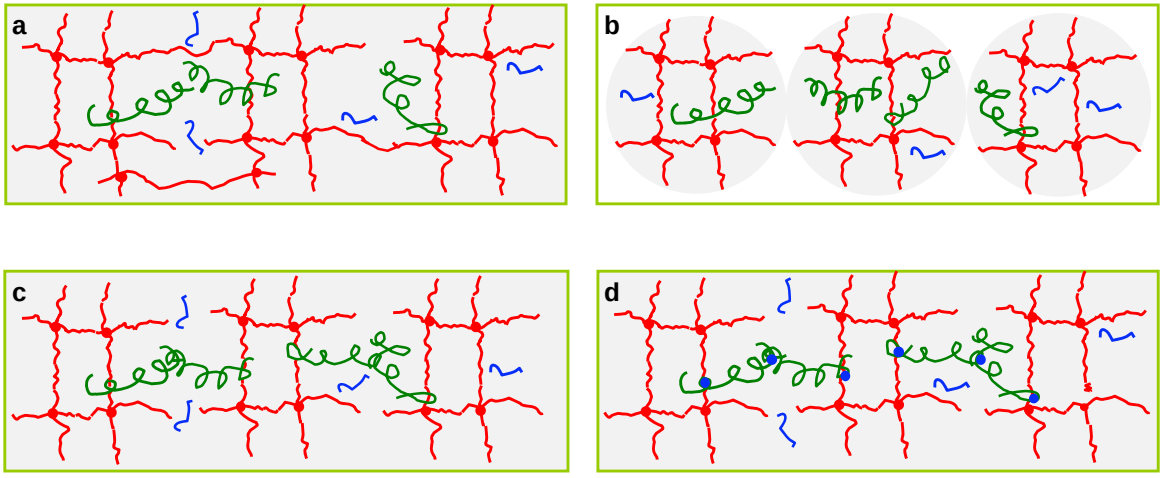

Figure 6.1: Schematic representation of the polymer microstructures of PSA films as well as the latex-based PSA film formation process. (a: solvent-based PSA film, b: latex particles, c: latex-based PSA film, d: post-treated latex-based PSA film.)

(Note: In images a through d, the grids and associated solid dots represent the gel polymers and their cross-link points, respectively; the long curled lines represent sol polymers with size larger than $2M_e$; and the short lines refer to the small sol polymers incapable of entanglement with other sol polymers or gel polymers. The solid dots in image d linking the grids and sol polymers represent newly formed cross-linking points during the post-treatment process for the latex-based PSA films.)

6.3.1 Polymer microstructure and performance changes during the post-treatment process of gel-free PSA 1B

Gel-free PSA 1B was heated in order to study the polymer microstructure and performance changes during the heating process and also to see if the post-treated PSAs have better performance than untreated PSAs with similar polymer microstructures. Two temperatures (i.e., 120 and 126^{o}C) were used to heat the PSA. The polymer microstructures and performance of the original and heated PSAs are shown in Table 6.2, and Figure 6.2, respectively.

Table 6.2: Polymer microstructures of the original and heated PSA 1B

PSA ID	Gel content (wt%)	M_w ($x10^{-3}$ g/mol)	M_n ($x10^{-3}$ g/mol)	MWD
1B	0	252	48	5.2
1B-H120/11	8	532	84	6.3
1B-H120/21	15	643	88	7.3
1B-H120/30	38	425	75	5.7
1B-H126/11	10	534	101	5.3
1B-H126/16	25	424	100	4.2
1B-H126/21	30	382	86	4.4

From Figure 6.2-A, one can see that at a given heating temperature, with the increase in heating time, the gel content increased (e.g., from 0 to 38 wt% at 120^{o}C). From Table 6.2, one can see that with the increase in gel content, M_w first increased to a maximum at a very small gel content (i.e., 15 wt% at 120^{o}C) and then decreased. This trend in M_w with increasing gel content observed with the heated PSAs was the same as that observed with the original PSAs (i.e., 1B-5B) discussed in Chapter 5. Through the reaction between the carboxyl and hydroxyl groups from the AA and HEMA units, two or more polymer chains could be chemically bonded and form one larger polymer chain. If the resulting polymer was sufficiently large, it would become gel polymer; otherwise, it would be sol polymer. If the heating time was not sufficient, most of the sol polymers grew into larger sol polymers while a small amount of them grew into gel polymers. Hence, M_w increased with the increase in gel content. Further increasing the heating time, a significant amount of gel polymers were formed in the treated PSAs, resulting in an increase in gel content. These gel polymers in the treated PSAs were mainly from the

larger sol polymers in the untreated PSAs, as they had more functional groups for reaction and consequently further growth. With the transformation of a significant amount of larger sol polymers into gel polymers, the average size of the sol polymers (M_w) became smaller.

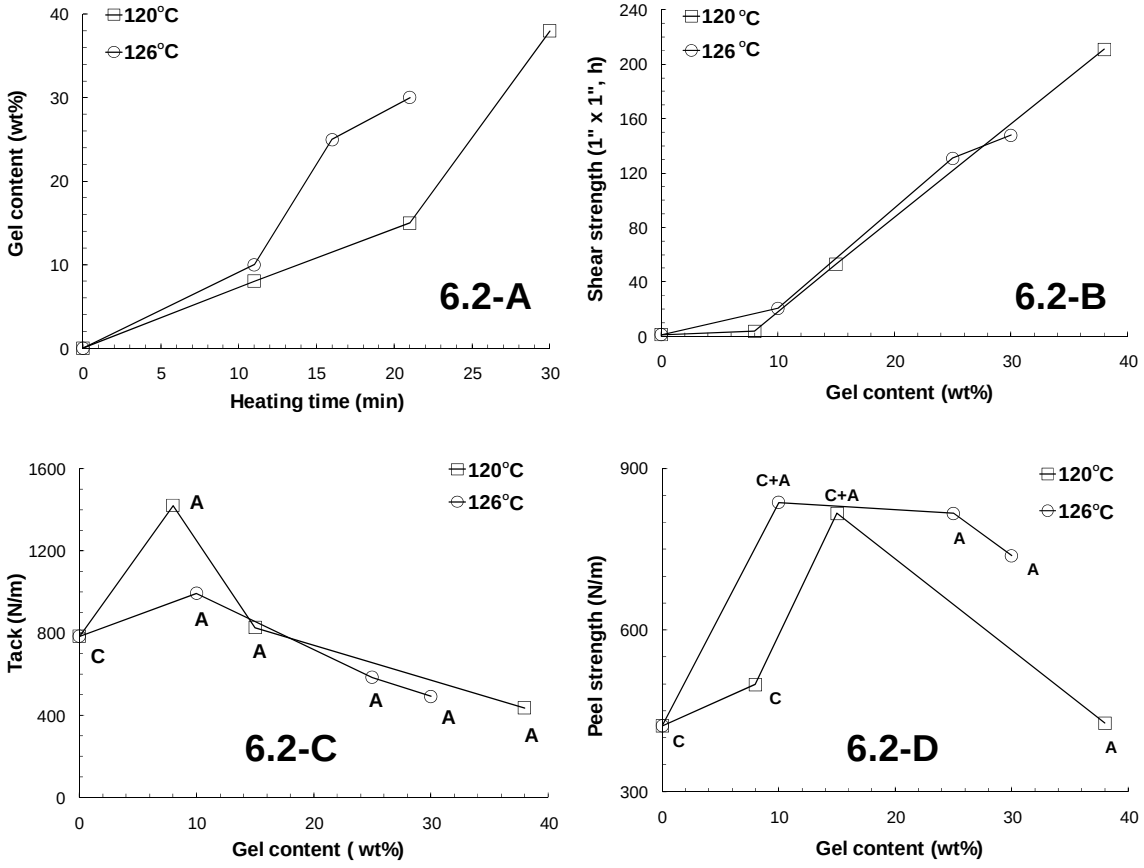

Figure 6.2: A-Gel content change with heating time during the heating process of PSA 1B; B, C, D-performance changes with gel content for the original and heated PSA 1B

(Note: In the tack and peel strength figures of Figure 6.2, "C", "A" and "C+A" refer to cohesive failure, adhesive failure, coexisting cohesive and adhesive failure, respectively.)

Figures 6.2-B, 6.2-C and 6.2-D show that with the increase in gel content, the shear strength increased; while tack and peel strength displayed maxima. This PSA performance trend with increasing gel content is very similar to that previously observed with the unheated latex-based PSAs 1B through 5B in Chapter 5. With the increase in gel content, the cohesive strength of the PSA films was enhanced, resulting in larger shear strength. Meanwhile, larger cohesive strength decreased the PSAs' deformability and flow ability, and led to less wetting of the PSA films on the substrate during the bonding process. In addition, the higher gel content lowered the PSA's capability for elongation,[12] and consequently the PSAs with a larger gel content could experienced a much smaller strain[13-14], compared to the PSAs with a lower gel content. Accordingly, the PSAs with larger gel content dissipated a smaller amount of energy during the debonding process. Less wetting as well as less dissipated energy led to a general decrease in tack and peel strength with increasing gel content. The special case of tack and peel strength increases with gel content observed at very low gel contents (e.g., from 0 to 15 wt%) can be explained as follows: (1) due to the very small gel content, the negative effect of gel on decreasing the PSAs' elongation capability was negligible; (2) when the gel content was low, the M_w increased with gel content as discussed earlier. The increase in M_w endowed the higher gel content PSAs with larger elongation capability compared to the lower gel content PSAs. Consequently, the larger gel content PSAs could have experienced larger strain and dissipated a larger amount of energy during the debonding process. For these very low gel content PSAs, the positive effect of a larger amount of dissipated energy on tack and peel strength might have counterbalanced the

negative effect of less wetting, hence the tack and peel strength increased with gel content.

6.3.2. Comparison of the performance of post-treated PSAs generated from PSA 1B to those of original latex-based PSAs 3B and 4B

The post-treated PSA films (i.e., 1B-H126/16 and 1B-H120/30) were compared to original PSA films 3B and 4B with respect to their polymer microstructure and performance in order to see whether the treated PSA films had better performance than the original ones with similar polymer microstructure. The polymer properties and performance of these PSAs are shown in Table 6.3 and Figure 6.3, respectively.

Table 6.3: Polymer properties of PSA films 3B, 4B, 1B-H126/16 and 1B-H120/30

PSA ID	Gel content (wt%)	M_w	M_n	M_c	M_e
		($x10^{-3}$ g/mol)			
3B	36	656	78	-	22
4B	51	443	105	82	21
1B-H126/16	25	424	100	-	-
1B-H120/30	38	425	75	-	-

From Table 6.3 and Figure 6.3, one can see that at a lower gel content, the post-treated PSA (i.e.,1B-H126/16, 25 wt% gel), showed significantly larger shear strength as well as larger tack and peel strength than the original PSAs 3B and 4B with higher gel contents (i.e., 3B: 36 wt%, 4B: 51 wt%). The better performance of the treated PSA was related to its unique microstructure. Since PSA 1B was gel free and had $M_w > 2M_e$ (see Table 6.1), the gel network in its corresponding treated PSAs should be continuous, while

the gels in the original PSAs 3B and 4B were discrete. Hence, the treated PSA (1B-H126/16) showed significantly larger shear strength than the original PSAs 3B and 4B, despite its lower gel content. The higher tack and peel strength of PSA 1B-H126/16 can be explained as follows: At significantly lower gel content, PSA 1B-H126/16 should have much larger deformability and flow ability, compared with PSAs 3B and 4B. Hence it could wet the substrate better during tack and peel strength testing. Meanwhile, due to its lower gel content, it should have much larger elongation capability and accordingly should have dissipated more energy by forming a larger strain during the debonding process of tack and peel strength testing. Both better wetting and a larger amount of dissipated energy contributed to the larger tack and peel strength of PSA 1B-H126/16.

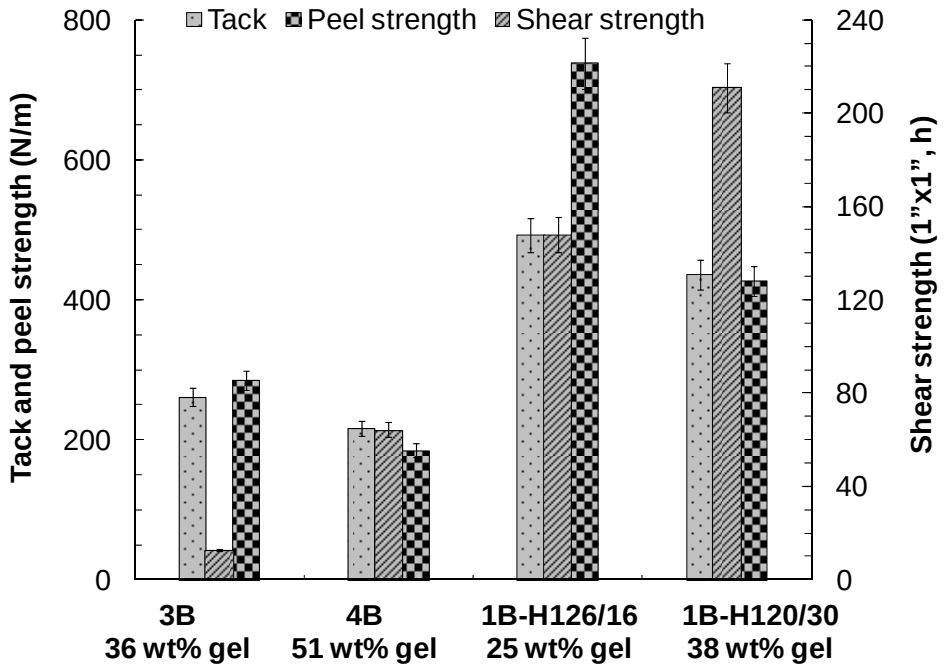

Figure 6.3: Performance of PSA films 3B, 4B, 1B-H126/16 and 1B-H120/30.

From Tables 6.3 and Figure 6.3, one can also see that at similar gel contents (i.e., ~36 wt%), the treated PSA film (i.e., 1B-H120/30) showed significantly larger shear strength as well as larger tack and peel strength, compared to the original PSA films (i.e., 3B). The larger shear strength was due to its continuous gel structure. The much larger tack and peel strength could be caused by two factors: (1) the heated PSA film (i.e., 1B-H120/30) may have had a loose gel network (larger M_c), compared to the original PSA film with similar gel content (i.e., 3B). Hence, it had larger deformability and could wet the substrate much better. (2) The heated PSA film might have had a much smoother surface, due to the possible flow of PSA polymers during the heating process.

6.3.3 Influence of very small sol polymers in the gel-free or low gel content latex-based PSAs on the performance of their treated PSAs

PSAs 1B and 2B were heated to study the influence of very small sol polymer (i.e., < $2M_e$) in the original PSAs on the performance of treated PSAs. The polymer properties of these two PSAs and their treated counterparts are shown in Table 6.4. The performance of the treated PSAs (i.e., 1B-H120/30 and 2B-H126/16) is shown in Figure 6.4.

Table 6.4: Polymer properties of the PSA 1B and 2B as well as their heated counterparts

PSA ID	Gel content (wt%)	M_w ($x10^{-3}$ g/mol)	M_n ($x10^{-3}$ g/mol)	M_e ($x10^{-3}$ g/mol)	*x** (wt%)
1B	0	252	48	26	32
1B-H120/30	38	425	75	-	-
2B	12	470	66	22	15
2B-H126/16	40	394	70	-	-

Note: **x* refers to the weight percentage of the very small sol polymers with sizes smaller than $2M_e$ in the total sol polymers. This number was obtained via GPC.

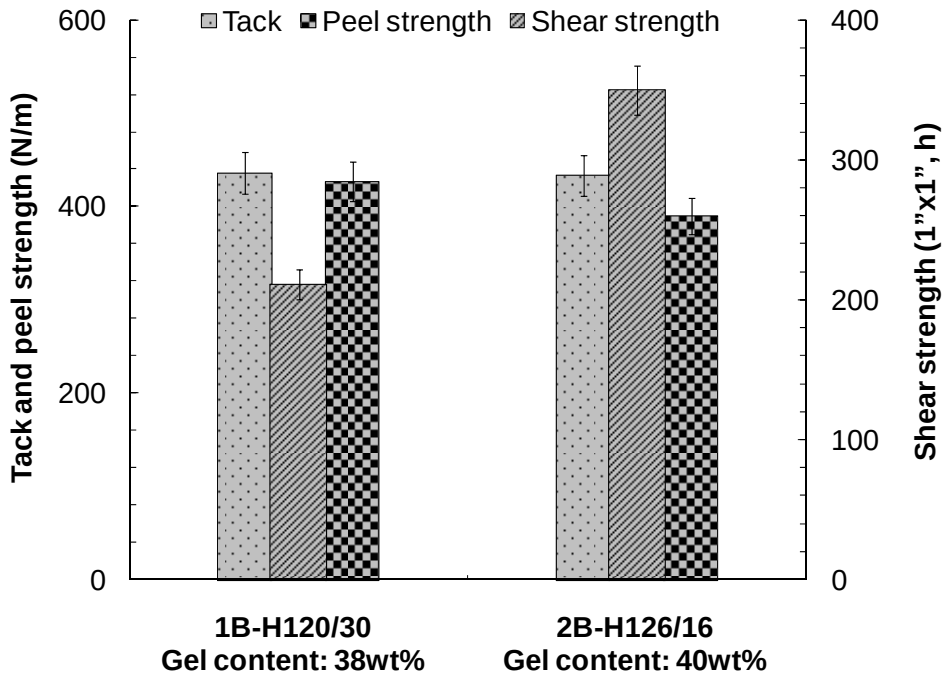

Figure 6.4: Performance of PSA films 1B-H120/30 and 2B-H126/16.

From Table 6.4 and Figure 6.4, one can see that at a similar gel content (i.e.~ 40 wt%), the post-treated PSA 1B-H120/30 had significantly smaller shear strength but similar tack and slightly higher peel strength, compared to the post-treated PSA 2B-H126/16. Considering the close tack and peel strength values, the M_c should be similar too. Otherwise, these two PSAs would have exhibited a significant difference in deformability and wetting capability on the testing panel, resulting in a significant difference in tack and peel strength values. Since PSAs 1B-H120/30 and 2B-H126/16 had similar gel contents and very likely, similar M_c, the significantly smaller shear strength of the former PSA likely resulted because it had a less perfect continuous gel network.

From Table 6.4, one can see that both PSAs 1B and 2B had very low gel contents as well as $M_w > 2M_e$. Hence, their respective treated PSAs (i.e., 1B-H120/30 and 2B-H126/16) should both have continuous gel networks.[1] Table 6.4 also shows that PSA 1B had a much larger amount of very small sol polymers (size < $2M_e$), compared with PSA 2B (i.e., 32 wt% vs. 15 wt%). These very small sol polymers could have a very negative effect on the gel network of the treated PSAs. This can be explained with the help of Figure 6.5. Very small sol polymers with size ≥ M_e but < $2M_e$ only entangled with other polymer chains at one end; while the very small sol polymers with size <M_e cannot entangle with other polymer chains (see image a in Figure 6.5). For example, even if a larger polymer chain formed a loop around a very small sol polymer with size <M_e, they cannot entangle. After treatment, the very small sol polymers with size ≥M_e but <$2M_e$ could become branches (see image b in Figure 6.5). Although these branches were part of the gel network, they could not enhance the network's capability to resist deformation. In addition, the presence of a significant amount of very small sol polymers (i.e., size <$2M_e$) in the original PSA films could cause a very large variance of the chain segments between two adjacent cross-linking points of the gel network in their corresponding post-treated PSAs (see image a and b of Figure 6.5). The formation of such an imperfect gel network would lower the post-treated PSA films' capability to resist deformation, and accordingly, would lead to smaller shear strength for the post-treated PSA films. From the above result and discussion, one can see that increasing the amount of very small sol polymers in very low gel content latex-based PSAs had a significant negative effect on the performance of their treated PSAs.

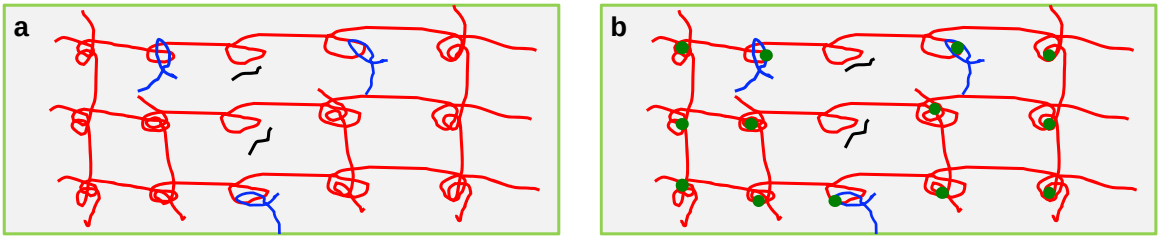

Figure 6.5: Schematic representation of the polymer microstructures of a latex-based PSA film with very small sol polymer (size < $2M_e$) as well as its post-treated counterpart. (a: original PSA film; b: post-treated PSA film)

6.3.4 Influence of simultaneously increasing the M_c and M_w of latex-based PSAs on the performance of their treated PSAs

PSAs 5B and 7B were post-treated under the same conditions (126^{o}C/11 min) to see if simultaneously increasing the M_c and M_w for similar gel content latex-based PSAs would result in better performance for the corresponding treated PSAs. The polymer properties and performance of PSAs 5B and 7B as well as their heated counterparts (i.e., 5B-H126/11 and 7B-H126/11) are shown in Table 6.5.

From Table 6.5, one can see that PSAs 5B and 7B had similar gel contents (~75 wt%), but the M_c and M_w of PSA 5B were much larger than those of PSA 7B. In addition, PSA 5B had $M_c > M_e$ and $M_w > 2M_e$, so the microgels in PSA 5B could be entangled by the sol polymers. As for PSA 7B, its M_w was also larger than $2M_e$ but its M_c was close to M_e. However, since M_c is only an average number of the size of the chain segments between two adjacent cross-linking points, the microgels in PSA 7B might be entangled by the sol polymers. In any case, compared with 7B, the microgels in PSA 5B should be better entangled by the sol polymers, due to its larger M_c and M_w. This has been confirmed by the larger shear strength of PSA 5B compared to PSA 7B (see Table

6.5). (Note: The detailed explanations for the difference in polymer microstructure, viscoelastic properties as well as performance between PSA 5B and 7B were provided previously in Chapter 5.)

Table 6.5: Polymer properties and performance of PSA 5B, 7B and their heated counterparts

PSA ID	Gel content (wt%)	M_w (x 10^3 kg/mol)	M_n (x 10^3 kg/mol)	M_c (x 10^3 kg/mol)	M_e (x 10^3 kg/mol)
5B	75	217	70	59	21
5B-H126/11	81	161	78	53	-
7B	74	87	42	20	23
7B-H126/11	79	73	42	22	-

PSA ID	Tack (N/m)	Peel strength (N/m)	Shear strength (h, 1/2" x 1/2")
5B	176	104	1.10
5B-H126/11	280	190	>336 h (2 weeks)[a]
7B	154	87	0.70
7B-H126/11	209	118	292.80

Note: [a]No sign of shear failure was observed after 2 weeks.

Table 6.5 also shows that the treated PSA from 5B (i.e., 5B-H126/11) had a larger gel content, smaller M_w and slightly smaller M_c compared to the original PSA 5B. Similar polymer microstructure difference was observed by comparing PSA 7B-H126/11 to 7B. The decrease in M_w with increase in gel content resulted as larger sol polymers in the original PSAs were more likely to undergo further growth and thereafter became part of the gel network during the heating process due to their larger size and consequently, the larger amount of functional groups present. The very small decrease in M_c observed after post-treating PSA 5B (i.e., M_c: 59 and 53 kg/mol for 5B and 5B-H126/11,

respectively) was unexpected. However, the gel content only increased by a small amount (i.e., 6 wt%) after post-treating PSA 5B, hence the M_c change could be also small. Also, the M_c of PSA 5B was about ~3M_e, hence some sol polymers trapped inside the microgels in PSA 5B, and some of them also entangled with the microgels (see image "a" of Figure 6.6). The transformation of this kind of entanglement points into cross-linking points during the heating process would tend to decrease the M_c (see Figure 6.6); in contrast, in PSA 5B, some sol polymer chains entangled with two adjacent microgels. If these types of entanglement points transformed into cross-linking points during the heating process, the M_c might tend to increase. The reason is the newly formed chain segment between the two adjacent cross-linking points was as big as the reacted sol polymers, which had sizes (M_w) much larger than the M_c of the original PSA 5B (see Figure 6.6). The two mentioned contradictory effects on M_c might have counterbalanced each other, resulting in a small change in M_c after post-treating PSA 5B.

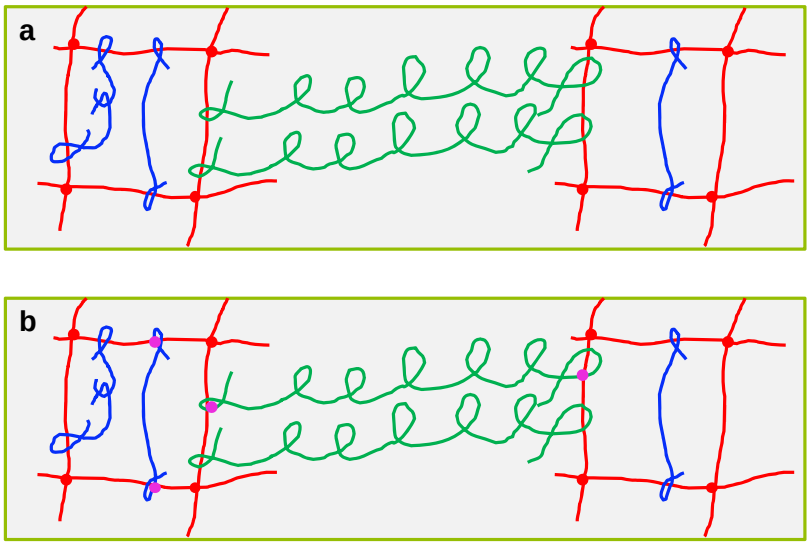

Figure 6.6: Scheme of the M_c change during the post-treatment process of PSA 5B. (a: before post-treatment, b: after post-treatment)

Table 6.5 shows that after post-treating PSAs 5B and 7B, the shear strength significantly increased, despite a small gel content change. For example, PSA 5B (gel content: 75 wt%) had a shear strength of 1.1 h and PSA 5B-H126/11 (gel content: 81 wt%) exhibited a shear strength larger than two weeks at the same contact area. This indicates that the discrete gel network had been changed into a continuous gel network after post-treating PSAs 5B and 7B. In addition, from Table 6.5, one can see that at similar gel content of about 80 wt%, PSA 5B-H126/11 had significantly larger shear strength, compared to PSA 7B-H126/11, despite its larger M_c (looser gel network). Clearly, a more perfect gel network was formed in PSA 5B-H126/11, compared to PSA 7B-H126/11. The reason behind this was that simultaneously increasing the M_c and M_w for similar gel content latex-based PSAs, could let more sol polymers entangle with the microgels and consequently the connection between the microgels were improved. Accordingly, a more perfect continuous gel network would form in its corresponding treated PSA, resulting in higher shear strength.

From Table 6.5, one could also see that after post-treating PSAs 5B and 7B, the tack and peel strength were also significantly increased. For example, the tack and peel strength was 170 and 104 N/m, respectively, for PSA 5B, and 280 and 190 N/m, respectively for PSA 5B-H126/11. This increase in tack and peel strength with gel content was unexpected, as it was found in a previous study that for BA/AA/HEMA (weight ratio: 96/2/2) PSAs, the tack and peel strength decreased with increasing gel content when the gel content was larger than about 15 wt% (see Chapter 5). It is suspected that the PSA surface tension might have changed after post-treatment, since it

is known that it is possible to increase PSA films' peel strength by increasing their surface tension and consequently the chemical interaction energy between the surfaces of these PSA films and substrate.[15-16] Hence, the surface tensions were measured for PSAs 5B and 5B-H126/11 (see Table 6.6). (Note: Details of the surface tension calculation are provided in the Appendix of this thesis.)

Table 6.6: Contact angle measurement data for PSA 5B and 5B-H126/11

PSA ID	Contact angle (^{o})		γ^d	γ^p	γ	I
	θ_1 (H_2O)	θ_2 (CH_2I_2)	($x10^{-3}$ N/m)			
5B	59	72	15	30	45	84
5B-H126/11	97	71	20	6	26	67

Note: γ_P, γ_P^d and γ_P^p are the PSAs' surface tension, and the dispersion and polar components of the surface tension. I is the chemical interaction energy between the surfaces of PSA film and the stainless steel testing panel.

From Table 6.6, one can see that PSA 5B-H126/11, the treated PSA, had smaller surface tension (γ_P) compared with PSA 5B, and consequently a smaller chemical interaction energy (I) between the PSA film and the stainless steel testing panel. Actually, the smaller surface tension of the heated PSA was consistent with the reaction between AA and HEMA during post-treatment. After reaction, the polar carboxyl and hydroxyl groups from AA and HEMA units became non-polar ester groups and tended to decrease the PSA's surface tension. However, considering the very large change in contact angle with water after post-treatment (i.e., 59 vs. 97 degrees) as well as the small amount of reacted AA and HEMA during the heating process, it is suspected that the PSA surface smoothness had changed. It is well known that smoother surfaces can lead to larger

contact angles. In order to confirm this, the surface of PSA 5B, 7B as well as their heated counterparts (i.e., PSA 5B-H126/11 and 7B-H126/11) were characterized via AFM (see Figure 6.7).

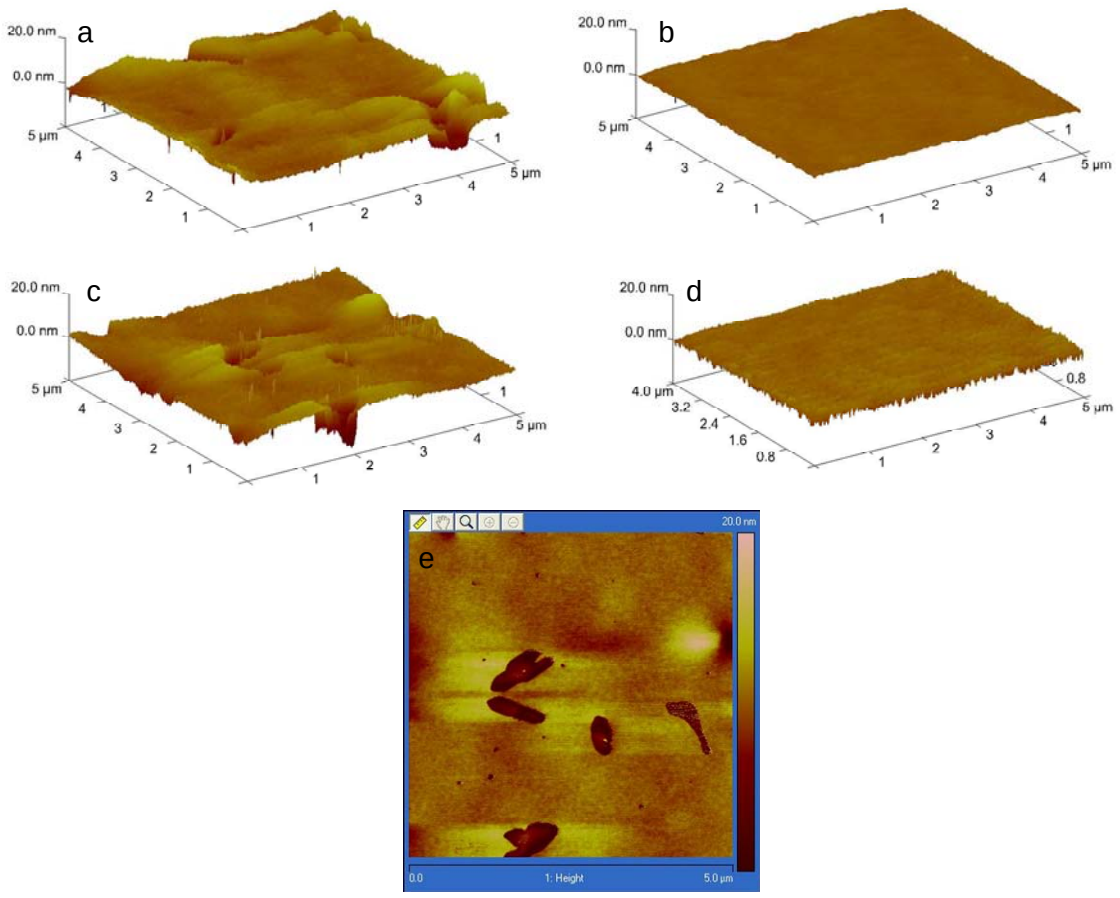

Figure 6.7: Surface images of PSA films 5B, 7B and their heated counterparts, 5B-H126/11 and 7B-126/11. (a-d are 3-D height images. a: 5B, b: 5B-H126/11, c: 7B, d: 7B-H126/11; e is the 2-D image height image of PSA 7B)

From Figure 6.7, one can see that the original PSA films (i.e., PSA 5B and 7B) had some defects, which were too small to be observed with naked eyes, but were detectable with AFM. These defects may have been caused by the slightly lower viscosity

of the latexes, or a very small amount of coagulated latex, which was too small to be removed from the latexes via filtration. In contrast, the heated PSAs (i.e., PSA 5B-H126/11 and 7B-H126/11) did not have these defects. In addition, the surfaces of the heated PSAs were much smoother than those of the unheated ones. Apparently, the PSA polymer flowed during the heating process, resulting in a smoother surface after post-treatment. Hence the post-treated PSAs showed higher tack and peel strength than their unheated counterparts. Moreover, comparing image "b" and "d" of Figure 6.7, one can see that the surface of PSA 5B-H126/11 was much smoother, compared to that of PSA 7B-H126/11. This might also have contributed to the higher tack and peel strength of the former PSA, in addition to their polymer microstructure differences mentioned earlier. The smoother surface of PSA 5B-H126/11, can be explained as follows: Both PSA 5B and 7B had a very large amount of gel polymer (~75 wt%), hence the property of their gel polymers (i.e., M_c) should have a significant influence on the polymer flow during the heating process. PSA 5B had a much looser gel structure (i.e., M_c: 59 kg/mol), compared with PSA 7B (i.e., M_c: 20 kg/mol), hence the microgel polymer of PSA 5B should have expanded more and thereafter flowed much more during the heating process. As a result, the treated PSA from 5B (i.e., 5B-H126/11) showed a smoother surface, compared with the treated PSA from 7B (i.e., 7B-H126/11).

From the above results, one can see that post-treatment can greatly improve the performance of latex-based PSAs. Shear strength can be increased along with tack and peel strength. In addition, simultaneously increasing the M_c and M_w for similar gel content latex-based PSAs, could impart better performance of the treated PSAs (e.g., larger shear strength as well as larger tack and peel strength).

6.3.5 Influence of increasing the amount of very small sol polymers in gel-containing latex-based PSAs on the performance of their treated PSAs

PSAs 4B and 6B were post-treated under the same conditions (126^{o}C/10 min) to study if increasing the amount of very small sol polymer in gel-containing latex-based PSAs (i.e., size <2M_e) could have a significant influence on the treated PSAs. The polymer properties and performance of PSA 4B, 6B as well as their heated counter parts (PSA 4B-H126/11 and 6B-H126/11) are shown in Table 6.7.

Table 6.7: Polymer properties and performance of PSA 4B, 6B and their heated counterparts as well as 5B

PSA ID	Gel content (wt%)	M_w (x 10^3 kg/mol)	M_n (x 10^3 kg/mol)	M_c (x 10^3 kg/mol)	M_e (x 10^3 kg/mol)	*x** (wt%)
4B	51	443	105	82	21	10
4B-H126/11	70	216	73	-	-	-
6B	49	113	28	38	27	48
6B-H126/11	63	109	43	-	-	-
5B[a]	75	217	70	59	21	-

PSA ID	Tack (N/m)	Peel strength (N/m)	Shear strength (h, 1/2” x 1/2”)
4B	216	185	0.52
4B-H126/11	323	236	11.30
6B	223	203	0.13
6B-H126/11	450	270	5.10
5B[a]	176	104	1.10

Note: (1): **x* refers to the weight percentage of the sol polymers with size smaller than 2M_e in the total sol polymers. (2) [a]5B was used as the control sample to compare the performance of latex-based PSAs with that of the post-treated PSAs.

From Table 6.7, one can see that PSAs 4B and 6B both had M_w larger than $2M_e$ and M_c larger than M_e. Hence the microgels could be entangled by the sol polymers in both PSAs. In addition, PSAs 4B and 6B had similar gel contents, but PSA 4B had a much larger M_c and M_w compared to PSA 6B. This is similar to the comparison of PSA 5B to 7B. Another significant difference between PSA 4B and 6B was that PSA 4B had a much smaller amount of very small sol polymers (i.e., size $<2M_e$) (i.e., 10 wt% vs. 48 wt% of the total sol polymers, see Table 6.7). Obviously, due to the larger M_c and M_w as well as a much smaller amount of very small sol polymers, PSA 4B should have had a better entanglement between the sol polymers and microgels, compared to PSA 6B. This is consistent with the significantly larger shear strength of PSA 4B (i.e., 0.52 h vs. 0.13 h). (Note: The detailed explanations with respect to the different microstructures, viscoelastic properties and performance between PSAs 4B and 6B were provided in Chapter 5.)

Table 6.7 also shows that after heating, PSAs 4B and 6B showed increase in gel content and decreases in M_w. Moreover, from Tables 6.7 and 6.5, one can see that after heating under the same conditions (126^{o}C/11 min), PSAs 4B and 6B showed much larger increases in gel content (i.e., 19 wt% and 14 wt%), compared with PSAs 5B and 7B (i.e., 6 wt% and 5 wt%). This occurred because PSAs 4B and 6B had more sol polymers available for further growth into gel polymers. In addition, from Table 6.7, one can see that after heating PSAs 4B and 6B the films showed a significant increase in not only shear strength but also tack and peel strength. Moreover, from Table 6.7, one can see that the treated PSAs (4B-H126/11 and 6B-H126/11) showed significantly larger shear strengths, compared to an original PSA with even much higher gel content (i.e., PSA 5B).

This confirmed that the discrete microgels in PSAs 4B and 6B transformed into continuous gel networks after post-treatment. In addition, the higher tack and peel strength of the post-treated PSAs (i.e., 4B-H126/11 and 6B-H126/11) should also be due to their smoother surfaces, compared with their respective untreated counterparts (i.e., 4B and 6B).

From Table 6.7, one can see that after heating under the same conditions, PSA 4B showed a larger increase in gel content (i.e., ~19 wt%), compared to PSA 6B (i.e., ~14 wt%). This was because PSA 6B has a significantly larger amount of very small sol polymers (i.e., $< 2M_e$), compared to 4B. Some of these very small sol polymers (i.e., $< M_e$) could not entangle with other polymer chains even at one end. Hence, during the heating process, they could not react with other polymers and become gel. Table 6.7 also showed that the heated PSA from 4B (i.e., 4B-H126/11) showed significantly larger shear strength than the treated PSA from 6B (i.e., 6B-H126/11) (i.e., 11.30 vs. 5.10 h). As the gel content difference between these two treated PSAs was small (i.e., 7 wt%), the significantly larger shear strength of PSA 4B-H126/11 should correspond to a more perfect continuous gel network compared to PSA 6B-H126/11. The formation of a less perfect continuous gel network in PSA 6B-H126/11 could be explained as follows: The presence of a significantly larger amount of very small sol polymers (i.e., $< 2M_e$) in PSA 6B should have caused much less entanglement between the sol polymers and the microgels, compared with PSA 4B. Accordingly, the gel network of the treated PSA from 6B (i.e., 6B-H126/11) had more weak points around the edges of the original microgels compared to PSA 4B. Moreover, PSA 4B-H126/11 exhibited significantly smaller tack compared to PSA 6B-H126/11 (323 vs. 450 /m). It is suspected that the larger gel content

of PSA 4B-H126/11 only played a minor role in achieving its much smaller tack, as the gel content difference between PSA 4B-H126/11 and 6B-H126/11 was very small (i.e., ~ 7wt%). The much smaller tack of PSA 4B-H126/11 compared to PSA 6B-H126/11, was likely due to its significantly higher surface roughness. This can be explained as follows: There were equal amounts of sol and gel polymer in PSAs 4B and 6B (e.g., gel content: ~50 wt%). Considering the much larger mobility of the sol polymers, compared with the microgel, the movement of sol polymers occurred during the heating process should have principally caused the surface change of the PSA films. PSA 6B had a significantly larger amount of very small sol polymers and these small sol polymers could have involved much more movement than the larger ones due to their much smaller size and much greater mobility. Hence, the sol polymer in PSA 6B should have flowed much more during the heating process, compared to PSA 4B. Consequently, the treated PSA from 4B (i.e., 4B-H126/11) should have higher surface roughness compared to that of the treated PSA from 6B (i.e., 6B-H126/11). The peel strength of PSA 4B-H126/11 was only slightly smaller than that of PSA 6B-H126/11 (i.e., 236 vs. 270 N/m). The much smaller difference in peel strength observed with PSA 4B-H126/11 and 6B-H126/11 compared with the difference in tack, was because peel strength is not as sensitive to surface smoothness of the PSA films as tack. During peel strength testing, a much longer contact time and also a much larger contact force were used compared to tack testing.

From the above results, one can see that increasing the amount of very small sol polymers in the original gel-containing latex-based PSAs had a significant negative influence on the performance of the treated PSAs. Decreasing the amount of very small sol polymers (i.e., size < $2M_e$) in the original gel-containing latex-based PSAs could lead

to significantly better performance for the treated PSAs. For example, shear strength could be greatly increased only at a small sacrifice of peel strength.

6.3.6 Influence of the amount of very large sol polymer in gel-containing latex-based PSAs on the performance of their treated PSAs

Tobing et al.[1] found that after post-treating a gel-containing latex-based PSA with M_w (604 kg/mol) of about $30M_e$ (M_e: ~20 kg/mol), the PSA's performance could not be greatly improved. Hence they pointed out that if the M_w of a gel-containing latex-based PSA is too large (e.g., > $20M_e$), then the microgel could not be turned into a continuous gel network after post-treatment. Since M_w is only an average number, we decided to study if increasing the amount of very large sol polymer (e.g., size > $20M_e$) in a latex-based PSA under the condition of $M_c > M_e$ and also $2M_e < M_w \leq 20M_e$ will have a significant influence on the performance of post-treated PSAs. For this purpose, PSAs 4B and 5B as well as their heated counterparts were studied. Their polymer microstructure and performance are shown in Table 6.8.

Table 6.8: Polymer properties and performance of PSA 4B, 5B and their heated PSAs

PSA ID	Gel content (wt%)	M_w	M_n	M_c	M_e	*x** (wt%)
		($\times 10^3$ kg/mol)				
4B	51	443	105	82	21	30
4B-H126/21	79	190	72	-	-	-
5B	75	217	70	59	21	12
5B-H126/11	81	161	78	53	-	-

PSA ID	Tack (N/m)	Peel strength (N/m)	Shear strength (h, 1/2" x 1/2")
4B	216	185	0.52
4B-H126/21	299	210	20.20
5B	176	104	1.10
5B-H126/11	280	190	>336 h (two weeks)[a]

Note: (1): * *x* The weight percentage of the sol polymers with size larger than $20M_e$ in the total sol polymers. (2) [a]No sign of PSA falling was observed after 2 weeks.

PSAs 4B and 5B both had $M_c > M_e$ as well as $2M_e < M_w \leq 20M_e$. As we have shown earlier, both PSAs could form a continuous gel network. PSA 4B had a lower gel content and a larger M_w compared with PSA 5B (see Table 6.8). In addition, PSA 4B had a much larger amount of very large sol polymers, compared to PSA 5B (i.e., ~30 vs. 12 wt% of the total sol polymers). From Table 6.8, one can see that at a similar gel content of ~80 wt%, the heated PSA film from 4B (i.e., 4B-H126/21) showed a much smaller shear strength as well as similar tack and peel strength compared with the heated PSA film from 5B (i.e., 5B-H126/11). It seems that tack and peel strength were mainly affected by gel content. Although the M_c of PSA 4B-H126/21 was not measured, based on the significantly smaller shear strength of PSA 4B-H126/21 compared with PSA 5B-

H126/11, one can see that a much less perfect continuous gel network should have formed in PSA 4B-H126/21.

This can be explained by examination of the film formation processes for latex-based PSAs and their heated counterparts. As shown in Figure 6.8, during the film formation process, some sol polymer chains of one latex particle could diffuse across particle boundaries. If their size was larger than $2M_e$, they would be able to entangle two adjacent microgels. Due to their much larger size, the very large sol polymers (e.g., $>20M_e$) could not move very fast, hence they tend to stay in their local latex particles and entangle with either the sol or microgel polymers there. In addition, due to their larger size and consequently intense entanglement with other small or medium size sol polymers in its local latex particle, these very large sol polymers might also have slowed the diffusion of other sol polymers during the film formation process as well as the conditioning process afterward. As a result, if there were a larger number of much larger sol polymers in the latexes, then the number of entanglement points for connecting two adjacent microgels would be much smaller in the corresponding latex-based PSAs. Consequently, much less cross-linking points for connecting two adjacent microgels were formed in the heated PSAs, resulting in much lower shear strength. (Note: In this case, a large portion of the gel increase caused by post-treatment was due to the reaction between the very large sol polymers with their nearby microgel and sol polymers. This kind of reaction cannot lead to the formation of a continuous gel structure.)

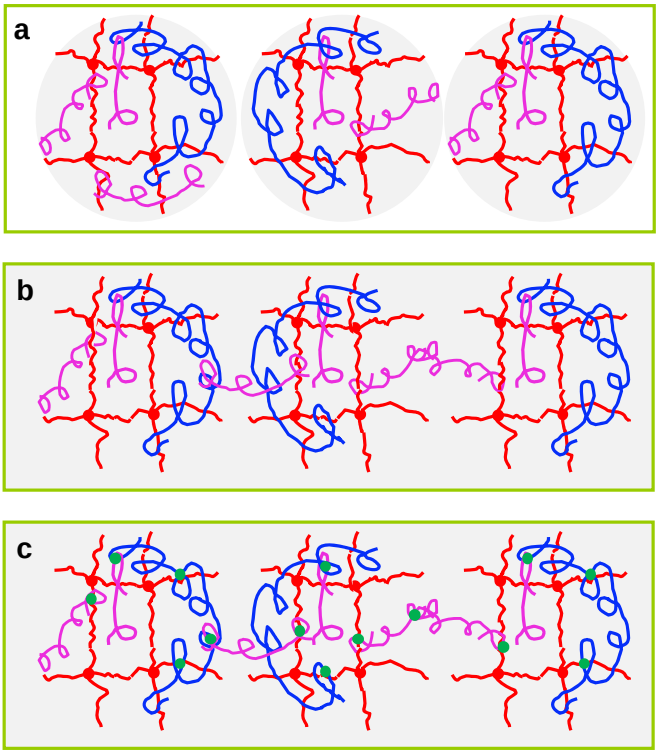

Figure 6.8: Scheme of formation of PSA films 4B and 4B-H126/21.
(a: Latex 4B, b: Latex-based PSA film 4B; c: Post-treated PSA film 4B-H126/21)

In order to confirm the above explanation with respect to the negative effect of very large sol polymer on the performance of heated PSAs, the heating of PSAs TK1 and 4B was studied. The polymer properties and performance of these two PSAs as well as their heated counterparts are shown in Table 6.9. PSA TK1 is a latex-based PSA from a previous study reported by Tobing et al.[17] It has a film thickness of about 30 μm, which is very close to the film thickness used in this study (~33 μm). In addition, its composition (i.e., BA/AA/IBMA (isobutoxy methyl acrylamide)/DDM (n-dodecyl mercaptan) weight ratio: 96.4/2.5/1/0.1) was homogenous and very similar to that of PSA

4B (i.e., BA/AA/HEMA weight ratio: 96/2/2). Hence, the copolymers of these two PSAs should also have very similar T_gs. Tobing et al. showed the heating of PSA TK1 as a good example of transforming the microgels into a continuous gel network. Its heated counterparts, PSA TK1-H121/10, showed significantly larger shear strength, compared with similar gel content unheated latex-based PSAs with the same composition. From Table 6.9, one can see that PSA TK1 had a similar gel content but smaller M_w than PSA 4B, hence it can be concluded that there was a much smaller amount of very large sol polymer in the original PSA TK1. The latex used for producing PSA TK1 should also have had a much smaller amount of very large sol polymers, compared to the latex used for casting PSA 4B. Hence the sol polymers' diffusion rate during the process of forming and conditioning PSA TK1 should be much larger compared with that for PSA 4B. If our previous explanation regarding the negative influence of very large sol polymers is correct, then using a shorter conditioning time for PSA TK1, compared with PSA 4B, could lead to a similar amount of diffused sol polymers. Consequently, in this case, the microgels were entangled with similar amounts of polymers in both PSAs. Accordingly, their heated counterparts might have continuous gel networks with a similar degree of perfection, resulting in similar shear strength if the heated PSAs had similar gel contents. This was confirmed with the following experiment results. Tobing et al. made the heated PSA (TK1-H121/10) by directly drying the still wet PSA TK1 at a high temperature (i.e., 121^{o}C for 10 min). So, the total time allowed for sol polymer diffusion in PSA TK1 was a maximum of 10 min before heating it;[17,1] in contrast, in our study, before heating PSA 4B, it was dried and then conditioned at room temperature for 24h. From Table 6.8, one can see that at similar gel contents (i.e., ~78 wt%), the PSA obtained from heating TK1

(i.e., TK1-H121/10) showed similar shear strength (~18.33 h) as that of the PSA obtained from heating 4B (i.e., 4B-H126/21) (~20.20 h). Based on this similar shear strength, one can conclude that similar gel content PSAs TK1-H121/11 and 4B-H126/21 should have continuous gel networks with similar degrees of perfection.

Table 6.9: Polymer properties and performance of PSA 4B, TK1 and their heated PSAs

PSA ID	Gel content (wt%)	M_w	M_n	M_c	M_e	x* (wt%)
		(x 10^3 kg/mol)				
4B	51	443	105	82	21	30
4B-H126/21	79	190	72	-	-	-
TK1[a]	45	188	36	143	25	-
TK1-H121/10[b]	77	100	30	76	23	-

PSA ID	Tack (N/m)	Peel strength (N/m)	Shear strength (h, 1/2" x 1/2")
4B	216	185	0.52
4B-H126/21	299	210	20.20
TK1[a]	193	246	0.83
TK1-H121/10[b]	211	123	18.33

Note: (1) *Weight percentage of sol polymers with size larger than $20M_e$ in the total sol polymers. (2) [a]TK1 is a latex-based BA/AA/IBMA (isobutoxy methyl acrylamide) (weight ratio: 96.4/2.5/1) PSA (see Table IV of ref. 1). (3) [b]TK1-H121/10 is the PSA obtained by heating PSA TK1 at 121°C for 10 min (see Table IV of ref. 1).

6.3.7 Comparison of the performance of post-treated latex-based PSAs and solvent-based PSAs with similar microstructure.

In order to check if the performance of post-treated latex-based PSA can be improved to the same level as that of a solvent-based PSA with similar polymer microstructure, PSA 5B-H126/11 obtained from this study was compared with PSA TK2-H121/10, a solvent-

based PSA. These two PSA films had similar thickness of about 30 μm. In addition, as mentioned earlier and as shown in Table 6.10, PSA 5B-H126/11 was obtained by heating a high gel content latex-based PSA 5B (i.e., ~75 wt%). PSA TK2-H121/10 was obtained from a gel-free PSA copolymer. PSA 5B-H126/11 and TK2-H121/10 had a very similar copolymer composition: BA/AA/HEMA weight ratio of 96/2/2 for the former and BA/AA weight ratio of 97.5/2.5 for the latter. In addition, these two PSAs had very similar polymer microstructures (see Table 6.10 for gel content, M_c and M_w). Figure 6.9 shows that the post-treated latex-based PSA 5B-H126/11 yielded a better performance than the solvent-based PSA TK-H121/10; for example, significantly larger shear strength as well as tack and peel strength. This was initially surprising, but can be explained. The higher tack and peel strength of PSA 5B-H126/11 might be caused by its smoother surface, compared to PSA TK2-H121/10. The much larger shear strength could be caused by two factors related to polymer microstructure: (1) the tighter gel network of PSA 5B-H126/11, compared to that of PSA TK2-121/10 (i.e., M_c: 53 vs. 63 kg/mol). However, considering the small difference in M_c, this factor should not have contributed a very large portion to the very large difference in shear strength. (2) The more perfect network of PSA 5B-H126/11, compared to that of PSA TK2-121/10. In our opinion, making the solvent-based PSA TK2-H121/10 by heating a gel-free PSA film made with a polymer solution is like making post-treated latex-based PSAs by heating a gel-free latex-based PSA. The reason is the latter process did not involve microgels either, like the former one. As shown earlier, even for gel-free or very low gel content latex-based PSAs with $M_w > 2M_e$, the amount of very small sol polymers in the PSA had a significant negative influence on the degree of perfection of the gel network in the heated latex-based PSA.

Accordingly, shear strength was greatly decreased. Based on this, it is suspected that in the original PSA for making the solvent-based PSA (i.e., TK2-H121/10), there might also have been a significant amount of very small sol polymers (i.e., $< 2M_e$) leading to a less perfect gel network for PSA TK2-H121/10, compared to the post-treated latex-based PSA 5B-H126/11. In addition, the significant shear strength difference between PSA 5B-H126/11 and TK2-H121/10 might be also related to their respective heating processes. From Table 6.10, one can see that the reaction rate between polymer chains during the heating process for forming PSA TK2-H121/10 was much larger than that for forming PSA 5B-H126/11. For example, the gel content increased by 80 wt% within 10 minutes during the former process; while only 6 wt% within 11 minutes during the latter process. The very large gel content increase during the heating process for forming PSA TK2-H121/10 means that the polymer chains reacted and thereafter incorporated into the gel network very quickly. Hence, the flow of these polymer chains during the heating process might be very limited. This is different from what reported earlier regarding the significant polymer flow during the heating process for forming PSA 5B-H126/11. As a result, in PSA TK2-H121/10 there might still be some defects, which was form its corresponding original PSA film TK-2. The gel network of PSA TK2-H121/10 was discontinuous around these defects, and consequently this might lead to smaller shear strength for it, compared to PSA 5B-H126/11.

Table 6.10: Polymer properties of PSAs 5B, TK2 and their heated counterparts

PSA ID	Gel content	M_w	M_n	M_c	M_e
	(wt%)	($x10^{-3}$ g/mol)			
5B	75	217	70	59	21
5B-H126/11	81	161	78	53	-
TK2[c]	0	271	75	-	23
TK2-H121/10[d]	80	79	30	63	23

Note: (1) [c]TK2 is BA/AA (weight ratio: 97.5/2.5) statistic copolymer produced by solution polymerization (see Table I of ref. 17) (2) [d]TK2-H121/10 is the PSA generated by heating the PSA film cast from "TK2" copolymer solution at 121°C for 10 min (see Table IV of ref. 17).

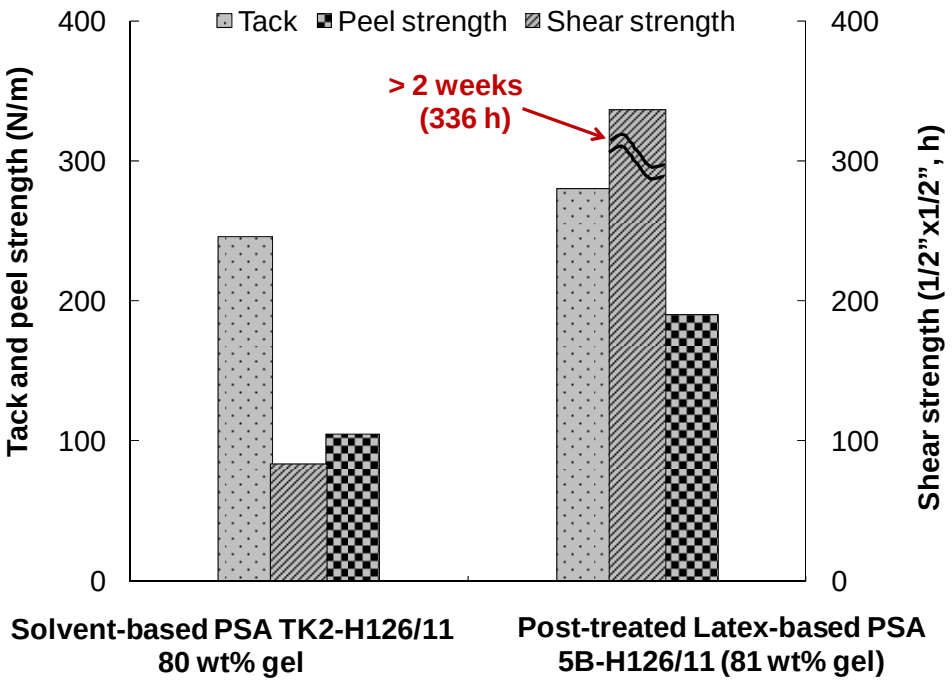

Figure 6.9: Performance of solvent-based PSA TK2-H126/11 and post-treated latex-based PSA 5B-H126/11.

6.4 Conclusions

Post-treatment by heating is a very effective way for improving the performance of latex-based PSAs, and the effect of treatment depends on the polymer microstructures of the untreated latex-based PSAs. For gel-free or very low gel content latex-based PSAs, decreasing the amount of very small sol polymers (i.e., size < $2M_e$) under the condition that M_w was larger than $2M_e$, could lead to improved entanglement between the polymer chains. Consequently, this would lead to the formation of a more perfect continuous gel network in the post-treated PSA. As a result, the post-treated PSA would exhibit significantly larger shear strength. As for gel-containing latex-based PSAs, if M_c is larger than or close to M_e and also the M_w is larger than $2M_e$ and smaller or close to $20M_e$, the microgels could be connected by the sol polymers. Improving the connection between the microgels in the latex-based PSAs is the key to get treated PSAs with better performance (i.e., larger shear strength), as in our case, a more perfect continuous get network would form in the treated PSAs. Better connection between the microgels in the untreated latex-based PSAs could be achieved in three ways: (1) simultaneously and properly increasing the M_c and M_w for similar gel content PSAs; (2) decreasing the amount of very small sol polymers (i.e., < $2M_e$). The negative effect of very small sol polymers was due to its incapability to effectively entangle with the microgels as well as other sol polymers in the latex-based PSAs; and (3) decreasing the amount of very large sol polymers (i.e., > 20 M_e). The negative effect of very large sol polymer was caused by its lower mobility.

Compared to the latex-based PSAs with similar polymer properties, the treated PSAs showed much better performance. They exhibited not only significantly larger shear strengths but also much larger tack and peel strengths. The larger shear strength

resulted because the gel network was continuous in the treated PSAs, while discrete in the untreated PSAs. The larger tack and peel strength was due to the much smoother surface of the treated PSAs. During the post-treatment process, the PSA polymer could flow and resulted in a much smoother surface for the treated PSAs compared with those of the untreated ones. In this study, it was also found that by optimizing the polymer microstructures of the latex-based PSAs, it was possible to generate a treated latex-based PSA with even better performance than that of a solvent-based PSA with similar polymer properties.

6.5 Acknowledgements

The authors thank the Natural Science and Engineering Research Council (NSERC) of Canada for financial support and Dr. Gabriela Fonseca for assistance with the AFM measurements.

6.6 References

1. Tobing S. D., A. Klein, Journal of Applied Polymer Science 2001, 79: 2558-2564.
2. Papsin J., George A., Patent No.: US 6281298B1.
3. Kavanagh M. A., Anderson K.S., Erdogan B., Patent No., US 7652103B2.
4. Krepski L. R., Filiatrault T. D., Mccracken S. D., Patent No.: US 7714076.
5. Filiatrault T. D., Kavanagh M. A., Anderson K. S., Patent No.: US 7652095.
6. Farwaha R., Boutillier D. N., Phan L., Patent No.: US 6541566.
7. Bernard M., Patent No.: US 5278227.
8. Keskey W., Schuetz J., Lee D. I., Patent No.: 4474923.

9. Tobing S. D., Klein A., Sperling L. H., Journal of Applied Polymer Science 2001, 81: 2109-2117.

10. Pressure Sensitive Tape Council, Test methods for pressure sensitive adhesive tapes 2004, 14th Edition, Northbrook, Illinois.

11. Qie L., Dubé M. A., European Polymer Journal 2010, 46(6): 1225-1236.

12. Zosel A., Ley G., Macromolecules 1993, 26: 2222-2227.

13. Deplace F., Carelli C., Mariot S., Journal of Adhesion 2009, 85: 18-54.

14. Lakrout H., Sergot P., Creton C., Journal of Adhesion, 1999, 69: 307-359.

15. Qie L., Dubé M. A., International Journal of Adhesion & Adhesives 2010, 30(7): 654-664.

16. Li L., Tirrell M., Korba G. A., Journal of Adhesion 2001, 76: 307-334.

17. Tobing S. D., Klein A., Journal of Applied Polymer Science 2001, 79: 2230-2244.

CHAPTER 7

GENERAL DISCUSSION AND RECOMMENDATIONS

In the past years, our society has realized the importance of protecting our environment. Therefore, green products, which are environmental friendly with respect to both their production and application, are in great need. Pressure sensitive adhesives (PSAs) are widely used in both our everyday life and in industrial settings. Two of the most important PSAs are solvent-based and latex-based PSAs.[1] While latex-based PSAs are more environmentally compliant than solvent-based PSAs, they tend to have inferior performance (e.g., lower shear strength at similar tack and peel strength).[2,3] Hence the performance of latex-based PSAs must be improved in order to replace solvent-based PSAs in some applications. The goal of this thesis was to greatly improve the shear strength of latex-based PSAs at little to no sacrifice to tack and peel strength.

In this project, controlling the polymer microstructure of the latexes (or their corresponding PSAs) was used as the main approach for improving the performance of latex-based PSAs. In addition, modifying the PSAs' composition and surface properties were also adopted as supplementary approaches.

This thesis started with modifying the concentrations of chain transfer agent (CTA) and cross-linker used in starved seeded semi-batch emulsion polymerization process to produce butyl acrylate (BA)/methyl methacrylate (MMA) latex copolymers with versatile polymer microstructures. Three techniques were used to produce the latexes: (1) adding CTA only, (2) adding cross-linker only, and (3) adding both CTA and cross-linker. The first two methods were widely used and well studied in the past;[4-7] while the last one was very rarely used and also not well studied.[8-9] Hence in this research, the influence of simultaneously adding CTA and cross-linker was thoroughly studied. In addition, in order to gain control over the latexes' polymer microstructure, a

2^3 factorial design involving two factors (CTA and cross-linker concentrations) and three levels was carried out. Based on the design, a model was established relating the polymerization condition to the latexes' gel content, which is the most important factor in a polymer's microstructure.

The influence of the BA/MMA latexes' polymer microstructure on the performance of their corresponding PSAs was studied. However, the relationship between the polymer microstructure and PSAs' performance could not be established for medium and high gel content BA/MMA PSAs, as they showed very low tack and peel strength as well as extremely large shear strength. In order to solve this problem, the polymerization factors including the feeding rates of monomer emulsion and initiator solution, the monomer composition, and emulsifier concentration were modified to produce latexes applicable for use as PSAs. In some cases, these polymerization parameters were manipulated simultaneously. Such comprehensive research has never been reported before, to our knowledge. In addition, the PSA films' thickness was also modified in order to increase the PSAs' tack and peel strength.

With the proper monomer composition and emulsifier concentrations found from the above study, two series of BA/acrylic acid (AA)/2-hydroxy ethyl methacrylate (HEMA) latexes were produced by varying the CTA concentration: one in the absence of cross-linker; the other in the presence of cross-linker. With the PSAs made from these latexes, the influence of polymer microstructure on PSA performance and viscoelasticity was studied. In particular, similar gel content latexes obtained with the above two different methods were compared regarding their corresponding PSA performance and viscoelastic properties. Such a study has never been reported, to our knowledge.

Finally, the performance BA/AA/HEMA latex-based PSAs was further improved by post-heating. Tobing et al.[3,10] reported that by properly post-treating latex-based PSAs with $M_c > M_e$ as well as $2M_e < M_w < 20M_e$, the performance (i.e., shear strength) of the PSAs could be greatly improved due to the transformation of a discrete microgel structure into a continuous gel network. (Note: M_c is the molecular weight between cross-linking points, M_w is the weight average molecular weight of the sol polymers, and M_e is the molecular weight between entanglement points). In this work, the influence of the presence of a significant amount of very small or very large sol polymers (i.e., size $<2M_e$ or size $>20M_e$) in the untreated PSAs on the performance of their corresponding treated PSAs was studied. In addition, the possibility of improving the performance (i.e., shear strength) of post-treated PSAs by simultaneously increasing the M_c and M_w of the original latex-based PSAs with similar gel contents was explored. Such studies have never been reported before, to our knowledge.

7.1 Main Contributions and Findings

7.1.1 Using CTA and cross-linker simultaneously to modify latexes' polymer microstructure (Chapter 3)

It was found that using CTA and cross-linker simultaneously allowed one to expand the range of latex microstructural possibilities as opposed to manipulating one concentration at a time. For example, similar gel content latex with much smaller M_c and M_w could be obtained when increasing the CTA and cross-linker concentrations simultaneously. In addition, the latexes' polymer microstructure change was studied under the condition of varying the amount of CTA at a constant amount of cross-linker. It was found that at a

constant cross-linker concentration (i.e., 0.2 phm), increasing the CTA concentration from 0 to 0.2 phm, generated a latex with lower gel content, looser gel network (i.e., larger M_c) as well as smaller sol polymers (i.e., smaller M_w). Further increasing the CTA concentration from 0.2 to 0.4 phm, the gel content further decreased and M_c further increased; but M_w increased due to the formation of branched sol polymers. The polymer microstructures of these latexes are shown in Figure 7.1.

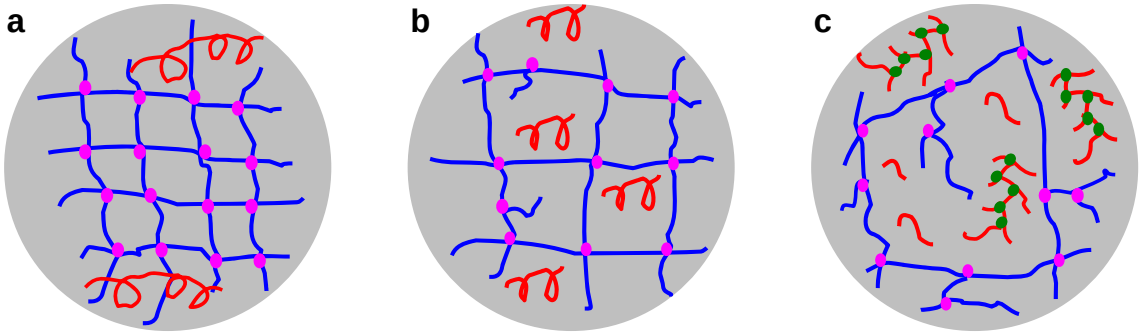

Figure 7.1: Polymer microstructure of latexes produced by varying the CTA concentrationat a constant cross-linker concentration (i.e., 0.2 phm)
(a: 0 phm CTA, b: 0.2 phm CTA, c: 0.4 phm CTA)

7.1.2 Improving the performance of latex-based PSAs by modifying the monomer mixture and the amount of emulsifier (Chapter 4)

It was found that changing the monomer mixture from BA/MMA to BA/AA/HEMA while simultaneously decreasing emulsifier concentration dramatically improved the corresponding PSAs' shear strength as well as tack and peel strength. Hence with this method, the goal of this research has been achieved. The reasons behind this result are: (1) addition of polar groups (i.e., carboxyl groups from AA and hydroxyl groups from HEMA) to the PSA increased its cohesive strength due to the strong hydrogen bonding

between these groups. Hence the shear strength was greatly increased; and (2) adding polar groups increased the PSA film's surface tension, and decreasing the amount of emulsifier enhanced the contact between PSA polymer and substrate. Consequently, the chemical interaction energy between PSA film and substrate surfaces greatly increased. As a result, the tack and peel strength were also greatly improved.

7.1.3 Improving the performance of latex-based PSAs by controlling their polymer microstructures (Chapter 5)

Two series of BA/AA/HEMA latexes were produced via starved seeded semi-batch emulsion polymerization by varying the amount of CTA either in the absence or presence of cross-linker. It was found that at similar gel content, the latexes generated in the absence of cross-linker had significantly larger M_c and M_w as well as a significantly smaller amount of very small sol polymer (i.e., size $<M_e$).

The performance of the PSA films mainly depended on gel content. In general, with the increase in gel content, the shear strength increased, while tack and peel strength decreased. In addition, at similar gel content, the PSAs with larger M_c and M_w showed significantly larger shear strength as well as similar tack and peel strength, compared to their counterparts with smaller M_c and M_w. Hence, simultaneously increasing the M_c and M_w for similar gel content latex-based PSAs was another tool for effectively improving PSA performance.

The reasons for the similar gel content PSAs' performance results include: (1) at similar gel content, increasing the PSAs' M_c and M_w enhanced the entanglement between their polymer chains. Consequently the PSAs' cohesive strength significantly increased,

as has been confirmed by their significantly larger shear moduli measured via dynamic mechanical analysis (DMA). Accordingly, the PSAs' shear strength was increased; and (2) at similar gel content, increasing the PSAs' M_c and M_w lowered their deformability and flow ability, as is consistent with their larger shear moduli. As a result, during the bonding process, PSAs with much larger M_c and M_w could not wet the substrate as well as its similar gel content counterpart with smaller M_c and M_w during the bonding process of tack and peel strength testing. This tended to lower its tack and peel strength.[11] Meanwhile, at similar gel content, increasing the PSAs' M_c and M_w enhanced their elongation capability,[12] which endowed the PSA with larger capability to form longer fibrils during the debonding process of tack and peel strength testing.[13-14] As a result, the PSA might have experienced much larger strain and consequently dissipated larger amounts of energy during the debonding process. This tended to increase the PSAs' tack and peel strength.[13-14] The positive effect of larger dissipated energy on increasing tack and peel strength might have counterbalanced the negative effect of less wetting. Hence PSAs with similar gel content showed similar tack and peel strength.

7.1.4 Improving the performance of latex-based BA/AA/HEMA PSAs by optimizing their polymer microstructure and post-treatment (Chapter 6)

It was found that post-heating is a very effective way for improving the performance of latex-based PSAs, and the effect of post-treatment depends on the polymer microstructures of the untreated latex-based PSAs. For gel-free or very low gel content latex-based PSAs, decreasing the amount of very small sol polymers (i.e., size $<2M_e$) under the condition that M_w was larger than $2M_e$, led to improved entanglement between

the polymer chains. Consequently, this led to the formation of a more perfect continuous gel network in the post-treated PSA. As a result, the post-treated PSA exhibited significantly larger shear strength. As for gel-containing latex-based PSAs, if the M_c was larger than or close to M_e and also the M_w was larger than $2M_e$ but smaller than or close to $20M_e$, then the microgels could be entangled by the sol polymers in these PSAs.[3] In this study, it was found that improving the connection between the microgels in the original latex-based PSAs was the key to improve PSA performance (i.e., larger shear strength), as in this case, a more perfect continuous get network would form in the treated PSAs. Better connection between the microgels in the untreated latex-based PSAs could be achieved in three ways: (1) simultaneously and properly increasing the M_c and M_w for similar gel content PSAs; (2) decreasing the amount of very small sol polymers (i.e., size $<2M_e$). The negative effect of these very small sol polymers was due to their incapability to effectively entangle with the microgels as well as other sol polymers in the latex-based PSAs; and (3) decreasing the amount of very large sol polymers (i.e., >20 M_e). The negative effect of these very large sol polymers was caused by their lower mobility.

Compared to the latex-based PSAs with similar gel contents, the treated PSAs showed much better performance. They exhibited not only significantly larger shear strengths but also much larger tack and peel strengths. The larger shear strength resulted because the gel network was continuous in the treated PSAs, while it was discrete in the untreated PSAs. The larger tack and peel strength were due to the much smoother surface of the treated PSA films. During the post-treatment process, the PSA polymer could flow and therefore resulted in a much smoother surface for the treated PSAs, compared with those of the untreated ones.

7.1.5 Publications

This thesis includes four manuscripts for publication in refereed journals. Two have been published, one has been submitted for publication, and the other is to be submitted shortly:

(1) Qie L., Dubé M. A., Chapter 3, European Polymer Journal 2010, 46: 1225-1236.

(2) Qie L., Dubé M. A. Chapter 4, International Journal of Adhesion and Adhesives 2010, 30: 654-664.

(3) Qie L., Dubé M. A, Chapter 5, accepted by Macromolecular Reaction Engineering in 2010.

(4) Qie L., Dubé M. A., Chapter 6, to be submitted to Journal of Applied Polymer Science.

7. 2 Recommendations for Future Research

In order to further improve the PSA performance gains presented in this thesis, the following research is recommended.

a) Exploring Methods for Making Better Latex-based PSA Films

The presence of defects such as holes and scratches in PSA films are very common due to unsuitable latex properties such as viscosity and particle size, casting tools for making PSA films, or conditions for making the PSA films with latexes or polymer solutions. The presence of these defects in PSA films can deteriorate their performance, and must be diminished.

In this study, the latex's solid content was modified in order to adjust the latex's viscosity and consequently, provide good PSA films. However, it was found that it was very difficult to produce defect-free PSA films. For example, Figure 7.2 shows the PSA films made by casting BA/AA/HEMA latex with a Meyer bar (see "e" of Figure 7.2 for the image of a Meyer bar). The latex had an average particle diameter of ~150 nm, a pH of about 5.5, and a solid content adjusted from 48, to 45, and to 42 wt%, respectively. One can see that at a latex solid content of 48 wt%, the resulting PSA film had many visible scratches (see "a" of Figure 7.2). This was because the latex's viscosity was too high, therefore the latex could not flow properly to totally diminish the lines left by the threads of the casting Meyer bar during the PSA film formation process. Decreasing the latex solid content slightly to 45 wt% resulted in a PSA film with hole-like defects, due to lower viscosity (see "b" of Figure 7.2). Decreasing the latex solid content further to 42 wt% resulted in an almost discontinuous PSA film, due to very low viscosity (see "c" and "d" of Figure 7.2). The PSA films made with late having solid content of 45 wt% and 42 wt% looked perfect with naked eye, and the defects were not visible; but the defects could be detected by atomic force microscopy (AFM). This was due to the very small size of the defects.

The observed sharp latex viscosity change around solids content of about 45 wt% for other latexes with average particle diameters of 150 nm has been reported elsewhere.[15] Thus, in order to solve the problems related with latex viscosity and produce defect-free PSA films, two methods may be useful: (1) choosing proper viscosity-adjusting additives for latexes to get better control over the latex viscosity. In addition, the chosen additives should not have any significant negative influence on PSA

performance; and (2) choose proper casting tools to make PSA films. For example, for high viscosity latex (i.e., the latex with 48 wt% solid content), choosing a casting tool without threads on it (e.g., knife blade) may be able to produce PSA films without scratches. The reason is in this case, it is not necessary for the latexes to flow in order to fill the gap left by the threads of the casting bar, and therefore form a continuous PSA film.

Making latexes with larger particle sizes (e.g., 250 – 400 nm) is another way to achieve defect-free PSA films, since in this case the impurities such as coagulated particles will be big enough to be removed by filtration from the latexes. It is well known that such impurities can also cause defects in PSA films.

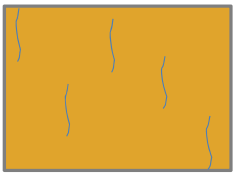

a: 48 wt% solid content

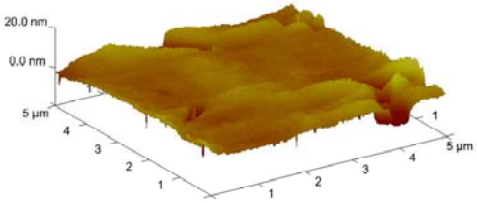

b: 45 wt% solid content

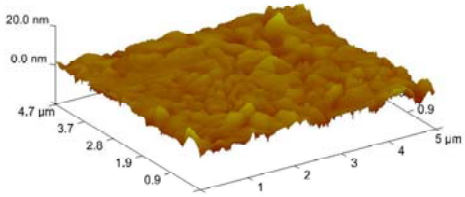

c: 42 wt% solid content

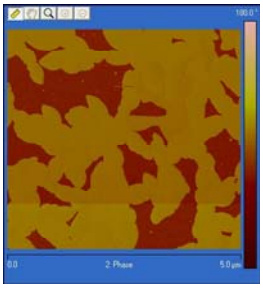

d: 42 wt% solid content

e: Meyer bar for casting PSA film

Figure 7.2: Influence of latex's solid content on PSA film
(a: Drawn image, b and c: 3-D height image by AFM, d: phase image by AFM)

b) Optimizing the amounts of functional groups in the original latex-based PSAs for improving the performance of post-treated PSAs.

In this study, the amount of functional groups in the original PSA copolymers was fixed. Varying the amounts of functional groups in the original latex-based PSAs can result in post-treated PSAs with different polymer microstructures and correspondingly different performance. Hence, optimizing the amount of functional groups in the original PSAs is one way to improve the performance of post-treated PSA films.

c) Optimizing the functional groups in the original latex-based PSAs for improving the performance of post-treated PSAs and simplifying the post-treatment process.

In this study, the functional groups in the latex-based PSAs were chosen as carboxyl groups from AA and hydroxyl groups from HEMA. The reaction between these two groups is slow and also only occurs at higher temperatures (e.g., >~110^{o}C). Hence, some of the entanglement points for connecting the microgels by sol polymers in the original latex-based PSAs might not have transformed into cross-linking points via reaction between these two groups during the post-treatment process. Consequently, even though the resulting gel network in the post-treated PSAs was continuous, it might have some weak points, which could cause lower shear strength for the treated PSAs. To solve this problem, the functional groups can be optimized, so that they can react very fast and effectively.

Moreover, if good original latex-based PSA films can be made by modifying latexes' viscosity, particle size, etc., then functional groups able to react at room temperature can be chosen for the original PSAs. In this case, it is not necessary to use

PSA polymer flow at the high temperature of the post-treatment process to make PSA films with defects. This way, the post-treatment process will be much easier to carry out and its cost will be much lower.

7.3 Final Remarks

The main objective of this thesis was to improve the performance of latex-based PSAs, which are more environmental friendly but have poorer performance, compared to another type of very important commercial PSA, solvent-based PSAs. With the above results, one can see that we have surpassed our original objective, which was to greatly improve the shear strength of latex-based PSAs at small or no sacrifice to tack and peel strength. In two cases, not only was shear strength greatly improved, but so were tack and peel strength due to the simultaneous modification of PSA bulk and surface properties.

Another supplementary objective was to study the influence of CTA and cross-linker concentrations on latexes' polymer microstructure, to gain better control over the polymer microstructure of the latexes and their corresponding PSAs. This was also accomplished.

While our objectives were fulfilled, some very interesting research such as that recommended above still needs to be done in order to further improve the performance of latex-based PSAs, and therefore make greener PSA products.

7.4 References

1. Jovanovic R., Dubé M. A., Journal of Macromolecular Science-Polymer Reviews 2004, C44(1): 1-51.

2. Tobing S. D., Klein A., Journal of Applied Polymer Science 2001, 79(12): 2230-2244.
3. Tobing S. D., Klein A., Journal of Applied Polymer Science 2001, 79(14): 2558-2564.
4. Shen H. Z., Zhang J. Y., Liu S. J., Journal of Applied Polymer Science 2008, 107(3): 1793-1802.
5. Plessis C., Arzamendi G., Leiza J., Journal of Polymer Science. Part A, Polymer Chemistry, Vol. 39, 1106–1119 (2001)
6. Bouvier-Fontes L., Pirri R., Asua J. M., Macromolecules 2005, 38: 1164-1171.
7. Bouvier-Fontes L., Pirri R., Asua J. M., Journal of Polymer Science. Part A, Polymer Chemistry 2005, 43: 4684–4694.
8. Chauvet J., Asua J. A., Leiza J. R., Polymer 2005, 46(23): 9555-9561.
9. Kajtna J., Golob J., Krajnc M., International Journal of Adhesion and Adhesives 2009, 29(2): 186-194.
10. Tobing S. D., Klein A., Sperling L.H., Journal of Applied Polymer Science 2001, 81(9): 2109-2117.
11. István B., Pressure-Sensitive Adhesives and Applications 2004, Marcel Dekker Inc., New York.
12. Zosel A., Ley G., Macromolecules 1993, 26: 2222-2227.
13. Deplace F., Carelli C., Mariot S., J. Adhesion 2009, 85: 18-54.
14. Zosel A., International Journal of Adhesion and Adhesives 1998, 18: 265-271.
15. Horsky J., Quadrat O., Porsch B., Colloids and Sufaces A: Physicochemical and Engineering Aspects 2001, 180: 75-85.

APPENDIX

This appendix includes five sections: (1) calculation of the instantaneous and overall monomer conversion for a polymerization process (Run 1 from Chapter 3 was used as an example); (2) study the influence of latexes' pH on their corresponding PSAs' performance with sample latexes 3 and 4 from Chapter 5; (3) study the influence of contact area on PSAs' shear strength. (PSA films 1A through 6A from Chapter 5 were used as samples); (4) calculation of PSA film's surface tension as well as the chemical interaction energy between the surfaces of PSA film and substrate. PSA film 5B and its post-treated counterpart, PSA film 5B-H126/11, were used as samples for this calculation; (5) Explanation about storage modulus (G'), loss modulus (G") and composite modulus (G*)

1 Monomer conversion calculation for Run 1 from Chapter 3

Instantaneous monomer conversion was calculated based on the total amount of monomer added to the reactor up to the sampling time; in contrast, the overall monomer conversion was calculated based on the total amount of monomer in the polymerization formulation. To obtain the monomer conversion values, both the polymerization and sample latexes information are required. Hereafter, the detailed calculation procedure is provided.

1.1 Polymerization formulation

The first step for the calculation was to get the polymerization formulation, which is shown in Table A1.

Table A1: Polymerization formulation of Run 1 from Chapter 3

Ingredients	Initial load (g)	Feeding composition	
		Initiator solution (g)	Monomer emulsion(g)
H_2O	217.19	90	88.49
BA/MMA	10.80/1.22	-	303.20/33.69
KPS	0.4003	0.8996	-
NDM	-	-	1.3534
AMA	-	-	0.7500
SDS	0.4506	-	6.7245
$NaHCO_3$	0.0491	-	-
Total weight	229.8980	90.8996	434.20

1.2 Added Reactants in the reactor during the polymerization process

The second step was to calculate the amount of added reactants. The added reactants in the reactor included two parts: one was from the initial load; the other was from the feeding. The amount of fed reactants were calculated with the feeding initiator solution and monomer emulsion compositions (see Table A1) and the feeding rates for Run 1 (i.e., 0.433 g/min and 2.412 g/min, respectively, for initiator solution and monomer emulsion). For example, the weight of fed monomer BA up to a feeding time of 20 min was calculated as follows:

$$W_{fBA,t} = (r_{ME} \times t) \times \frac{W_{BA,ME}}{W_{ME}} \qquad (A1)$$

$$W_{fBA,20min} = \left(2.412\frac{g}{min} \times 20min\right) \times \frac{303.20g}{434.20g} = 33.686g \qquad (A2)$$

In Equation A1, $W_{f\,BA,\,t}$ is the weight of fed monomer BA up to a feeding time of 20 min; r_{ME} is the feeding rate of monomer emulsion; t is the feeding time. (Note: The total feeding times are 180 min and 210 min for monomer emulsion and initiator solution, respectively.) $W_{BA,\,ME}$ is the weight of BA in the monomer emulsion; and W_{ME} is the weight of monomer emulsion.

So the total amount of BA added to the reactor up to a feeding time of 20 min ($W_{aBA,20min}$) was calculated as follows:

$$W_{aBA,20min} = W_{iBA} + W_{fBA,20min} = 10.80 + 33.686 = 34.486g \qquad (A3)$$

In the above equation, $W_{i,BA}$ is the weight of BA from initial load. Similarly, the amounts of other reactants added to the reactor up to the sampling time were also calculated, and the obtained data are shown in the following Table A2.

Table A2: Weight of added reactants for Run 1 from Chapter 3

Feeding Time (min)	Added reactants (g)				
	Monomer (BA+MMA+AMA)	H_2O	KPS+SDS +$NaCO_3$	NDM	Total
20	49.4483	235.5855	1.7325	0.0270	286.7933
60	124.3127	272.3984	3.3979	0.0809	400.1899
120	236.6131	327.6088	5.8958	0.1619	570.2796
180	348.9058	382.8172	8.3936	0.2428	740.3594
210	348.9058	395.6790	8.5218	0.2833	753.3899
End of Run 1	348.9058	395.6790	8.5218	0.2833	753.3899

1.3 Solid content of sample latexes taken during the polymerization of Run 1

The third step to calculate monomer conversion was to obtain the solid contents for the latex samples taken during the polymerization. To calculate the solid content, about 1 g latex was weighed and put in an aluminum dish, then the dish was dried in a fume hood at room temperature for a week and then in an vacuum oven at 30°C for 2 days to get dry latex. Then the solid contents of sample latexes were calculated according to the following equation.

$$S_t = \frac{W_{DLS,t}}{W_{LS,t}} = \frac{W_{dish+DLS,t} - W_{dish}}{W_{dish+LS,t} - W_{dish}} \qquad (A4)$$

In Equation A4, S_t is the solid content of latex sample taken at feeding time t; $W_{DLS,t}$ is the weight of the dry latex sample; $W_{LS,t}$ is the weight of the latex sample; $W_{dish+DLS,t}$ is the total weight of dish and dry latex sample; W_{dish} is the dish weight; $W_{dish+LS,t}$ is the total weight of dish and latex sample. The results are shown in Table A3.

Table A3: Solid content of sample latexes of Run 1 from Chapter 3

Latex ID	Feed time (min)	Weight (g)			Solid content (wt%)
		Pan	Pan + latex	Pan +dry latex	
1	20	1.0349	1.2985	1.0752	15.3%
2	60	1.0336	1.6836	1.2210	28.8%
3	120	0.9953	2.0182	1.4053	40.1%
4	180	0.9955	1.7315	1.3321	45.7%
5	210	1.0045	1.9121	1.4260	46.4%
6	End of Run 1	1.0418	2.1515	1.5658	47.2%

1.4 Calculate the instantaneous and overall monomer conversion during the polymerization process of Run 1

The last step was to calculate the instantaneous and overall monomer conversion using the data in Tables A2 and A3. The following equations were used for the calculation.

$$x_{I,t} = \frac{W_{P,t}}{W_{TM,t}} \qquad (A5)$$

$$x_{O,t} = \frac{W_{P,t}}{W_{TM}} \qquad (A6)$$

In the above two equations, $x_{I,t}$ and $x_{O,t}$ are the instantaneous and overall monomer conversion at feeding time t, respectively; $W_{P,t}$ is the amount of polymer produced in the reactor up to feeding time t; $W_{TM,\,t}$ is the total amount of monomer added to the reactor up to the sampling time; and W_{TM} is the total amount of monomer in the formulation, which is the same as the total amount of monomer added to the reactor up to the end of polymerization.

In order to get the values of the parameters in the above two equations, the following equations were used.

$$W_{TM,t} = \sum W_{Mi,t} \qquad (A7)$$

$$\begin{aligned} W_{P,t} &= W_{DL,t} - \left(W_{KPS,t} + W_{SDS,t} + W_{NaCO3,t}\right) \\ &= W_{TL,t} \times S_t - \left(W_{KPS,t} + W_{SDS,t} + W_{NaCO3,t}\right) \end{aligned} \qquad (A8)$$

$$W_{TM} = \sum W_{Mi,ER} \qquad (A9)$$

In the above equations, $W_{Mi,t}$ the amount of monomer i added to the reactor up to feeding time t; $W_{Mi,ER}$ is the amount of monomer i added to the reactor till the end of the Run. $W_{DL,t}$ is the amount of dry latex in the reactor at feeding time t; while $W_{L,t}$ is the amount of latex in the reactor at feeding time t. $W_{KPS,t}$, $W_{SDS,t}$ and $W_{NaCO3,t}$ are the amount of KPS, SDS and $NaCO_3$ added to the reactor up to feeding time t, respectively. These data are provided in Table A2. In addition, Equation A8 was established as the added KPS, SDS and $NaCO_3$ also existed in the dry latex together with the polymer.

Combining Equations A5 through A9, the instantaneous and overall monomer conversions were calculated, and the corresponding data are shown in Table A4.

Table A4: Instantaneous and overall monomer conversion
(Run 1 from Chapter 3)

		Monomer conversion (wt%)	
		Instantaneous	Overall
Start of the Run		0	0
Feeding time (min)	20	85.3	12.1
	60	90.1	32.1
	120	94.1	63.8
	180	94.6	94.6
	210	97.8	97.8
End of the Run		99.5	99.5

2 Study the Influence of latexes' pH on their corresponding PSAs' performance

In this study, two film types were cast for each PSA formulation: one at a pH of 3.0 and the other at a pH of 5.5. The increase in pH yielded fairly similar or slightly lower tack and peel strength results but significantly higher shear strength values. Two examples of this effect using PSAs 3A vs. 3B and 4A vs. 4B are shown in Table A5. Previous studies showed that ionization of the carboxyl groups in PSAs could lead to higher elastic modulus, and correspondingly higher cohesive strength and larger shear strength.[1] However, it seems that this was not the case here as the pH change was not as great and the AA was evenly distributed throughout the latex particles as opposed to residing primarily on the particle surface (Note: The carboxyl groups on the latex particle surface could be ionized by adjusting pH; while those inside the particle could not). This was further confirmed by DMA analysis: the pH of the latex did not show significant influence on the modulus frequency curves of the corresponding PSAs. Although the effect of pH on cohesive strength was not observable with the PSAs for DMA testing, it could be significant for the PSA films for performance measurement, as the two PSAs were prepare differently (i.e., the former by drying latex for one month while the latter for 24 h). It is known that an increase in pH could cause the latex particles to swell.[2] As a result, the latex viscosity increased as we noticed while filtering the latex, and thereafter resulted in better packing of latex particles during the film casting process. Consequently, within a certain drying time frame, the improved packing could have led to greater diffusion of polymer chains into neighboring particles and promoted greater polymer chain entanglement. Hence, the cohesive strength of the corresponding PSAs (i.e., PSAs for performance measurement) was enhanced, and accordingly larger shear strength

resulted. In contrast, if the drying time was long enough, then the polymer chains in the PSAs made from latexes with different pH could reach a similar equilibrium state. Therefore the cohesive strength of these PSAs (i.e., PSAs for DMA testing) was not significantly affected by the pH of the corresponding latex.

Table A5: Influence of latexes' pH on corresponding PSAs' performance

Latex ID	Latexes' pH	PSA ID	Tack (N/m)	Peel strength (N/m)	Shear strength (1"x1", h)
3	3	3A	285	318	7.3
	5.5	3B	261	285	12.7
4	3	4A	230	216	41.2
	5.5	4B	216	185	64.2

3 Study on the **influence of contact area on PSA shear strength**

In this study, two different contact areas were used to measure the shear strength, as some of the shear strength of the high gel content PSAs were too large to be measured with a contact area of 1" by 1". Thus, shear strength testing using a smaller contact area of ½" by ½" was also employed. Figure A1, obtained with PSAs 1A through 6A, shows the correlation between the shear strengths resulting from these two different methods is in polynomial form.

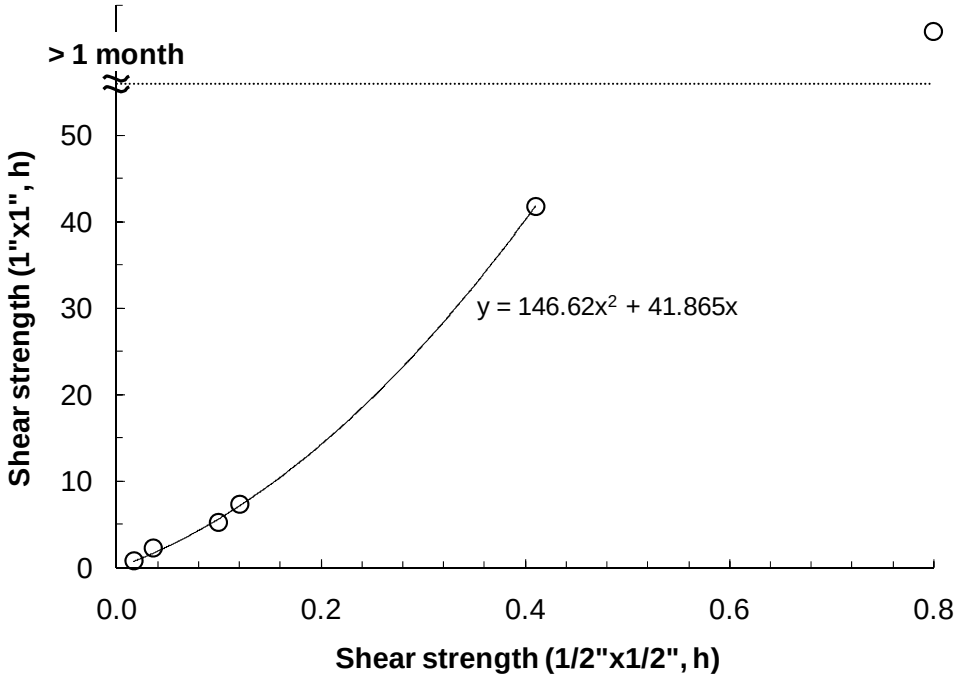

Figure A1: Influence of contact area on shear strength.

The above mentioned result differs from previous work regarding the influence of contact area on shear strength as shown in Eq. A10:[3]

$$T = \frac{L^2 W \eta}{2tMg} \qquad (A10)$$

where T is the shear strength, L is the length of contact area between the PSA and the testing panel, W is the width of the contact area, η is the zero shear viscosity of the PSA, t is the thickness of the PSA film, M is the testing load and g is the gravitational constant. According to Equation A10, a linear relationship should exist between the 1"x 1" shear strength and ½" x ½" shear strength, and the former should be 8 times that of the latter. In

addition, the measured 1" x 1" shear strength in our study was far larger than that predicted by Equation A10. Besides, the larger the ½" x ½" shear strength, the larger was the difference between our measurement and the Equation A10 prediction using a contact area of 1" x 1". The differences likely arose for two reasons. In our study, the PSA samples are versatile, ranging from gel-free to high gel content PSAs, while the PSAs used for generating Equation A10 were all gel-free polymers. First, it is suspected that for the PSAs produced in this study (especially those with medium to high gel contents), the shear strength change with contact area was affected not only by the area but also by the accompanying change in the packing state of the polymer chains in the PSA films. It is known that the time needed for the polymer chains in a PSA to reach an equilibrium state depends on the PSA's microstructure. Higher gel contents and smaller M_c should correspond to longer equilibrium times. Therefore, if all the PSAs were conditioned for the same time (24 h, in this study), the polymer chains in the low gel content PSAs might have reached an equilibrium state, whereas those in the high or even medium gel content PSAs may not have. If the contact area was ½" x ½", the PSAs fell from the testing panel within a very short time (from several minutes to about 1 h for the PSAs in this study) in contrast to when a contact area of 1" x 1" was used (from several hours to more than 1 month). This longer contact period in the case of the 1" x 1" contact area may have allowed the polymer chains to migrate and form better entanglements during the shear strength testing, therefore resulting in improved shear strength. This coincides with our experimental data that revealed how PSAs conditioned for a longer time had significantly larger shear strengths for the same contact area. For example, after increasing the conditioning time of PSA 6A (gel content: 75 wt%) from 24 h to 2 weeks, the shear

strength at ½" x ½" was increased from about 0.8 h to 2 h. Nonetheless, the above mentioned data also indicated that polymer chain diffusion should make only a minor contribution to the very large difference between the 1" x 1" shear strength data measured in our study and those predicted by Equation A10. A second, more compelling reason for these shear strength differences however, arises from the generation of Equation A10. The data used to generate Equation A10 were obtained from gel-free PSAs with very low shear strengths. These PSAs had a more liquid-like behavior relative to the PSAs in our study. Hence their deformation under a shear force could be roughly explained by viscosity alone (e.g., not including elasticity) as in Equation A10. In fact, Figure A1 shows that a linear relationship exists between 1" x 1" and ½" x ½" shear strength measurements at very low shear strength levels. This linear relationship is consistent with what predicted by Equation A10. Figure A1: Influence of contact area on shear strength.

4 PSA film surface tension and chemical interaction energy between the surfaces of PSA films and stainless steel testing panels

PSA film 5B and its post-heated counterpart, 5B-H126/11, were used for the relative measurement and calculation. A contact angle method was used to measure the surface tension of the PSA films with VCA Optima contact angle equipment from AST Products Inc. DDI water and di-iodomethane (CH_2I_2) were used as the testing liquids with known surface tensions.

4.1 Calculation of the surface tension for PSA films

The surface tension of a PSA film was calculated with the following three equations.[1]

$$(1 + cos\theta_1)\gamma_1 = 4\left(\frac{\gamma_1^d \gamma_P^d}{\gamma_1^d + \gamma_P^d} + \frac{\gamma_1^p \gamma_P^p}{\gamma_1^P + \gamma_P^p}\right) \quad (A11)$$

$$(1 + cos\theta_2)\gamma_2 = 4\left(\frac{\gamma_2^d \gamma_P^d}{\gamma_2^d + \gamma_P^d} + \frac{\gamma_2^p \gamma_P^p}{\gamma_2^P + \gamma_P^p}\right) \quad (A12)$$

$$\gamma_P = \gamma_P^d + \gamma_P^p \quad (A13)$$

In the above equations, θ_1 and θ_2 are the contact angles measured with water and di-iodomethane (CH_2I_2), respectively; γ_P, γ_P^d and γ_P^p are the PSA film's surface tension as well as its dispersion and polar components, respectively; γ_1 (72.8 dyne/cm), γ_1^d (22.1 dyne/cm) and γ_1^p (50.7 dyne/cm) are the surface tension of water as well as its dispersion and polar components, respectively; γ_2 (50.8 dyne/cm), γ_2^d (44.1 dyne/cm) and γ_2^p (6.7 dyne/cm) are surface tension of di-iodomethane as well as its dispersion and polar components, respectively.[4]

4.2 Calculation of the chemical interaction energy between the surfaces of PSA films and stainless steel testing panels

This calculation was done according to.[4]

$$I = 2\left(\gamma_P^d \gamma_S^d\right)^{1/2} + 2\left(\gamma_P^p \gamma_S^p\right)^{1/2} \quad (A14)$$

In the above equation, I is the chemical interaction energy between the surfaces of PSA film and stainless steel testing panel; γ_S^d (29 dyne/cm) and γ_S^p (15 dyne/cm) are the

dispersion and polar component of the surface tension of the stainless steel testing panel.[4]

4.3 Calculation results

The contact angle data and the calculation results are shown in the following table. (Note: The surface tension results obtained from Equation A13 and the interaction energy (*I*) obtained from Equation A14 both had units of dyne/cm. These results were converted to N/m according to 1dyne/cm = 10^{-3} N/m, and are shown in Table A6.)

Table A6: Contact angle measurement data for PSA 5B and 5B-H126/11

PSA ID	Contact angle (^{o})		γ^d	γ^p	γ	*I*
	θ_1 (H_2O)	θ_2 (CH_2I_2)	($x10^{-3}$ N/m)			
5B	59	72	15	30	45	84
5B-H126/11	97	71	20	6	26	67

5 Explanation about storage modulus (G'), loss modulus (G"), and composite modulus (G*)

Many polymer materials are viscoelastic materials. If under a dynamic stress (σ), they will develop a strain (ε) which is not in the same phase as the stress (see Equation A15-A16).

$$\sigma = \sigma_0 \sin(\omega t + \delta) \qquad (A15)$$

$$\varepsilon = \varepsilon\sigma_0 \sin(\omega t) \qquad (A16)$$

In the above equations, ω is the frequency of strain oscillation; t is time; δ is the phase lag between the strain and stress.

The storage and loss modulus (G' and G") of viscoelastic materials respectively measure the stored energy, representing the elastic portion, and the energy dissipated as heat, representing the viscous portion. The storage and loss moduli are defined as follows:

$$G' = \frac{\sigma_0}{\varepsilon_0} cos\delta \qquad (A17)$$

$$G'' = \frac{\sigma_0}{\varepsilon_0} sin\delta \qquad (A18)$$

Composite modulus (G*) reflect materials' capability to resist deformation caused by stress. It is defined as follows;

$$G^* = \sqrt[2]{(G')^2 + (G'')^2} = \frac{\sigma_0}{\varepsilon_0} \qquad (A19)$$

6 References

1. T. Wang, E. Canetta, T. G. Weerakkody, Acs Appl. Mater. Interface 2009, 1, p. 631-639.
2. J. Horsky, O. Quadrat, B. Porsch, L. Mrkvickova, Colloid Surfaces A 2001, 180, p. 75-85.
3. D. Satas, Handbook of Pressure Sensitive Adhesive Technology, 2nd edition, Van Nostrand Reinhold, New York, 1989, p. 105.
4. Yang H. W. H., Chang E. P., Trends in Polymer Science 1997, 5: 380-384.